# The causes and consequences of demographic variation

**Simon Patrick Rolph**

Department of Animal and Plant Sciences

The University of Sheffield

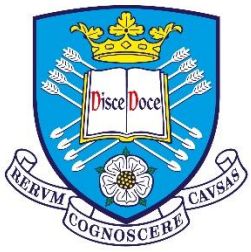


The University Of Sheffield.

A thesis submitted for the degree of Doctor of Philosophy

April 2021

Curiously enough, the only thing that went through the mind of the bowl of petunias as it fell was Oh no, not again. Many people have speculated that if we knew exactly why the bowl of petunias had thought that we would know a lot more about the nature of the Universe than we do now.

Douglas Adams, The Hitchhiker's Guide to the Galaxy

# Summary

Demography aims to understand the changes in population numbers or density arising from individual-level variation in fertility, mortality, and migration. Understanding and predicting population dynamics remains an important keystone for ecologists in order to identify population management strategies and explore evolutionary optimisation of timings and energetic allocations of life history strategies. In chapter two, I examine how comparative analysis of published plant matrix population models (MPMs) from the COMPADRE Plant Matrix Database can be used to determine axes of life history variation using principal component analysis. I simulate population models under the assumption that density dependence constrains growth rates as a result of a carrying capacity: a non-adaptive constraint. I found density dependent constraints explained much of the covariance patterns in life history metrics. In chapter three, I use this simulated population model framework to explore the link between life history and transient dynamics, quantified as responses to perturbations. Indices of transient response derived from population models also exhibited non-adaptively constrained covariance patterns. Transient response was characterised on two axes; magnitude of transient response and tendency to attenuated as opposed to amplify. In chapter four, I show that how we model the interannual fluctuations in vital rates affects our model's resulting population dynamics, life history metrics and responses to perturbations, using data from Soay Sheep population on the island of St Kilda. I show this by modelling vital rates with generalised linear mixed-effects models (GLMMs) and hierarchical generalised additive models (HGAMs) and comparing the resulting integral projection models. In chapter five, I discuss the need to be precise in interpretating results of demographic approaches. How we model populations, and the resulting non-adaptive constraints, play an important role in shaping these results. I outline future uses of this simulated population model framework for time-varying population models and single species study systems.

- Old version
- Demography aims to understand the changes in population numbers or density arising from individual-level variation in fertility, mortality, and migration.
- Understanding and predicting population dynamics remains an important keystone for ecologists in order to identify effective population management strategies and explore how evolution optimises the timings and energetic allocations of life history strategies.
- Comparative analyses of metrics derived from demographic models are a proposed approach to identify these energetic allocations.
- in demographic models for hundreds of species from the COMPADRE Plant Matrix Database.
- We applied our simulated population model framework to explore the link between life history and transient dynamics in the context of density dependent constraints. We found that over 50% of magnitude for transient response was predicted by a fast-slow continuum, but the tendency to amplify or attenuate was poorly linked to life history.
- The general discussion summarises our key findings in the link between demography and life history, reviews how demographic research should be interpreted whilst taking account of non-adaptive constraints and outlines future uses of the simulated population model approach.

# Acknowledgements

I am writing these acknowledgements after a very strange year in a global pandemic and so I'm extra thankful to everyone who helped me to complete my PhD.

First, thanks to Dylan for taking me on as a PhD student and steering my research to what it is today. Thank you for your academic support, countless comments and edits on my drafts, and for being understanding when things went wrong. Thanks to Rob Salguero-Gómez for providing me with the opportunity to embark on this PhD journey and thanks to the Leverhulme Trust funded Centre for Advanced Biological Modelling for making this PhD happen.

This research was made possible by the enormous collaborative effort to produce the open-access data in the COMPADRE Plant Matrix Database. Thanks to the COMPADRE Plant Matrix Database team, supported by the Max Planck Institute for Demographic Research (MPIDR), for data digitalization and error-checking. This research was also made possible by many people involved in the data collection for the long-running Soay Sheep project, it was a real privilege to work with this dataset.

I am so very grateful to have Nat in my life for her love, support, delicious baking, and miraculous ability to keep me being productive through the endless monotony of working from home.

Thanks to my family for their enduring support and belief in me throughout this PhD. I know how proud of me you are for finishing this PhD.

It wouldn't have been the same if it weren't for my fantastic lab group and fellow office mates: Tamora, Simran, Bethan, Alison, Kim, Shaun, Jason, Tom, Rob, John, and James. Thanks for the coffee breaks, the many pints in Interval, the cheese-filled lab meetings (apologies to the people who used the room after us) and lab group walks. Thanks to Tamora, Kim and Bethan for providing valuable comments and edits on my drafts.

Thanks to everyone in the Animal and Plant Science research community but special thanks to my fellow writing-retreaters: Roberta, Jönny, Emma, Joe, and Tom. Through Google Meet we managed to recreate the closest approximation to an office environment and supported one another through the final stretches of our PhDs.

Thanks to Luke and the fellow volunteers at Sheffield and Rotherham Wildlife Trust who helped me feel myself again whilst I took leave of absence from the PhD. Also, thanks to Dale from the University Counselling Service for her advice and guidance during this period.

Thanks to Ronan, not just a housemate of three years, but a good friend who immediately made me feel welcome in Sheffield.

I want to thank the many fantastic people I met at conferences who made me feel a part of the ecological research community; conferences were real highlights of my PhD experience because of them. Special thanks to the immensely welcoming research community at the Zoology and Botany Departments of Trinity College Dublin who hosted me in autumn 2019.

Lastly, thanks to the Rivelin Valley, whose many interweaving footpaths were an essential source of strength throughout this PhD.

# Statement of intellectual contribution

The work in this thesis would not have been possible without the intellectual contributions listed below. All data chapters (Chapters 2-4) are presented as manuscripts for publication. Major contributions are listed below, and additional contributions noted in the acknowledgements of each chapter.

**Chapter 1:** S. P. R. wrote the manuscript. D.Z.C. contributed critically to the manuscript.

**Chapter 2:** S. P. R. and D.Z.C. conceived and designed the study. S. P. R. prepared the data, carried out the analysis and wrote the manuscript. D.Z.C. contributed critically to the manuscript.

**Chapter 3:** S. P. R. and D.Z.C. conceived and designed the study. S. P. R. prepared the data, carried out the analysis and wrote the manuscript. D.Z.C. contributed critically to the manuscript.

**Chapter 4:** S. P. R. and D.Z.C. conceived and designed the study. S. P. R. prepared the data, carried out the analysis and wrote the manuscript. D.Z.C. contributed critically to the manuscript.

**Chapter 5:** S. P. R. wrote the manuscript. D.Z.C. contributed critically to the manuscript.

# Declaration

This thesis contains original work and does not contain material previously published or written by other persons, except where due reference has been made in the text. The contribution of collaborators to the conceptualisation, data collection, statistical analysis, authorship, and editing of this thesis has been clearly stated. The thesis content results from work I have undertaken since starting my research higher degree and includes no work submitted to qualify for any other degree or diploma in any university or other institution. I, the author, confirm that the Thesis is my own work. I am aware of the University's Guidance on the Use of Unfair Means (www.sheffield.ac.uk/ssid/unfair-means).

# Contents

# Chapter 1

# General introduction

# Why do we care about demographic variation?

Demography aims to understand the changes in population numbers or density arising from individual-level variation in fertility, mortality, and migration. In the hierarchy of ecological complexity, demography provides a vital link between the individual and the population. Across time, space and phylogeny, populations exhibit a diverse array of dynamics. Understanding and predicting population dynamics remains an important keystone for ecologists to identify effective population management strategies and explore how evolution optimises the timings and energetic allocations of life history strategies. Studying processes at the population level is key to determining why demographic rates, such as survival and fecundity, vary (and covary) on spatial and temporal scales (Sutherland et al., 2013). Features of populations in which ecologists are interested, such as population growth rate, are typically not easy to measure; we cannot simply take a cursory look at a population and determine its population trajectory. However, we can more easily measure the features of individuals: physical traits, fecundity, and mortality. Demographic approaches provide the toolbox to translate from this individual-level data to the population. Ultimately, demographic approaches provide a framework for studying population dynamics in which demographic rates vary over the lifespan of individuals. These approaches provide mechanistic insight into the processes that shape population dynamics.

Within the framework of demography, demographic variation describes among-individual differences in survival, growth, maturation, and reproduction. A fundamental challenge in demography is to understand the causes and consequences of this variation; why do individuals have different demographic rates and what does this mean for the population? There are different dimensions to demographic variation: that which occurs between individuals, through the changing environment and over the course of an individual's life. Demographic variation will arise because individuals are not identical and exhibit variation in physical traits, which can be summarised as an individual's phenotype: the physical expression of the underlying genotype and its interaction with the environment. Phenotypic variation takes many forms such as body mass, size, age, and life stage. Some phenotypes will be better suited for a certain environment resulting in higher survival, faster growth, or higher fecundity (Csergő

et al., 2017). The environment which individuals experience varies in space and time, driving further demographic variation (Crowley et al., 2016). In addition, an individual will be subjected to different environmental conditions throughout their life. We must also consider that some individuals are simply luckier than others: individual stochasticity plays a role in the distribution of demographic variation (Caswell, 2009). Ultimately, demographic rates are a result of a composition of all of these drivers of demographic variation. Consequences of demographic variation can be quantified as variation in fitness and population dynamics, features that are fundamental to our understanding of evolutionary and ecological processes.

Demographic studies have a long history of adopting both empirical and theoretical approaches. Empirical approaches seek to isolate causes of demographic variation using experimental treatments, submitting different groups of organisms to alternative environmental conditions and looking for variation in response. Experiments have been used in demographic research for insects (Tenhumberg et al., 2009) and plants (Bullock et al., 1994) but are not feasible for larger, longer lived, or more widely roaming species (e.g. Jackson et al., 2019). Relying on experimental approaches would limit the taxonomic breadth of any comparative analysis and make it harder to test the generality of hypotheses. Another strand of empirical work uses observational studies to collect longitudinal, individual-level demographic data with environmental covariates. This data can be used to infer the dependence of demographic rates on an individual's state, such as age or size, and/or environmental conditions. A range of statistical and modelling tools are used to link the individual to the population. This approach has been applied to a wide range of taxa but often only focuses on a portion of the life cycle. A subset of these studies calculates demographic rates for the entire life cycle and can be used to develop population models. Bypassing the need for field data, theoretical approaches use mathematical models to understand generic patterns whilst not being tied to a particular system or species. For example, theoretical demographic approaches have applied to investigate how life stage structure impacts population dynamics (de Roos, 2018) and the role of individual stochasticity in human populations (Hartemink et al., 2017). Ultimately, the toolkit needed to apply these approaches have methodological

similarities: we build models that can express between-individual differences to examine the consequences of demographic variation.

# Understanding demography through mathematical models

Modelling has a central role in overcoming one of the greatest challenges in ecology: the incredible complexity of ecological systems. Population models are mechanistic models that allow us to capture key components of natural populations. Population models typically use variables and relationships between those variables to portray a simplified population process. For example, a simple model of a self-contained population without migration could look like

$$n_{t+1} = s\, n_t + b\, n_t \qquad (1.1)$$

where $n_t$ is the population size at time $t$ and $n_{t+1}$is the population size at $t + 1$. In this model, $s$ and $b$ are constants that describe the survival rate and birth rate. Early prominent theoretical population models were not structured demographically and considered population state simply as a number of individuals, assuming the same vital rates for each individual. Considering demography when doing ecological, and thus incorporating demographic structure in mathematical models, is widely recognised as an important component of ecology and evolution (Metcalf & Pavard, 2007).

An important step in demographic modelling was the development of the discrete-time, discrete state, age-classified matrix model (Leslie, 1945). This type of model is often referred to as a Leslie matrix. The Leslie matrix brought the application of matrix calculus to analysing population dynamics (Hansen, 1989). A Leslie matrix classifies individuals by their age and each age class can have different rates of survival and reproduction. The model can be written out in a matrix representation like so

$$\begin{bmatrix} n_0 \\ n_1 \\ \vdots \\ n_{w-1} \end{bmatrix}_{t+1} = \begin{bmatrix} f_0 & f_1 & \cdots & f_{w-1} \\ s_0 & 0 & \cdots & 0 \\ \vdots & \vdots & \ddots & \vdots \\ 0 & 0 & s_{w-2} & 0 \end{bmatrix} \begin{bmatrix} n_0 \\ n_1 \\ \vdots \\ n_{w-1} \end{bmatrix} \quad (1.2)$$

where w is the maximum attainable age in the population, $f_a$ is the fecundity rate of each age class, $s_a$ is the survival of each age class and $n_a$ is the abundance of each age class. It can be written as

$$n_{t+1} = An_t \quad (1.3)$$

where $A$ is the transition matrix and $n_t$ is now a vector of age class abundances. This transition matrix can represent transitions between states other than age. The Lefkovitch model (Lefkovitch, 1965) classifies individuals by other factors; factors such as size or life stage can be a more important predictor of demographic variation than age. These tools are more broadly recognised as matrix population models (MPMs) (Caswell, 2001) or sometimes referred to as population projection matrices (PPMs) (e.g. Stott et al., 2011). MPMs are a generic tool for describing the transitions between states, constituting a transition matrix A with elements $a_{ij}$ representing the rate of transition from stage j to stage i. The transition matrix may be separated based on the type of transition. For example, a two-stage model could be written out as such:

$$A = P + F = \begin{bmatrix} a_{11} & a_{12} \\ a_{21} & a_{22} \end{bmatrix} = \begin{bmatrix} p_{11} & p_{12} \\ p_{21} & p_{22} \end{bmatrix} + \begin{bmatrix} f_{11} & f_{12} \\ f_{21} & f_{22} \end{bmatrix} \quad (1.4)$$

with a survival matrix, P, where class-specific rates $p_{ij}$ are constrained to be between zero (0% survival) and one (100% survival), and a fecundity matrix, F, in which class-specific transition values $f_{ij}$ can exceed one.

Matrix population models have emerged as a popular and important tool for modelling populations of plants and animals. In the scientific literature, there are matrix population models for hundreds of species (Salguero-Gómez et al., 2015, 2016a). Part of the reason that MPMs received such a successful integration into population ecology is that they are intuitive and relatively accessible. MPMs are rarely mentioned without reference to their 'tractability'. Supported by a growing literature base and synthesised in the comprehensive book 'Matrix Population Models' (Caswell, 2001), the MPM established itself as an important part of the ecologist's tool kit. Another strength was the wide range

of analyses and outputs that could be derived from MPMs. Perturbation analyses were used to determine the relative importance of different stages in the life cycle (De Kroon et al., 2000): a useful tool for population management (e.g. Wisdom & Mills, 1997) and explaining life history evolution (Wilbur & Rudolf, 2006).

In addition to standard population outputs such as growth rates, MPMs have also had many applications as a tool for analysing life histories. Matrix population models explicitly describe population-level transitions between discrete stages but if we consider individual stochasticity this information can also be interpreted as a description of life histories. Individual stochasticity describes how individuals will have different trajectories throughout their life. For example, if at the population level the survival rate for a specific year for a specific stage is 0.6, at an individual level this means that 60% of individuals survived and 40% did not. We can use these percentages as probabilities in a Markov chain which is a stochastic model describing a sequence of possible events where the probability of each event depends on the state. We can use Markov chain theory to proliferate through all possible life history pathways and derive life history metrics. Markov chain theory can be employed to calculate age-specific rates from stage-specific models to produce survivorship curves and fecundity curves. The derived age-specific rates can be used to calculate life history traits such as age at first reproduction, mean life expectancy and average lifetime reproduction (Caswell, 2009, 2011; van Daalen & Caswell, 2017). These methods can be generalised to variable environments (Caswell, 2009).

Classifying individuals into discrete classes is always an approximation when the underlying state variable is continuous, such as an individual's size (Picard & Liang, 2014). MPM outputs are sensitive to model parameterisation in terms of how the classes are defined by discretising a continuous variable (Salguero-Gómez & Plotkin, 2010; Tenhumberg et al., 2009). Integral projection models (IPMs) have emerged as a different way of modelling populations by classifying individuals on a continuous state variable which governs variation in vital rates. Instead of a population vector, the state of a population at time $t$ is described with a continuous state distribution such that individuals with state $z$ in the interval $[a, b]$ at time $t$ is

$$\int_a^b n(z,t)dz. \tag{1.5}$$

The IPM equivalents for the MPM survival and fecundity (Equation 1.4) transition matrices are two functions $P(z',z)$ representing survival/growth and $F(z',z)$ representing per capita fecundity where $z$ is the state at time $t$ and $z'$ is the state at time $t+1$. The full kernel comprising both $P(z',z)$ and $F(z',z)$ is usually notated as $K(z',z)$ such that $K(z',z) = P(z',z) + F(z',z)$. The population at time $t+1$ can be written out as

$$n(z',t+1) = \int_L^U K(z',z)n(z,t)dz \tag{1.6}$$

where $U$ and $L$ are the upper and lower limits of state $z$, respectively. The above equation represents a single state IPM where individuals are classified by size $z$ and no other factor. This simple model provides the foundation that all IPMs are based upon.

All modelling approaches have considerations to make that may affect their robustness and effectiveness; IPMs are no exception. Vital rates such as the probability of survival or the probability of reproduction are parameterised via regression. The choice of regression model has implications on the reliability and flexibility of the model. For example, a very simple regression model like a linear model might not capture the intricacies of a vital rate relationship, but an overly complex model may introduce excessive parameter uncertainty and/or overfit the relationship. Whilst almost any regression framework could be used, most IPMs are parametrised with generalised linear models (GLMs) or generalised linear mixed models (GLMMs) (Ellner et al., 2016b, 2016a). Without exploring the use of other regression frameworks, we could be missing out on improvements to our models, their analyses, and their interpretation. The main issue is that the relationships between state variables and vital rates in real populations may not be adequately described by generalised linear models. One area of concern is individuals at the extremes of the observed size range: whereas a linear model may be a suitable approximation for the intermediate sizes, this may extrapolate poorly to very large or small individuals.

Some notable exceptions to the predominant use of GL(M)Ms include the use of generalised additive models (GAMs) (Dahlgren et al., 2011; González et al., 2013). GAMs can fit smooth functions using splines which may better reflect vital rate relationships and therefore improve demographic models. These methodological advances reflect a wider shift in ecology towards data-driven approaches.

# The comparative analysis of demographic data

The comparative analysis of demographic data, or comparative demography, encompasses research that compares the demography of different populations or species. Early examples of comparative demography carried out fieldwork to compare a handful of species or populations and compared demographic traits such as the survivorship of two salamander populations (Tilley, 1980) and reproduction in three desert rodents (Christian, 1979). Subsequent comparative research identified that published MPMs could be used to compare the demography of species without the need to do additional fieldwork. For example, Silvertown et al. (1992) used published MPMs from 18 plant species to look at life history trade-offs. The scale of these analyses soon expanded; published MPMs for 83 species were used in an examination of the fast-slow continuum (Franco & Silvertown, 1996) and MPMs for 200 species were used to compare population dynamics of invasive and native plants (Ramula et al., 2008). These large-scale, comparative analyses can be classed as macroecological studies: macroecology encompasses research that spans large spatial, taxonomic, or temporal scales. Ultimately, these analyses were made possible because a set of different MPMs from different sources can be used to derive the same set of metrics.

The development of repositories for published MPMs provided the catalyst for a boom in research papers using comparative demography as a new approach for a range of ecological questions. The COMPADRE Plant Matrix Database (Salguero-Gómez et al., 2015) and COMADRE Animal Matrix Database (Salguero-Gómez et al., 2016a) are repositories for published plant and animal MPMs respectively, and together contain MPMs for 1174 species. The data for COM(P)ADRE can be

downloaded as a data object for the R programming language, reflecting R's growing popularity as the go-to tool for analysis in ecology. There has also been the development of R packages for the construction and analysis of MPMs (Stubben et al., 2014) and the analysis of transient dynamics of MPMs (Stott et al., 2012). These databases of MPMs facilitated comparative research across hundreds of species and have been used to classify plant life history strategies (Salguero-Gómez et al., 2016b), compare transient dynamics for different species (Stott et al., 2010) and search for senescence across the tree of life (Jones et al., 2014).

MPMs are well suited for comparative analysis because the same outputs can be derived from different MPMs; however, the results of comparative studies may be affected by issues such as fundamental methodological errors in MPM construction (Kendall et al., 2019). There are inconsistencies in the discrete stage structure from one MPM to the next and the number of stage classes used for an MPM has been shown to affect model outputs (Salguero-Gómez & Plotkin, 2010). Furthermore, different study systems present issues in making sure that all demographic transitions are accounted for; for example, cryptic life stages such as seedbanks or dormancy, cryptic transitions such as shrinkage (Salguero-Gómez & Casper, 2010), and conflating migrations with presumed mortality. Whilst the challenges mentioned here are known to persist, there are still unknowns in how these factors play out when individual demographic studies form part of broader macroecological approaches. In addition, there isn't a standardised way of testing for these effects.

Asymptotic population growth rate is a common focus of comparative studies because it is an established indicator of whether a population is declining or increasing. Growth rate is also important for assessing habitat suitability (Csergő et al., 2017) and fitness (Coulson et al., 2006). Population growth rate has been shown to vary more in time than space (Buckley et al., 2010) and interpolating growth rates is difficult (Coutts et al., 2016). Error is introduced into estimated growth rates because studies often do not span a sufficient timeframe to reliably estimate long term growth rate (Clark, 2003). A related consideration is that demographic studies, such as those in COM(P)ADRE, are motivated by different research interests. One example of this is that a common motivation for building a population model is to test potential management strategies (Crone et al., 2011), therefore endangered or invasive

species are oversampled. This will introduce further variance into the distribution of growth rates of demographic studies. It is unclear what impact this variance in growth rates has on how we can interpret the results of comparative analyses.

# Life history through the lens of demography

Demography and life history are fundamentally linked but we do not have a well-developed understanding of these connections (Coulson et al., 2010). Life histories describe regimes of survival, growth, and reproduction through an organism's life. Life history strategies describe the timings of life events such as birth and maturation and allocation of resources towards survival, growth, and reproduction. Life history theory aims to understand the adaptive significance of the timing of life history events and patterns of resource allocation. At the core of life history theory is the concept that energetic investments into survival, growth, and reproduction constrain the range of life history strategies (Stearns, 1976). Investing from a finite resource must lead to trade-offs where the increase in allocation towards one process must result in a decrease in others. In the absence of trade-offs, fitness-correlated traits would be selected until they were only limited by evolutionary history and physiological constraints. Life history strategies are complex and multidimensional: there are many ways in which an individual of a species could invest energy throughout their life into survival, growth, and reproduction. There have been many attempts, theory and data-driven, to classify life history strategies (Bielby et al., 2007; Bonser & Aarssen, 1996; Pierce et al., 2013; Salguero-Gómez et al., 2016b; Southwood, 1988; Stearns, 1983).

Frameworks for classifying life histories have typically attempted to place species along continuums ('axes'). An important early theory for classifying life histories placed strategies along an axis from r-selected strategies to K-selected strategies (MacArthur & Wilson, 1967; Pianka, 1970). r-selected strategies optimised growth and fecundity for unpredictable environments and K-selected strategies optimised survival and parental investment to operate in stable environments at the population's

carrying capacity. Another theory, the CSR strategies (Grime, 1977) placed plant life histories in a three-way space between the allocation of resources to growth, reproduction, and maintenance. The parallels between the CSR strategies and the demographic process of survival, growth and reproduction were not lost on Silvertown et al. (1992). They hypothesised that the importance of survival, growth, and reproduction for long term growth rate, as calculated through sensitivity analysis, related to the CSR strategies: stress tolerators (S) must optimise survival, competitors (C) must optimise growth, and ruderals (R) must optimise reproduction. However, their attempt to match the CSR strategies to the species' demography found limited correlation, ascribed to differences in where and how the data was collected for the demographic studies versus the data for CSR studies.

Another data-driven approach is to look for variance-covariance patterns of life history traits, typically at the species level, under the assumption that these life history traits are manifestations of the underlying budgetary trade-offs. Early use of this approach by Stearns (1983) used life history traits from field observations, such as clutch size and life expectancy, and suggested that a two-axis framework absorbed much of the variance and covariance in life history traits in mammals when controlled for body size. These axes were derived from a principal component analysis (PCA) on life history traits, a multivariate dimensional reduction technique. Following research continued to interrogate patterns of life history variation across animals (Heppell et al., 2000; Promislow & Harvey, 1990) and plants (Eriksson & Jakobsson, 1998; Franco & Silvertown, 2004). MPMs were used in comparative approaches looking at native and invasive populations (Ramula et al., 2008) and short-term dynamics (Stott et al., 2010). Data-driven approaches for classifying life histories became more ambitious in terms of taxonomic breadth as data availability increased through databases such as COMPADRE (Salguero-Gómez et al., 2015) and COMADRE (Salguero-Gómez et al., 2016a).

Salguero-Gómez et al (2016) was the first in a series of studies (Capdevila et al., 2019; Healy et al., 2019; Paniw et al., 2018; Salguero-Gómez, 2017) that used data from COMPADRE to classify life history strategies using a PCA of MPM derived life history traits. This analysis found that 55% of covariation in nine plant life history traits could be captured in two main axes of variation. These traits were: generation time, R0, survivorship curve type, age at sexual maturity, degree of iteroparity, net

reproductive rate, mature life expectancy and vital rates for progressive growth, retrogressive growth and mean sexual reproduction. The first axis represented the ‘pace of life' from short-lived, high turnover life histories to long-lived slow turnover life histories. The second axis captured variation in reproductive strategies from reproducing throughout life to reproducing once at the end of life: from iteroparity to semelparity. The position of a species in this two-axis space was later shown to correlate with population growth rate, conservation status, aridity index and specific leaf area (Salguero-Gómez, 2017). A similar approach was applied to animal population models using the COMADRE Animal Matrix Database and found that two PCA axes accounted for 71% of life history (co)variation using a different set of life history metrics (Healy et al., 2019). An extension of this comparative PCA approach used multiple transition matrices per species to classify life histories and predicted responses to environmentally stochastic environments (Paniw et al., 2018).

Each of these studies alludes to the existence of life history trade-offs explaining these patterns but these studies are purely correlative. These correlative patterns could be generated by a combination of different processes which may or may not include trade-offs in the allocation of energy towards survival, growth, and reproduction. The correlative patterns may be shaped by adaptive constraints: the selection of sets of life history traits through evolution. The correlative patterns could also be driven by environmental factors such as different levels of resource availability. However, patterns of covariance between life history metrics may also be driven by ecological factors that are unrelated to, or at least indirectly related to, species’ life histories, which we refer to as non-adaptive constraints. Density dependence is one such factor, for which there is evidence of its effects across a broad range of taxa (Brook & Bradshaw, 2006; Sibly et al., 2005). Density dependence’s potential impact on life history traits was formalised by Sutherland et al. (1986). Given a population of constant structure, let $\pi$ be the probability of surviving to reproduction and $\mu$ be the mean adult mortality per year. L is the expected reproductive lifespan and M is the average number of offspring produced by a female chosen at random from these reproducing in a given year. Then

$$\pi LM = \frac{\pi M}{\mu} = 2 \tag{1.7}$$

Essentially, this says that we should expect to see (co)variances between measures of demography and life history. Density dependence limits the possible combinations of these measures. One way to determine how important density dependence is in shaping life history trait (co)variance patterns would be to develop a null model. A null model could explore the life history trait (co)variance patterns created by density-dependent constraints, in the absence of energetic trade-offs, and compare this to the empirical findings from COMPADRE.

# Using null models to explore the effects of non-adaptive constraints

A null model is a general tool used across scientific disciplines: it is a pattern-generating routine that aims to hold some features of a dataset constant while allowing others to vary that can then be compared to an empirical dataset (Gotelli & Graves, 1997). The goal is to generate patterns expected in the absence of some process or mechanism. Typically, the null model's routine is designed to not explicitly include the mechanism that is presumed to be causing the pattern in question. The key purpose of a null model is to provide a baseline from which to compare any trend or finding; this gives insight as to whether the trend is a result of factors of interest or simply an emergent property of the system. Null models have an increasingly prominent role in community ecology which may be partly due to the innate complexity of ecological systems: high-dimensionality, non-linearity and stochasticity operating at different spatial and temporal scales. As a result of this complexity, interesting patterns will undoubtedly emerge, but because of this complexity, it can be hard to determine the underlying factors causing these patterns. Null models have not been formally applied to the comparative analyses of demographic data but here we outline why they might be a useful tool.

Inherent properties of MPMs have been shown to produce non-random patterns in comparative analyses. For example, $R_0$, the per generation growth rate, is mathematically constrained with asymptotic growth rate ($\lambda$) and generation time, $T$, such that

$$T = \frac{\log(R_0)}{\log(\lambda)} \tag{1.8}$$

and since generation time, $T$, must be positive, $\log(R_0)$ and $\log(\lambda)$ must have the same sign. Researchers have found the best way to assess how comparative analyses are being impacted by these sorts of properties is to simulate MPMs. McDonald et al. (2017) used simulated MPMs with temporal replicates to examine the demographic buffering hypothesis (DBH). Generated in the absence of natural selection, 96% of simulated population models showed a negative correlation between the importance and variability of demographic vital rates: evidence of the DBH. They used this finding to apply a link scaling to stabilise the relationship between importance and variability before carrying out the analysis on empirical data. Takada et al. (2018) simulated 24,000 MPMs with 4 life stages, calculated elasticities for survival, growth, and reproduction on population growth rate. Takada et al. (2018) found the combinations of elasticities were mathematically constrained and that the slope of a relationship in a ternary plot of elasticities was mathematically tied to the dimension of the MPM. These examples are not formally null models because they are not explicit in their constraints or they don't sample from a distribution, but they are motivated by a similar requirement. These studies have shown that these sorts of tools are useful when interpreting results of comparative demography because it allows us to interrogate whether a pattern is a result of a statistical artefact and allows us to correct for this when designing analyses or interpreting results.

# Outline of my research

This body of work aims to contribute to our understanding of the causes and consequences of demographic variation. Using two approaches, comparative and single system, we show how we can better use demographic data to understand the complex relationships between vital rates, life history traits and population performance. The thesis is a compilation of three manuscripts written as part of my PhD where each piece of research is distinct but cohesive with parallel themes of demography and life history. In this work, we use macroecological and comparative approaches using aggregated demographic data that has been compiled from many sources but have been distilled to a single transition matrix that is representative of the demography of a whole species. We also use highly detailed, study system-specific, individual-based, long-term demographic data for a single population.

In chapter two, *Density dependence limits the comparative analysis of demographic data*, we show that demographic data simulated under the non-adaptive constraint of density dependence, as a result of a population fluctuating around a carrying capacity, produced similar patterns of life history trait covariance when compared to life history trait covariance of empirical data from the COMPADRE Plant Matrix Database. We simulate population models to express plausible plant life history dynamics using an IPM framework. These IPMs were discretised to MPMs to facilitate reasonable comparisons between simulated and empirical demographic data. Our main conclusion is that demography-derived patterns of life history traits, previously described as a fast-slow continuum and possibly a symptom of underlying energetic budgetary trade-offs, are primarily shaped by density dependence, a non-adaptive constraint.

In chapter three, *Linking life history to transient dynamics via population models*, we investigate the link between life history and short-term, transient dynamics in the context of non-adaptive constraints. In this chapter, we use our novel simulated population model framework to derive both life history traits and measures of transient dynamics, under the assumption that density dependence constrains growth rates. With this dataset, we explore the patterns of covariance between each set of metrics using partial

least squares regression, also known as projection to latent space (PLS), and find a link between life history and transient dynamics. We show that 50% of the variance in the magnitude of transient response is explained by a fast-slow continuum, but there is substantial unexplained variance, despite working with purely simulated demographic models. Furthermore, by discretising demographic data to matrix population models, we show that the link between life history and transient dynamics can be obscured by discretisation artefacts.

In chapter four, *Time-varying vital rates for population modelling: how flexible do we need to be?*, we retain the key themes of life history and optimisation from chapter two and three but step away from the comparative analyses to focus on the demography of a single population; the long-studied population of Soay sheep (*Ovis aries*) on the island of St Kilda. We investigate how capturing the vital rates, the fundamental link between individual traits and demographic rates, in time-varying environments is affected by how much flexibility we afford in our modelling approach. We compare IPM constructed from vital rates fitted with generalised linear mixed-effects models (GLMMs) or more flexible hierarchical generalised additive model (HGAMs). We find that how we model time-varying vital rates does affect outputs, and that the more flexible HGAMs might be an ideal choice for modelling study systems with hidden state variables.

In chapter 5, the general discussion, I review the key findings of this body of work in terms of our understanding of demography, life history and transient dynamics. I use our findings to outline how we need to consider the implications of a demographic perspective of life history and how non-adaptive constraints should be considered when interpreting comparative analyses. Finally, I outline future directions for research using the simulated population model framework we pioneer in this research.

# References

Bielby, J., Mace, G. M., Bininda-Emonds, O. R. P., Cardillo, M., Gittleman, J. L., Jones, K. E., … Purvis, A. (2007). The fast-slow continuum in mammalian life history: An empirical reevaluation. *American Naturalist*, *169*(6), 748–757.

Bonser, S. P., & Aarssen, L. W. (1996). Meristem Allocation: A New Classification Theory for Adaptive Strategies in Herbaceous Plants. *Oikos*, *77*(2), 347.

Brook, B. W., & Bradshaw, C. J. A. (2006). Strength of evidence for density dependence in abundance time series of 1198 species. *Ecology*, *87*(6), 1445–1451.

Buckley, Y. M., Ramula, S., Blomberg, S. P., Burns, J. H., Crone, E. E., Ehrlén, J., … Wardle, G. M. (2010). Causes and consequences of variation in plant population growth rate: a synthesis of matrix population models in a phylogenetic context. *Ecology Letters*, *13*(9), 1182–1197.

Bullock, J. M., Hill, B. C., & Silvertown, J. (1994). Demography of Cirsium Vulgare in a Grazing Experiment. *The Journal of Ecology*, *82*(1), 101.

Capdevila, P., Beger, M., Blomberg, S. P., Hereu, B., Linares, C., & Salguero-Gómez, R. (2019). Aquatic and terrestrial organisms display contrasting life history strategies as a result of environmental adaptations. *BioRxiv*.

Caswell, H. (2001). *Matrix population models*. (L. John Wiley & Sons, Ed.).

Caswell, H. (2009). Stage, age and individual stochasticity in demography. *Oikos*, *118*(12), 1763–1782.

Caswell, H. (2011). Beyond R0: Demographic models for variability of lifetime reproductive output. *PLoS ONE*, *6*(6).

Christian, D. P. (1979). Comparative Demography of Three Namib Desert Rodents: Responses to the Provision of Supplementary Water. *Journal of Mammalogy*, *60*(4), 679–690.

Clark, J. S. (2003). Uncertainty and variability in demography and population growth: A hierarchical

approach. *Ecology*, *84*(6), 1370–1381.

Coulson, T., Benton, T. G., Lundberg, P., Dall, S. R. X., Kendall, B. E., & Gaillard, J. M. (2006). Estimating individual contributions to population growth: Evolutionary fitness in ecological time. *Proceedings of the Royal Society B: Biological Sciences*, *273*(1586), 547–555.

Coulson, T., Tuljapurkar, S., & Childs, D. Z. (2010). Using evolutionary demography to link life history theory, quantitative genetics and population ecology. *Journal of Animal Ecology*, *79*(6), 1226–1240.

Coutts, S. R., Salguero-Gómez, R., Csergő, A. M., & Buckley, Y. M. (2016). Extrapolating demography with climate, proximity and phylogeny: approach with caution. *Ecology Letters*, *19*(12), 1429–1438.

Crone, E. E., Menges, E. S., Ellis, M. M., Bell, T., Bierzychudek, P., Ehrlén, J., … Williams, J. L. (2011). How do plant ecologists use matrix population models? *Ecology Letters*, *14*(1), 1–8.

Crowley, P. H., Ehlman, S. M., Korn, E., & Sih, A. (2016). Dealing with stochastic environmental variation in space and time: bet hedging by generalist, specialist, and diversified strategies. *Theoretical Ecology*, *9*(2), 149–161.

Csergő, A. M., Salguero-Gómez, R., Broennimann, O., Coutts, S. R., Guisan, A., Angert, A. L., … Buckley, Y. M. (2017). Less favourable climates constrain demographic strategies in plants. *Ecology Letters*.

Dahlgren, J. P., García, M. B. M. B., & Ehrlén, J. (2011). Nonlinear relationships between vital rates and state variables in demographic models. *Ecology*, *92*(5), 1181–1187.

De Kroon, H., Van Groenendael, J., & Ehrlén, J. (2000). Elasticities: A review of methods and model limitations. *Ecology*, *81*(3), 607–618.

de Roos, A. M. (2018). When individual life history matters: conditions for juvenile-adult stage structure effects on population dynamics. *Theoretical Ecology*, *11*(4), 397–416.

Ellner, S. P., Childs, D. Z., & Rees, M. (2016a). Environmental Stochasticity. In *Data-driven Modelling of Structured Populations: A Practical Guide to the Integral Projection Model* (pp. 187–227).

Ellner, S. P., Childs, D. Z., & Rees, M. (2016b). General Deterministic IPM. In *Data-driven Modelling of Structured Populations: A Practical Guide to the Integral Projection Model* (pp. 139–185).

Eriksson, O., & Jakobsson, A. (1998). Abundance, distribution and life histories of grassland plants: a comparative study of 81 species. *Journal of Ecology*, *86*(6), 922–933.

Franco, M., & Silvertown, J. (1996). Life history variation in plants : An exploration of the fast-slow continuum hypothesis. *Philosophical Transactions of the Royal Society B: Biological Sciences*, *351*(1345), 1341–1348.

Franco, M., & Silvertown, J. (2004). A comparative demography of plants based upon elasticities of vital rates. *Ecology*, *85*(2), 531–538.

González, E. J., Rees, M., & Martorell, C. (2013). Identifying the demographic processes relevant for species conservation in human-impacted areas: does the model matter? *Oecologia*, *171*(2), 347–356.

Gotelli, N. J., & Graves, G. R. (1997). *Null Models in Ecology. Ecology* (Vol. 78). Cambridge.

Grime, J. P. (1977). Evidence for the existence of three primary strategies in plants and its relevance to ecological and evolutionary theory. *The American Naturalist*, *111*(982), 1169–1194.

Hansen, P. E. (1989). Leslie matrix models. *Mathematical Population Studies*, *2*(1), 37–67.

Hartemink, N., Missov, T. I., & Caswell, H. (2017). Stochasticity, heterogeneity, and variance in longevity in human populations. *Theoretical Population Biology*, *114*, 107–116.

Healy, K., Ezard, T. H. G., Jones, O. R., Salguero-Gómez, R., & Buckley, Y. M. (2019). Animal life history is shaped by the pace of life and the distribution of age-specific mortality and reproduction. *Nature Ecology and Evolution*, *3*(8), 1217–1224.

Heppell, S. S., Caswell, H., & Crowder, L. B. (2000). Life histories and elasticity patterns: Perturbation

analysis for species with minimal demographic data. *Ecology*, *81*(3), 654–665.

Jackson, J., Childs, D. Z., Mar, K. U., Htut, W., & Lummaa, V. (2019). Long-term trends in wild-capture and population dynamics point to an uncertain future for captive elephants. *Proceedings. Biological Sciences*, *286*(1899), 20182810.

Jones, O. R., Scheuerlein, A., Salguero-Gómez, R., Camarda, C. G., Schaible, R., Casper, B. B., … Vaupel, J. W. (2014). Diversity of ageing across the tree of life. *Nature*, *505*(7482), 169–173.

Kendall, B. E., Fujiwara, M., Diaz-Lopez, J., Schneider, S., Voigt, J., & Wiesner, S. (2019). Persistent problems in the construction of matrix population models. *Ecological Modelling*, *406*(June), 33–43.

Lefkovitch, L. P. (1965). The Study of Population Growth in Organisms Grouped by Stages. *Biometrics*, *21*(1), 1.

Leslie, P. H. (1945). On the use of matrices in certain population mathematics. *Biometrika*, *33*, 183–212.

MacArthur, R., & Wilson, E. O. (1967). *The Theory of Island Biogeography*. Princeton University Press.

McDonald, J. L., Franco, M., Townley, S., Ezard, T. H. G., Jelbert, K., & Hodgson, D. J. (2017). Divergent demographic strategies of plants in variable environments. *Nature Ecology and Evolution*, *1*(2), 0029.

Metcalf, C. J. E., & Pavard, S. (2007). Why evolutionary biologists should be demographers. *Trends in Ecology and Evolution*, *22*(4), 205–212.

Paniw, M., Ozgul, A., & Salguero-Gómez, R. (2018). Interactive life-history traits predict sensitivity of plants and animals to temporal autocorrelation. *Ecology Letters*, *21*(2), 275–286.

Pianka, E. R. (1970). On r- and K-Selection. *The American Naturalist*, *104*(940), 592–597.

Picard, N., & Liang, J. (2014). Matrix models for size-structured populations: Unrealistic fast growth

or simply diffusion? *PLoS ONE*, *9*(6), e98254.

Pierce, S., Brusa, G., Vagge, I., & Cerabolini, B. E. L. (2013). Allocating CSR plant functional types: The use of leaf economics and size traits to classify woody and herbaceous vascular plants. *Functional Ecology*, *27*(4), 1002–1010.

Promislow, D. E. L., & Harvey, P. H. (1990). Living fast and dying young: A comparative analysis of life-history variation among mammals. *Journal of Zoology*, *220*(3), 417–437.

Ramula, S., Knight, T. M., Burns, J. H., & Buckley, Y. M. (2008). General guidelines for invasive plant management based on comparative demography of invasive and native plant populations. *Journal of Applied Ecology*, *45*(4), 1124–1133.

Salguero-Gómez, R. (2017). Applications of the fast-slow continuum and reproductive strategy framework of plant life histories. *New Phytologist*, *213*(4), 1618–1624.

Salguero-Gómez, R., & Casper, B. B. (2010). Keeping plant shrinkage in the demographic loop. *Journal of Ecology*, *98*(2), 312–323.

Salguero-Gómez, R., Jones, O. R., Archer, C. R., Bein, C., de Buhr, H., Farack, C., … Vaupel, J. W. (2016a). COMADRE: A global data base of animal demography. *Journal of Animal Ecology*, *85*(2), 371–384.

Salguero-Gómez, R., Jones, O. R., Archer, C. R., Buckley, Y. M., Che-Castaldo, J., Caswell, H., … Vaupel, J. W. (2015). The compadre Plant Matrix Database: An open online repository for plant demography. *Journal of Ecology*, *103*(1), 202–218.

Salguero-Gómez, R., Jones, O. R., Jongejans, E., Blomberg, S. P., Hodgson, D. J., Mbeau-Ache, C., … Buckley, Y. M. (2016b). Fast-slow continuum and reproductive strategies structure plant life-history variation worldwide. *Proceedings of the National Academy of Sciences of the United States of America*, *113*(1), 230–235.

Salguero-Gómez, R., & Plotkin, J. B. (2010). Matrix dimensions bias demographic inferences: Implications for comparative plant demography. *The American Naturalist*, *176*(6), 710–722.

Sibly, R. M., Barker, D., Denham, M. C., Hone, J., & Pagel, M. (2005). On the regulation of populations of mammals, birds, fish, and insects. *Science*, *309*, 607–610.

Silvertown, J., Franco, M., ., & McConway, K. (1992). A demographic interpretation of grime's triangle. *Functional Ecology*, *6*(2), 130.

Southwood, T. R. E. (1988). Tactics, Strategies and Templets. *Oikos*, *52*(1), 3.

Stearns, S. C. (1976). Life-History Tactics: A Review of the Ideas. *The Quarterly Review of Biology*, *51*(1), 3–47.

Stearns, S. C. (1983). The influence of size and phylogeny on patterns of covariation among life-history traits in the mammals. *Oikos*, *41*(2), 173.

Stott, I., Franco, M., Carslake, D., Townley, S., & Hodgson, D. (2010). Boom or bust? A comparative analysis of transient population dynamics in plants. *Journal of Ecology*, *98*(2), 302–311.

Stott, I., Hodgson, D. J., & Townley, S. (2012). Popdemo: An R package for population demography using projection matrix analysis. *Methods in Ecology and Evolution*, *3*(5), 797–802.

Stott, I., Townley, S., & Hodgson, D. J. (2011). A framework for studying transient dynamics of population projection matrix models. *Ecology Letters*, *14*(9), 959–970.

Stubben, A. C., Milligan, B., Nantel, P., & Stubben, M. C. (2014). Package ' popbio .'

Sutherland, W. J., Freckleton, R. P., Godfray, H. C. J., Beissinger, S. R., Benton, T., Cameron, D. D., … Wiegand, T. (2013). Identification of 100 fundamental ecological questions. *Journal of Ecology*, *101*(1), 58–67.

Sutherland, W. J., Grafen, A., & Harvey, P. H. (1986). Life history correlations and demography. *Nature*.

Takada, T., Kawai, Y., & Salguero, R. (2018). A cautionary note on elasticity analyses in a ternary plot using randomly generated population matrices. *Population Ecology*, 1–11.

Tenhumberg, B., Tyre, A. J., & Rebarber, R. (2009). Model complexity affects transient population

dynamics following a dispersal event: A case study with pea aphids. *Ecology*, *90*(7), 1878–1890.

Tilley, S. G. (1980). Life Histories and Comparative Demography of Two Salamander Populations. *Copeia*, *1980*(4), 806.

van Daalen, S. F., & Caswell, H. (2017). Lifetime reproductive output: individual stochasticity, variance, and sensitivity analysis. *Theoretical Ecology*, *10*(3), 355–374.

Wilbur, H. M., & Rudolf, V. H. W. (2006). Life-history evolution in uncertain environments: Bet hedging in time. *American Naturalist*, *168*(3), 398–411.

Wisdom, M. J., & Mills, L. S. (1997). Sensitivity Analysis to Guide Population Recovery: Prairie-Chickens as an Example. *The Journal of Wildlife Management*, *61*(2), 302.

# Chapter 2

# Density-dependence limits the comparative analysis of demographic data

Simon Rolph[1]*, Roberto Salguero-Gómez[2], Robert Freckleton[1], Jonathan Potts[3], Dylan Childs[1].

[1] Department of Animal & Plant Sciences, University of Sheffield, Alfred Denny Building, Western Bank, Sheffield, S10 2TN, UK.

[2] Department of Zoology, University of Oxford, Zoology Research and Administration Building, 11a Mansfield Road, Oxford, OX1 3SZ, UK.

[3] School of Mathematics and Statistics, University of Sheffield, Hicks Building, Hounsfield Road, Sheffield, S3 7RH, UK.

*Contact author: srolph1@sheffield.ac.uk

# Summary

1. Life history trade-offs predict that life history strategies are fundamentally constrained and that patterns of covariance between life history traits should provide a basis to classify life histories. Demographic data provide a potentially valuable resource to explore these covariance patterns. For example, matrix population models (MPMs) are versatile population modelling tools describing transitions between discrete states and published MPMs have been compiled into the COMPADRE Plant Matrix Database. However, patterns of covariance between life history traits may be driven by density dependence. This work aims to determine whether density-dependent constraints and parameter uncertainty from sampling variation influence the patterns of covariance between life history metrics, and thus, does density dependence limit the comparative analysis of demographic data.
2. A previous study carried out a principal component analysis (PCA) of key life history metrics derived from plant MPMs and found two important axes of life history variation: fast-slow continuum and reproductive strategies. Our approach is to simulate sets of density-independent, size-structured integral projection models (IPMs) under the constraint that log(λ) (log long-term growth rate) is close to 0. The variance in the log(λ) distribution acts as a surrogate for sampling variation. These IPMs are discretised to MPMs to mimic the discrete stage structures found in a COMPADRE subset. We used PCA to identify whether the composition of the principal components is affected by sampling variation and MPM discretisation.
3. When sampling to a similar log(λ) distribution as observed in COMPADRE, our simulated demographic data produced strikingly similar patterns of life history trait covariance as observed in COMPADRE. Population performance was predicted primarily by $R_0$. Altering the mean and standard deviation of the target log(λ) affected the results of comparative analyses by altering patterns of covariance. Confidence intervals for the COMPADRE PCA highlighted uncertainty in the rotations and weightings of MPM-derived life history metrics.
4. **Synthesis:** Comparative analysis of matrix population models does not identify fundamental budgetary life history trade-offs. A significant component of the covariance among MPM-

derived life histories is consistent with non-adaptive constraints on these patterns, arising from density dependence. When projecting performance metrics onto the life history PCA space, the resulting associations should be interpreted with care.

**Keywords:** Density-dependence, comparative demography, life history strategies, matrix population model, integral projection model.

# Introduction

Life history strategies are descriptions of an organism's investment in growth, reproduction, and survival over its lifetime. Life histories underpin organismal fitness and are fundamental to our understanding of population dynamics and evolution (Metcalf & Pavard, 2007). Across the tree of life, we observe a fascinating diversity of forms, traits and strategies inhabiting a diverse array of environments (Kreft & Jetz, 2007). Nevertheless, a central tenet of life history theory is that budgetary trade-offs between investment in survival, growth and reproduction ultimately limit the diversity of strategies we observe (Stearns, 1992). This leads to the prediction that life histories are fundamentally constrained and that patterns of covariance between traits should provide a basis to classify life histories. For example, early work by MacArthur and Wilson (1967; reviewed in Parry, 1981) identified K-selected and r-selected strategies: r-selected, 'fast' strategies exhibit rapid growth, early maturity, short lifespan and high reproduction but low survival, especially in early life stages, whereas K-selected, 'slow' life histories exhibit the opposite. Universal adaptive strategy theory (UAST) developed by Grime et al. (1977) positioned plant life histories in a three-way trade-off space according to how an organism's resources are allocated to growth, maintenance or regeneration. Stearns (1983) identified two key axes of life history variation in mammals; the slow-fast continuum accounted for 68-75% of covariation, with a secondary axis describing reproductive strategies.

Comparative analysis of matrix projection models (MPMs) is increasingly used to classify life history strategies. MPMs are data-driven models parametrised from individual-level schedules of reproduction and mortality, from which population-level processes such long term asymptotic growth rates, transient dynamics and responses to perturbation can be calculated, as well as key life history traits such as mean life expectancy and age at maturity. Silvertown et al. (1992) were the first to use stage-based MPMs to investigate life history correlates, by linking UAST to the demographic processes of fecundity, growth and survival. MPMs have since been produced for hundreds of plant and animal species, providing the opportunity to use stage-based demographic models for large-scale comparative research (e.g. Salguero-Gómez et al., 2015, 2016a; Sibly et al., 2005). Salguero-Gómez et al. (2016b) used principal

component analysis (PCA) to classify plant life history strategies from life history traits derived from the density-independent, mean-matrices of 418 species. This PCA framework suggests that 55% of life history variation can be positioned on two axes: a fast-slow continuum and a 'reproductive strategies' axis. This two-axis framework has subsequently been used to correlate life history strategies with population growth rate, functional traits, conservation status (Salguero-Gómez, 2017), response to temporal autocorrelation (Paniw et al., 2018), and applied to animals (Healy et al., 2019).

Such broad-scale patterns are compelling, but their interpretation is hampered by several factors. An MPM can be structured with any number of discrete classes, typically defined by combinations of age, size and reproductive status. Although comparable sets of demographic and life history metrics can be calculated for any set of MPMs, some variation will inevitably reflect differences in the structural assumptions of different models. For example, demographic processes such as shrinkage, clonality and seedbanks are often ignored in plant populations (Janovský et al., 2017; Salguero-Gómez & Casper, 2010). MPMs also require continuous state variables such as body size to be divided into a discrete set of classes. Artefacts due to discretisation have been shown to affect predicted population performance (McDonald et al., 2017; Picard & Liang, 2014; Salguero-Gómez & Plotkin, 2010) though reducing MPMs to a consistent number of discrete classes can partially ameliorate this issue providing a consistent model structure for comparative purposes (Salguero-Gómez & Plotkin, 2010).

Patterns of covariance between life history metrics may also be driven by ecological factors that are unrelated to, or at least indirectly related to, species' life histories. Density dependence is one such factor, for which there is evidence of its effects across a broad range of taxa (Brook & Bradshaw, 2006; Sibly et al., 2005). Density dependence describes an inverse relationship between population growth rate and population density therefore resulting in fluctuations around a population's carrying capacity. As a result, the mean predicted asymptotic growth rate, log(λ), despite being calculated from density independent population models is constrained by density dependence through the mechanism of a carrying capacity. We see this in empirical data, the log(λ) of populations in the COMPADRE plant MPM database is approximately 0 (Fig. 2.1). This implies that schedules of growth, reproduction and mortality are constrained by density-dependent feedbacks, which in turn, may impose negative, species-

level correlations between life history metrics (Lande et al., 2002; Sutherland et al., 1986). For example, species with long generation times must exhibit reduced annual recruitment rates relative to short-lived species when log(λ) is constrained to ~ 0. Nonetheless, considerable variation in log(λ) exists in COMPADRE. Much of this variation is likely to be environmental in origin (Sibly et al., 2007). Many plant populations exhibit large variance in annual fecundity and recruitment (Kalisz & McPeek, 1992; Meyer et al., 1986) yet demographic data sets are typically short (<5 years) (Menges, 2000). Obtaining precise estimates of mean demographic parameters is not possible under these circumstances. For example, it has been shown that the temporal replication required to reliably estimate stochastic population growth rate far exceeds the length of most demographic studies (Metcalf et al., 2015). Finally, even the most temporally extensive demographic studies derive from annual censuses of a few hundred individuals at most, meaning that individual vital rate parameters must be estimated from a limited number of demographic events (Crone et al., 2011).

This raises the following question: do density-dependent constraints and parameter uncertainty influence the observed patterns of covariance between life history metrics? And thus, how should we interpret these patterns of covariation? This study aims to address these questions. We use Markov chain Monte Carlo (MCMC) to simulate a set of density-independent, size-structured integral projection models (IPMs) under the constraint that log(λ) is close to 0. The IPMs are discretised to MPMs to mimic the stage-based structure of comparable models in the COMPADRE database. We then use PCA to investigate how the composition of principal components is sensitive to the between-population variance of λ and chosen MPM dimension. Because these simulated population models do not incorporate budgetary trade-offs, the resulting set of models represent a 'neutral model' for plant demography, where the variance in the λ distribution acts as a surrogate for sampling variation.

# Methods

## Modelling life history strategies

To simulate a range of plausible plant life history strategies we defined a size-structured, post-reproductive census IPM with a time interval of one year. We chose an IPM as the underlying model because it allowed us to assess the effects of discretising a continuous trait. The full IPM kernel describes the transitions between two size distributions, immature, $n_I(z,t)$, and mature, $n_M(z,t)$, and from size $z$ to size $z'$ over a discrete-time interval. The transitions for the immature plants take the form

$$n_I(z',t+1) = \int_L^U s(z)(1-m(z))G(z',z)n_I(z,t)dz + \int_L^U p_b(z)b(z)p_r(1-m(z'))c_0(z')\ n_M(z,t)dz \quad (2.1)$$

and the transitions for the mature plants take the form

$$n_M(z',t+1) = \int_L^U s(z)G(z',z)n_M(z,t)dz + \int_L^U s(z)m(z)G(z',z)n_{\mathrm{I}}(z,t)dz + \int_L^U p_b(z)b(z)p_r m(z')c_0(z')n_M(z,t)dz \quad (2.2)$$

where $n_M(z,t)$ is the size distribution of mature individuals at time t, $n_I(z,t)$ is the size distribution of immature individuals at time t, $s(z)$ is the size-dependent survival function, $G(z',z)$ is the size-dependent growth kernel, $m(z)$ is size-dependent maturity, $p_b(z)$ is size-dependent flowering probability, $b(z)$ is size-dependent number of offspring, $c_0(z')$ is the size at birth and $p_r$ is the probability of survival and recruitment from seed to seedling. U is the upper size limit of the kernel and L is the lower size limit of the kernel. The IPM can be represented schematically in "mega-matrix" notation to combine the size distributions (Ellner et al., 2016), where the survival/growth kernel, *P*, can be written as

$$\begin{bmatrix} n_I(z',t+1) \\ n_M(z',t+1) \end{bmatrix} = \begin{bmatrix} s(z)(1-m(z))G(z',z) & 0 \\ s(z)m(z)G(z',z) & s(z)G(z',z) \end{bmatrix} \begin{bmatrix} n_I(z,t) \\ n_M(z,t) \end{bmatrix} \quad (2.3)$$

and the fecundity kernel, *F*, can be written as

$$\begin{bmatrix} n_I(z', t+1) \\ n_M(z', t+1) \end{bmatrix} = \begin{bmatrix} 0 & p_b(z)b(z)p_r\big(1-m(z')\big)c_0(z') \\ 0 & (z)b(z)p_r m(z')c_0(z') \end{bmatrix} \begin{bmatrix} n_I(z,t) \\ n_M(z,t) \end{bmatrix}. \quad (2.4)$$

The underlying demographic functions for all IPM components are given in Table 2.1 and IPM parameters are given in Table 2.2. The survival function, $s(z)$, is a logistic function with parameters for the slope, $\tau_z$, and intercept at $z = 0.5$, $\tau_{int}$, of a linear function that undergoes the logistic transformation to probability from 0 to 1. The growth function, $G(z', z)$, is a probability density function for size at next census, $z'$, conditional on current size $z$. The growth function has two parameters; the 'pace of growth' parameter, $\gamma_p$, (described in more detail in the following paragraph) and standard deviation, $\gamma_\sigma$. The following vital rates are logistic functions with parameters for slope and intercept; probability of flowering function, $p_b(z)$ with parameters $\beta_z$ and $\beta_a$, and probability of maturation function, $m(z)$ with parameters $\varphi_z$ and $\varphi_a$. The seed production function, $b(z)$, is the exponential of a linear function with two parameters: slope, $\omega_z$, and intercept at $z = 0.5$, $\omega_a$. Size at birth, $c_0(z')$, is a normal distribution with a mean of zero and standard deviation $\vartheta_\sigma$. First-year survival/recruitment is a one parameter constant, $\varepsilon$, constrained from zero, no seeds survive/recruit, to one, where all seeds survive/recruit. The resulting IPM could capture a wide range of life histories and incorporated key demographic processes typical of published IPMs of plant systems (e.g. Kuss et al., 2008; Ramula et al., 2009; Rees & Rose, 2002).

We placed constraints on the IPM parameters to prevent them from describing unrealistic life history strategies (Table 2.2). 'Size' in our model represented a dimensionless measure of development. The probability of survival, probability of flowering and number of offspring produced all increased with size. To prevent plants from having an unrealistic 0% probability of mortality we did not allow the survival probability at any size to exceed 0.99. We defined $z = 0$ as a standardised mean size at birth and $z = 1$ as a standardised size that a surviving plant will converge towards. We implemented this by fixing the linear $z' \sim z$ component of the probability density function to pass through $z = 1, z' = 1$. The slope and intercept parameters are constrained resulting in a single 'pace of growth' parameter, $\gamma_p$. Under this constraint, the pace of growth (or development) is determined by the slope of the expected size function.

# Sampling life history strategies

We sampled IPM parameters that result in an asymptotic growth rate log(λ) ~ 0 using an adaptive Metropolis (AM) algorithm with delayed rejection (Haario et al., 2001) where the target distribution was

$$P(\log(\lambda)) = \prod_{i=1}^{n} \mathcal{N}(\mu, \sigma^2) f_i \quad (2.5)$$

where $n$ is the number of steps in the AM algorithm, $\mathcal{N}$ is a Gaussian distribution with mean $\mu$ and variance $\sigma^2$, and $f_i$ are the constraint distributions. Metropolis algorithms are a Markov chain Monte Carlo (MCMC) method for generating random samples from a probability distribution for which direct sampling is difficult. At each iteration, a candidate parameter set was proposed from the adaptively updated proposal distribution, the corresponding IPM kernel was constructed, and $log(\lambda)$ was calculated from the dominant eigenvalue of the kernel. The acceptance ratio for the accept-reject step was calculated from a target Gaussian density function with a mean of zero, and pseudo-priors (Table 2.2) defined to steer the sampler towards more realistic life histories.

The AM algorithm required informative constraints, $f_i$, to prevent the oversampling of 'immortal' strategies with very high survival and negligible fecundity, and annual monocarpic strategies with very low survival but for high fecundity. These strategies lie at the boundaries of parameter space where the acceptance ratio is essentially constant. Once attained, these strategies lead to very poor mixing of the MCMC chain, preventing the sampler from exploring the whole parameter space. Gaussian priors were fitted on the slope and intercept of the survival function and the slope and intercept of the seed production function (Table 2.2). The AM algorithm was implemented in R using the modMCMC function from R package FME (Soetaert & Petzoldt, 2010). The parameter covariance matrix was re-evaluated every 500 iterations to improve the acceptance rate of proposed parameter sets. The first 25,000 parameter sets were discarded as burn-in to allow the adaptation of the covariance matrix to occur. The remaining parameter sets were thinned to 1000 parameter sets to remove autocorrelation.

# Derived matrix population models

We constructed stage-structured MPMs from each IPM to ensure that we were making a fair comparison between the simulated population model and empirical data from the COMPADRE Plant Matrix Database (Fig. 2.2) It also provided an exploration of the consequences of imposing discrete stage structure on continuously structured populations. The discretisation of the state distribution preserved log(λ) but induced biases in the derived life history metrics. To construct an MPM, the continuous size domain was first divided into contiguous discrete intervals. The mean rate of growth-survival and reproduction were then derived by calculating an expectation with respect to the normalised stable size distribution over each interval.

The discretisation of the growth-survival kernel $P(z', z)$ to the growth-survival matrix **P** with elements $p_{IIij}$ was calculated for transitions from immature individuals to immature individuals as

$$p_{IIij} = s\left(z_{[L_j,U_j]}\right)\left(1 - m\left(z_{[L_i,U_i]}\right)\right) G\left(z'_{[L_i,U_i]}, z_{[L_j,U_j]}\right) = \frac{\int_{L_i}^{U_i}\int_{L_j}^{U_j} n_I(z)s(z)\left(1 - m(z')\right)G(z', z)dzdz'}{\int_{L_j}^{U_j} n_I(z)dz} \quad (2.6)$$

and transitions from immature individuals to mature individuals $p_{MIij}$ was calculated as

$$p_{MIij} = s\left(z_{[L_j,U_j]}\right) m\left(z_{[L_i,U_i]}\right) G\left(z'_{[L_i,U_i]}, z_{[L_j,U_j]}\right) = \frac{\int_{L_j}^{U_j}\int_{L_i}^{U_i} n_I(z)s(z)m(z)G(z', z)dzdz'}{\int_{L_j}^{U_j} n_I(z)dz} \quad (2.7)$$

and transitions from mature individuals to mature individuals $p_{MMij}$ was calculated as

$$p_{MMij} = s\left(z_{[L_j,U_j]}\right) G\left(z'_{[L_i,U_i]}, z_{[L_j,U_j]}\right) = \frac{\int_{L_j}^{U_j}\int_{L_i}^{U_i} n_M(z)s(z)G(z', z)dzdz'}{\int_{L_j}^{U_j} n_M(z)dz} \quad (2.8)$$

where $U_i$ and $L_i$ were the upper and lower size limits of size class $i$, $U_j$ and $L_j$ were the upper and lower size limits of size class $j$ and $n(z)$ was the stable size distribution of the full IPM kernel $K(z', z)$ calculated as the dominant eigenvector. U and L were determined by computing the cumulative stable state distribution of the IPM and calculating size limits that split this distribution into predetermined percentiles.

Similarly, the discretization of the fecundity kernel $F(z', z)$ to fecundity matrix **F** with elements $f_{IMij}$ was calculated for transitions from mature individuals to immature individuals as

$$f_{IMij} = p_b\left(z_{[L_j,U_j]}\right) b\left(z_{[L_j,U_j]}\right) p_r\, c_0\left(z'_{[L_i,U_i]}\right)\left(1 - m\left(z'_{[L_i,U_i]}\right)\right) \quad (2.9)$$

$$= \frac{\int_{L_i}^{U_i}\int_{L_j}^{U_j} n_M(z) p_b(z) b(z) c_0(z')\left(1 - m(z')\right) dz dz'}{\int_{L_j}^{U_j} n_M(z) dz}$$

and calculated for transitions from mature individuals to mature individuals as

$$f_{MMij} = p_b\left(z_{[L_j,U_j]}\right) b\left(z_{[L_j,U_j]}\right) p_r\, c_0\left(z'_{[L_i,U_i]}\right) m\left(z'_{[L_i,U_i]}\right) \quad (2.10)$$

$$= \frac{\int_{L_i}^{U_i}\int_{L_j}^{U_j} n_M(z) p_b(z) b(z) c_0(z') m(z') dz dz'}{\int_{L_j}^{U_j} n_M(z) dz}.$$

The full matrix, **A**, describing all growth, survival and reproductive transitions was calculated as $\mathbf{A} = \mathbf{P} + \mathbf{F}$.

# Life history metrics

For each simulated population model and population model from COMPADRE, we calculated nine life history metrics commonly used in comparative analyses and used in Salguero-Gómez et al. (2016b) (Table 2.3). To apply these calculations to our simulated MPMs we made some alterations to the original calculations outlined here. Three of the following life history metrics are derived from the age-specific survivorship curve $l_a$, and the age-specific fertility trajectory $f_a$. In Salguero-Gómez et al. (2016b), $l_a$ and $f_a$ were calculated from the **P** matrix and the **F** matrix according to Caswell (2001, pp. 118–121) conditional on starting in a single life stage. This was not appropriate for our simulated population models because offspring were born from a size distribution and therefore a single life stage of the discretised MPM could not accurately represent size at birth. In this analysis we calculated $l_a$ and $f_a$ for a cohort of individuals from an initial discrete state distribution $c_j$ , notated as $\widetilde{l_a}$ and $\widetilde{f_a}$. $c_j$ was calculated by the stable stage distribution matrix multiplied by the **F** matrix resulting in the size class distribution of a new cohort of a population operating at its asymptotic stable stage distribution and can be represented as

$$c_j = \sum_{1}^{m} F_j \; w_j \tag{2.11}$$

Where $w_j$ is the stable stage distribution, dominant eigenvector, of $\boldsymbol{A}$ and $m$ is the number of discrete stages.

The *survivorship curve type* describes the shape of decay of survivorship over the lifespan of an individual. The shape of the age-specific survivorship curve is calculated from the age-specific survival $\widetilde{l_a}$ as quantified by Keyfitz' entropy (H) calculated as

$$H = \frac{-\log(\widetilde{l_a})\widetilde{l_a}}{\sum \widetilde{l_a}}. \tag{2.12}$$

Survivorship curves types I, II, and III correspond to $H$ >1, = 1, <1, respectively. *The degree of iteroparity* describes a life history strategy's position between two extremes of reproductive strategy; semelparity is characterised by a single reproductive event before mortality whereas iteroparity is characterised by many reproductive events before mortality. This was calculated in MPMs as the spread of reproduction throughout the lifespan of the individual as quantified by Demetrius' entropy (S) calculated as

$$S = -e^{-\log(\lambda)} \widetilde{l_a}\widetilde{f_a} \log\left(e^{-\log(\lambda)} \widetilde{l_a}\widetilde{f_a}\right) \tag{2.13}$$

where λ was the dominant eigenvalue of the full matrix $A$. High S values correspond to iteroparous strategies whereas low S values correspond to semelparous strategies.

Demographic vital rates summarise population-level transitions between life stages whilst a population has reached a stable stage distribution. The *progressive growth vital rate*, $\gamma$, describes the mean probability of an individual transitioning to a more developed stage once the population has converged to the stable stage distribution. $\gamma$ is calculated from an MPM as

$$\gamma = \sum_{1}^{m} P'_{i,j} \; w_j|_{i<j} \tag{2.14}$$

where $P' = P/s_j$, $s_j$ is the stage-specific survival, $w_j$ is the stable stage distribution and m is the number of classes in the MPM. The *retrogressive growth vital rate*, $\rho$, describes the mean probability of transitioning to a less developed stage once the population has converged to the stable stage distribution. The retrogressive growth rate is calculated from an MPM as

$$\rho = \sum_{1}^{m} P'_{i,j}\ \bar{w}_j|_{i>j} \tag{2.15}$$

where $P' = P/s_j$, $s_j$ is the stage-specific survival and $w_j$ is the stable stage distribution. *Mean sexual reproduction*, Φ, describes the mean year to year per-capita number of sexual reproductive events once the population has converged the stable stage distribution and is calculated as

$$\emptyset = \sum_{1}^{m} F_j\ w_j\ . \tag{2.16}$$

*Net reproductive rate*, $R_0$, describes the mean number of recruits produced during the mean life expectancy of an individual in the population

$$R_0 = \int_0^{\infty} \tilde{l_a}\tilde{f_a} dx\ . \tag{2.17}$$

*Generation time*, *T*, is a measure of population turn-over; the number of years necessary for the individuals of a population to be fully replaced by new ones. Generation time (*T*) is calculated as

$$T = \frac{\log(R_0)}{\log\ (\lambda)}. \tag{2.18}$$

*Age at maturity*, $L_{\alpha,}$ is the number of years that it takes an average individual in the population to enter a mature life stage, defined as one in which an individual can potentially reproduce. *Mature life expectancy*, $L_{w,}$ is the log ratio of mean age at sexual maturity ($L_\alpha$) and the mean life expectancy (ηe) of an individual in the population and is calculated as $L_w = \log(\eta_e) - \log(L_\alpha)$.

## Demographic data

Demographic data were used to characterise the MPM intervals used to discretise the simulated IPMs to MPMs. This ensured that they exhibited realistic MPM dimensions and stable stage distributions (Fig. 2.2). We used the COMPADRE Plant Matrix Database (version 4.0.1) for this purpose; however, to ensure we were making reasonable comparisons to our simulated population models, only a subset of COMPADRE was used. Only MPMs with size-classified discrete stages were included and all woody species were excluded because they generally exhibit low variation in growth trajectories (Zuidema et al., 2010). MPMs that used secondary state variables, such as flowering, were excluded because size was the only state variable in our model. Only MPMs with a matrix projection interval of one year were used to be consistent with the time interval of our IPM. MPMs with clonal reproduction were not included because the only form of reproduction in the IPM was sexual reproduction. MPMs that were subject to an experimental treatment were not used. A by-product of this selection process was the deselection of annual monocarpic plants. One MPM was calculated per species capturing the average population dynamics; the spatial and temporal element-wise arithmetic mean average of all unmanipulated years and sites available in COMPADRE. This produced a sample of 95 MPMs, which we hereafter refer to as our COMPADRE subset.

## Dimension reduction via PCA

Principal component analysis (PCA) was carried out on life history metrics calculated for each set of MPMs to determine the key axes of (co)variation. Due to the irreducibility and ergodicity of some MPMs in COMPADRE (Stott et al., 2010b), the calculation of a demographic metric may result in an NA or infinite value. These values were imputed using the 'regularised' method in the imputePCA function of R package missMDA (Josse & Husson, 2016) to maximise sample size. Generation time (T), mean sexual reproduction (Φ), survivorship curve type (H), age at sexual maturity $L_\alpha$ and $R_0$ were log-transformed, then all life history metrics were scaled to unit variance and mean-centred. The sign of scores and loadings in PCA are arbitrary; however, to allow comparison we inverted scores and loadings to ensure consistency, if required. When PCAs were carried out on multiple simulates,

rotations and weightings were inverted, if needed, so that the life history metrics associated with each principal component fit with recognised patterns; mean sexual reproduction was always negatively loaded on PC1, mature life expectancy was always negatively loaded on PC2.

## Investigating the effects of sampling variation and density-dependent constraints

To investigate how the amount of sampling variation affects the composition of PC1+2 we compared simulated population models sampled from Gaussian $\log(\lambda)$ distributions with a range of standard deviations but a constant mean and distributions with a range of means but a constant SD. The first set, the standard deviations of the target $\log(\lambda)$ distributions, $\log(\lambda)_\sigma$, ranged from 0.01 to 0.1 and the mean of the target $\log(\lambda)$ distributions, $\log(\lambda)_\mu$, was 0. For the second set the standard deviation, $\log(\lambda)_\sigma$, was 0.1 and the values for the mean $\log(\lambda)_\mu$ were between -0.5 and 0.5. For reference, the COMPADRE subset had $\log(\lambda)_\sigma = 0.134$ and $\log(\lambda)_\mu = 0.01$.

Each resulting set of IPM parameters were thinned to 1000 parameter sets and discretised to MPMs with the same ratio of matrix dimensions and stable stage distributions as observed in the COMPADRE subset. PCAs were carried out on each set of MPMs, including the COMPADRE subset. The COMPADRE subset was bootstrapped 1000 times to observe intervals. To visualise the composition of the first two principal components we produced a biplot of each of the resulting PCAs. For each PCA we calculated the weighted rotation of each life history metric; the weighted rotation is the rotation of a life history metric towards a PC, weighted by the proportion of variance explained by the respective PC.

# Results

In our PCA of a COMPADRE subset, 60% of variation in the nine life history metrics were captured by the first two principal components (Fig. 2.4). Positive values on the first principal component (40% variance explained) represent less reproductive, slower growing and later maturing, semelparous strategies. Positive values on the second principal component (20% of variance explained) represent greater mature life expectancy and less retrogressive growth. The life history metrics most strongly weighted towards PC1 were degree of iteroparity (0.50), mean sexual reproduction (-0.45), progressive growth (-0.39) and R0 (-0.38). The life history metrics most strongly weighted towards PC2 were mean age at maturity (0.67), R0 (0.37), progressive growth (-0.35) and retrogressive growth (-0.37). Bootstrapped confidence intervals highlighted the uncertainty in the weighted rotations of derived life history metrics in the COMPADRE PCA, with considerable overlap for PC2 (Fig. 2.5). For PC1, degree of iteroparity and generation time, mean sexual reproduction, R0 and progressive growth had the most robust weighted rotations with the smallest bootstrapped intervals.

The distributions of life history metrics (Fig. 2.3) and the resulting PCA axes (Fig. 2.4 B) from the simulated populations resembled those associated with the population models from our COMPADRE subset. Simulated population models sampled from a target log(λ) distribution with a standard deviation of 0.2 and a mean of 0 produced a similar log(λ)distribution to our COMPADRE subset and represented our best simulated analogue to the COMPADRE subset. Simulated population models showed, on average, more retrogressive growth, and more progressive growth, and thus reduced stasis than the population models in COMPADRE. Simulated population models also showed less variance in R0, despite similar variance in log(λ). Our COMPADRE subset and simulated population models exhibit clear non-linear constraints between life history metrics (Fig. 2.3). Projecting log(λ) onto the PCA space shows a clear trend of log(λ) across the PCA space which is positively associated with $R_0$.

Increasing the standard deviation of the target log(λ) distribution altered the relative contributions of some life history metrics to the first two principal components in simulated population models (Fig. 2.5). As the standard deviation of the target log(λ) increased, R0 became more important on PC1,

survivorship curve type and mean age at maturity became less important. The importance of other life history metrics did not change for PC1. As for PC2, as the standard deviation of the target $\log(\lambda)$ increased, mean age at maturity and progressive growth became more important towards PC2. Changes in $\log(\lambda)_{\sigma}$ did not consistently affect the weighting towards either PC1 or PC2 of mean sexual reproduction, degree of iteroparity, generation time and retrogressive growth.

Sampling simulated MPMs using target $\log(\lambda)$ distribution with a non-zero mean produced principal components with life history metrics weighted differently on each axis (Fig. 2.5). The most observable difference is in $R_0$; at $\log(\lambda)_{\mu}$ = -1 $R_0$ is strongly negatively weighted on PC1 whereas at $\log(\lambda)_{\mu}$ = 1 $R_0$ is strongly positively weighted on PC1. Progressive growth and retrogressive growth saw some change for different values of $\log(\lambda)_{\mu}$. Generation time and survivorship curve type and mean age at maturity did not show much change across different values of $\log(\lambda)_{\mu}$ for PC1 or PC2.

# Discussion

At the core of life history theory is the idea that an organism's finite energy budget constrains the allocation of effort toward the processes of growth, survival and reproduction (Stearns, 1992). Because quantifying such trade-offs is extremely challenging under natural conditions (Reich, 2014; Wenk & Falster, 2015), comparative approaches are often used to explore patterns of life history (co)variation between species (Jervis et al., 2001; Rochet, 2000; Sæther & Bakke, 2007; Stearns, 1983). Comparative analysis of stage-based MPMs has the potential to reveal these key axes of life history variation (Franco & Silvertown, 1996; Salguero-Gómez et al., 2016b). A robust life history classification framework should reflect the underlying budgetary trade-offs rather than non-adaptive constraints. We simulated MPM-derived life history strategies in the absence of budgetary constraints but mimicked the consequences of density dependence by restricting the log asymptotic population growth rate, $\log(\lambda)$, to have a mean of 0. This constraint on $\log(\lambda)$ was representative of population densities fluctuating around a carrying capacity. When we decomposed the resulting life history 'strategies' using PCA, we found that the composition of the first two principal components is broadly similar to PCA results for the COMPADRE database (Salguero-Gómez et al., 2016b). This indicates that a significant component of the covariance among MPM-derived life histories is consistent with non-adaptive constraints on these patterns.

If the principal components do not capture pure budgetary trade-offs, how should they be interpreted? The interpretation by (Salguero-Gómez et al., 2016b) implies that the emerging fast-slow axis in a PCA of MPM-derived life history traits is further evidence for a fast-slow continuum that describes life histories along an axis of allocation towards reproduction to high allocation to survival. We show in this work that this form of analysis cannot be used as evidence for the presence/absence of a life history axis based on energetic allocation. Instead, these axes, and the axes of similar studies (Capdevila et al., 2019; Healy et al., 2019; Paniw et al., 2018), must be interpreted with an appreciation that patterns of life history covariance may arise from a range of factors: fundamental budgetary trade-offs, non-adaptive constraints, or environmental effects. Interpretation of the principal components is speculative

at best when using only demographic data from published population models because these data cannot differentiate the different underlying factors of these patterns of life history covariance. Fundamentally, some degree of correlation between life history metrics is expected, given that the assumption of density dependence requires demographic trade-offs between survival and reproduction to support a persistent population (Sutherland et al., 1986). As such, dimension reduction tools like PCA will always find axes of variation and we should be careful not to prescribe our preferred interpretation onto those axes. Therefore, interpretation of these analyses cannot simply highlight the presence of correlations as an interesting result, they must go further to interrogate these correlations to understand their underlying drivers.

This research has implications on how we link the covariance patterns of life history metrics to other data. Salguero-Gómez (2017) showed that the position of a population on the first two axes predicted its asymptotic growth rate but we observe similar patterns using the simulated strategies. When projecting metrics of population performance (e.g. $\lambda$ or measures of transient growth) onto the life history PCA space, the resulting associations should be interpreted with care. Our work shows that the PCA axes are a composite of life history strategy and population performance because the MPM derived life history metrics are not independent of MPM derived population performance. Given our findings, we can say that this correlation between life history and population performance is an innate feature arising from a combination of non-adaptive constraints, environmental variation, and sampling variation in $\lambda$, rather than an indication that some life histories are of greater fitness than others. In another example, Adler et al. (2014) found that functional traits directly affected only a limited set of physiological processes and demographic rates but still explained considerable variation in overall life history. In addition to the mechanistic explanations offered, an alternative explanation for the strength of this link may be that there is less possible (co)variation in life history under non-adaptive constraints. As such, a functional trait only requires a correlation with one life history metric for it to subsequently account for a large proportion of (co)variation in life history.

The consequences of imperfect sampling of environments, parameter uncertainty and model structure are difficult to assess directly (Knape & de Valpine, 2012) because published population models are

not perfect representations of real systems. However, our simulated population model framework provides a novel approach to testing these assumptions. Sampling variation is especially a concern in demographic data because of the extensive temporal replication required for reliable long-term performance estimates (Metcalf et al., 2015). When the majority of demographic data sets are <5 years (Menges, 2000) it is imperative to understand the role of sampling error in shaping the patterns of life history covariance. By assuming that persistent populations are constrained such that $\log(\lambda) \approx 0$ and sampling sets of models with different magnitudes of between-model variance in $\log(\lambda)$ we emulated the consequences of varying the level of sampling variation. Our results showed that the magnitude of sampling error did not substantially affect the composition of the life history PC1 and PC2. Therefore, within the variance range, we explored our work indicates that the presence of this variance not a key factor in shaping covariance patterns in MPM-derived metrics. However, we do see that the mean value of lambda severely impacts the covariance patterns of MPM derived metrics. One of the reasons the variance in $\log(\lambda)$ has a negligible impact may be the predominant influence of the $\log(\lambda) \approx 0$ constraint limiting how life history metrics can co-vary. However, an important assumption here is that in our simulated population models the distribution of growth rates is independent of any factors of life history or environment. Populations are disproportionately modelled when they are invasive or endangered because of the need to produce models to inform management (Crone et al., 2011; Jelbert et al., 2015). These sorts of biases will need to be considered when interpreting comparative analyses.

Going forward, we can use the simulated population model as a null model in comparative work and more constrained setting such as multiple populations of a single species. A null model is a general tool used across scientific disciplines: it is a pattern-generating routine that aims to hold some features of a dataset constant while allowing others to vary that can then be compared to an empirical dataset (Gotelli & Graves, 1997). We could also use the null model to explore links between different population-level metrics. For example, further investigating the links between life history and transient dynamics (Stott et al., 2010a). An advantage of using a simulated population model approach would be that some of the issues of MPM, such as construction errors (Kendall et al., 2019) and spatial/taxonomic sampling biases (Salguero-Gómez et al., 2015, 2016a), could be dismissed as explanatory factors, whilst being able to

interrogate many of the same research questions. This approach could also be applied to research on a single species, such as PlantPopNet (Buckley et al., 2014) a globally distributed population study of *Plantago lanceolata*. Adapting the approach to a single species setting would involve constraining the underlying IPM to reflect a more limited range of life histories plausible for the target species, but with added realism through time-variant vital rates. This would provide a baseline from which we could identify areas in the possible life history space that are not occupied by real populations. With this approach, we could investigate how evolution and/or environmental effects are constraining the range of possible life histories, against the background of non-adaptive constraints.

Ultimately, how we use comparative analysis of demographic data to explore patterns of life histories depends on our definition of 'life histories'. Sutherland et al., (1986) suggested over three decades ago that life histories "may be more profitably viewed as consequences of [organisms'] actions (which may be evolved strategies), environmental effects and demographic constraints". Given this view, demographic data should remain as a useful resource to describe life histories, on the condition that environmental factors and demographic constraints are incorporated into the interpretation. Here we have provided a framework for exploring how demographic non-adaptive constraints affect patterns of life history covariance and showed that comparative work determining differences across species and populations will be subject to the effects of non-adaptive constraints. Comparative approaches using demographic data may hold valuable insights into ecology, population biology and demography, but we have shown that an understanding of non-adaptive constraints will be vitally important for gaining those insights.

# Acknowledgements

This research was supported by the Centre for Advanced Biological Modelling funded by the Leverhulme Trust. We thank the COMPADRE Plant Matrix Database team, supported by the Max Planck Institute for Demographic Research (MPIDR), for data digitalization and error-checking.

# References

Adler, P. B., Salguero-Gómez, R., ., Compagnoni, A., Hsu, J. S., Ray-Mukherjee, J., … Franco, M. (2014). Functional traits explain variation in plant life history strategies. *Proceedings of the National Academy of Sciences*, *111*(2), 740–745.

Brook, B. W., & Bradshaw, C. J. A. (2006). Strength of evidence for density dependence in abundance time series of 1198 species. *Ecology*, *87*(6), 1445–1451.

Buckley, Y. M., Blomberg, S. P., Csergo, A., Ehrlén, J., Gonzalez, M. B., Garcia, … Wardle, G. M. (2014). PlantPopNet: A Spatially Distributed Model System for Population Ecology. *Ecology Society of Australia 2014 Annual Conference*.

Capdevila, P., Beger, M., Blomberg, S. P., Hereu, B., Linares, C., & Salguero-Gómez, R. (2019). Aquatic and terrestrial organisms display contrasting life history strategies as a result of environmental adaptations. *BioRxiv*.

Caswell, H. (2001). *Matrix population models*. (L. John Wiley & Sons, Ed.).

Crone, E. E., Menges, E. S., Ellis, M. M., Bell, T., Bierzychudek, P., Ehrlén, J., … Williams, J. L. (2011). How do plant ecologists use matrix population models? *Ecology Letters*, *14*(1), 1–8.

Ellner, S. P., Childs, D. Z., & Rees, M. (2016). General Deterministic IPM. In *Data-driven Modelling of Structured Populations: A Practical Guide to the Integral Projection Model* (pp. 139–185).

Franco, M., & Silvertown, J. (1996). Life history variation in plants : An exploration of the fast-slow continuum hypothesis. *Philosophical Transactions of the Royal Society B: Biological Sciences*, *351*(1345), 1341–1348.

Gotelli, N. J., & Graves, G. R. (1997). *Null Models in Ecology. Ecology* (Vol. 78). Cambridge.

Grime, J. P. (1977). Evidence for the existence of three primary strategies in plants and its relevance to ecological and evolutionary theory. *The American Naturalist*, *111*(982), 1169–1194.

Haario, H., Saksman, E., & Tamminen, J. (2001). An adaptive Metropolis algorithm. *Bernoulli*, *7*(2), 223.

Healy, K., Ezard, T. H. G., Jones, O. R., Salguero-Gómez, R., & Buckley, Y. M. (2019). Animal life history is shaped by the pace of life and the distribution of age-specific mortality and reproduction.

*Nature Ecology and Evolution*, *3*(8), 1217–1224.

Janovský, Z., Herben, T., & Klimešová, J. (2017). Accounting for clonality in comparative plant demography – growth or reproduction? *Folia Geobotanica*, *52*(3–4), 1–10.

Jelbert, K., Stott, I., Mcdonald, R. A., & Hodgson, D. (2015). Invasiveness of plants is predicted by size and fecundity in the native range. *Ecology and Evolution*, *5*(10), 1933–1943.

Jervis, M., Heimpel, G., Ferns, P., Harvey, J., & Kidd, N. (2001). Life-history strategies in parasitoid wasps: A comparative analysis of "ovigeny." *Journal of Animal Ecology*, *70*(3), 442–458.

Josse, J., & Husson, F. (2016). missMDA : A Package for Handling Missing Values in Multivariate Data Analysis. *Journal of Statistical Software*, *70*(1), 1–31.

Kalisz, S., & McPeek, M. A. (1992). Demography of an age-structured annual: resampled projection matrices, elasticity analyses, and seed bank effects. *Ecology*, *73*(3), 1082–1093.

Kendall, B. E., Fujiwara, M., Diaz-Lopez, J., Schneider, S., Voigt, J., & Wiesner, S. (2019). Persistent problems in the construction of matrix population models. *Ecological Modelling*, *406*(June), 33–43.

Knape, J., & de Valpine, P. (2012). Are patterns of density dependence in the Global Population Dynamics Database driven by uncertainty about population abundance? *Ecology Letters*, *15*(1), 17–23.

Kreft, H., & Jetz, W. (2007). Global patterns and determinants of vascular plant diversity. *Proceedings of the National Academy of Sciences*, *104*(14), 5925–5930.

Kuss, P., Rees, M., Ægisdóttir, H. H., Ellner, S. P., & Stöcklin, J. (2008). Evolutionary demography of long-lived monocarpic perennials: A time-lagged integral projection model. *Journal of Ecology*, *96*(4), 821–832.

Lande, R., Engen, S., Sæther, B. E., Filli, F., Matthysen, E., & Weimerskirch, H. (2002). Estimating density dependence from population time series using demographic theory and life-history data. *American Naturalist*, *159*(4), 321–337.

MacArthur, R., & Wilson, E. O. (1967). *The Theory of Island Biogeography*. Princeton University Press.

McDonald, J. L., Franco, M., Townley, S., Ezard, T. H. G., Jelbert, K., & Hodgson, D. J. (2017).

Divergent demographic strategies of plants in variable environments. *Nature Ecology and Evolution*, *1*(2), 0029.

Menges, E. S. (2000). Population viability analyses in plants: Challenges and opportunities. *Trends in Ecology and Evolution*, *15*(2), 51–56.

Metcalf, C. J. E., Ellner, S. P., Childs, D. Z., Salguero-Gómez, R., Merow, C., Mcmahon, S. M., … Rees, M. (2015). Statistical modelling of annual variation for inference on stochastic population dynamics using Integral Projection Models. *Methods in Ecology and Evolution*, *6*(9), 1007–1017.

Metcalf, C. J. E., & Pavard, S. (2007). Why evolutionary biologists should be demographers. *Trends in Ecology and Evolution*, *22*(4), 205–212.

Meyer, J. S., Ingersoll, C. G., McDonald, L. L., & Boyce, M. S. (1986). Estimating uncertainty in population growth rates: jackknife vs. bootstrap techniques. *Ecology*, *67*(5), 1156–1166.

Paniw, M., Ozgul, A., & Salguero-Gómez, R. (2018). Interactive life-history traits predict sensitivity of plants and animals to temporal autocorrelation. *Ecology Letters*, *21*(2), 275–286.

Parry, G. D. (1981). The meanings of r- and K-selection. *Oecologia*, *48*, 260–264.

Picard, N., & Liang, J. (2014). Matrix models for size-structured populations: Unrealistic fast growth or simply diffusion? *PLoS ONE*, *9*(6), e98254.

Ramula, S., Rees, M., & Buckley, Y. (2009). Integral projection models perform better for small demographic data sets than matrix population models: A case study of two perennial herbs. *Journal of Applied Ecology*, *46*(5), 1048–1053.

Rees, M., & Rose, K. E. (2002). Evolution of flowering strategies in Oenothera glazioviana: an integral projection model approach. *Proceedings of the Royal Society B: Biological Sciences*, *269*(1499), 1509–1515.

Reich, P. B. (2014). The world-wide "fast-slow" plant economics spectrum: A traits manifesto. *Journal of Ecology*, *102*(2), 275–301.

Rochet, M.-J. (2000). A comparative approach to life-history strategies and tactics among four orders of teleost fish. *Journal of Marine Science*, *57*, 228–239.

Sæther, B.-E., & Bakke, Ø. (2007). Avian life history variation and contribution of demographic traits to the population growth rate. *Ecology*, *81*(3), 642–653.

Salguero-Gómez, R. (2017). Applications of the fast-slow continuum and reproductive strategy framework of plant life histories. *New Phytologist*, *213*(4), 1618–1624.

Salguero-Gómez, R., & Casper, B. B. (2010). Keeping plant shrinkage in the demographic loop. *Journal of Ecology*, *98*(2), 312–323.

Salguero-Gómez, R., Jones, O. R., Archer, C. R., Bein, C., de Buhr, H., Farack, C., … Vaupel, J. W. (2016a). COMADRE: A global data base of animal demography. *Journal of Animal Ecology*, *85*(2), 371–384.

Salguero-Gómez, R., Jones, O. R., Archer, C. R., Buckley, Y. M., Che-Castaldo, J., Caswell, H., … Vaupel, J. W. (2015). The compadre Plant Matrix Database: An open online repository for plant demography. *Journal of Ecology*, *103*(1), 202–218.

Salguero-Gómez, R., Jones, O. R., Jongejans, E., Blomberg, S. P., Hodgson, D. J., Mbeau-Ache, C., … Buckley, Y. M. (2016b). Fast-slow continuum and reproductive strategies structure plant life-history variation worldwide. *Proceedings of the National Academy of Sciences of the United States of America*, *113*(1), 230–235.

Salguero-Gómez, R., & Plotkin, J. B. (2010). Matrix dimensions bias demographic inferences: Implications for comparative plant demography. *The American Naturalist*, *176*(6), 710–722.

Sibly, R. M., Barker, D., Denham, M. C., Hone, J., & Pagel, M. (2005). On the regulation of populations of mammals, birds, fish, and insects. *Science*, *309*, 607–610.

Sibly, R. M., Barker, D., Hone, J., & Pagel, M. (2007). On the stability of populations of mammals, birds, fish and insects. *Ecology Letters*, *10*(10), 970–976.

Silvertown, J., Franco, M., ., & McConway, K. (1992). A demographic interpretation of grime's triangle. *Functional Ecology*, *6*(2), 130.

Soetaert, K., & Petzoldt, T. (2010). Inverse modelling, sensitivity and Monte Carlo analysis in R using package FME. *Journal of Statistical Software*, *33*(3), 1–28.

Stearns, S. C. (1983). The influence of size and phylogeny on patterns of covariation among life-history traits in the mammals. *Oikos*, *41*(2), 173.

Stearns, S. C. (1992). *The evolution of life histories*. Oxford: Oxford University Press.

Stott, I., Franco, M., Carslake, D., Townley, S., & Hodgson, D. (2010a). Boom or bust? A comparative

analysis of transient population dynamics in plants. *Journal of Ecology*, *98*(2), 302–311.

Stott, I., Townley, S., Carslake, D., & Hodgson, D. J. (2010b). On reducibility and ergodicity of population projection matrix models. *Methods in Ecology and Evolution*, *1*(3), no-no.

Sutherland, W. J., Grafen, A., & Harvey, P. H. (1986). Life history correlations and demography. *Nature*.

Wenk, E. H., & Falster, D. S. (2015). Quantifying and understanding reproductive allocation schedules in plants. *Ecology and Evolution*, *5*(23), 5521–5538.

Zuidema, P., Jongejans, E., Chien, P. D., During, H. J., & Schieving, F. (2010). Integral Projection Models for trees: a new parameterization method and a validation of model output. *Journal of Ecology*, *98*(2), 345–355.

# Figures

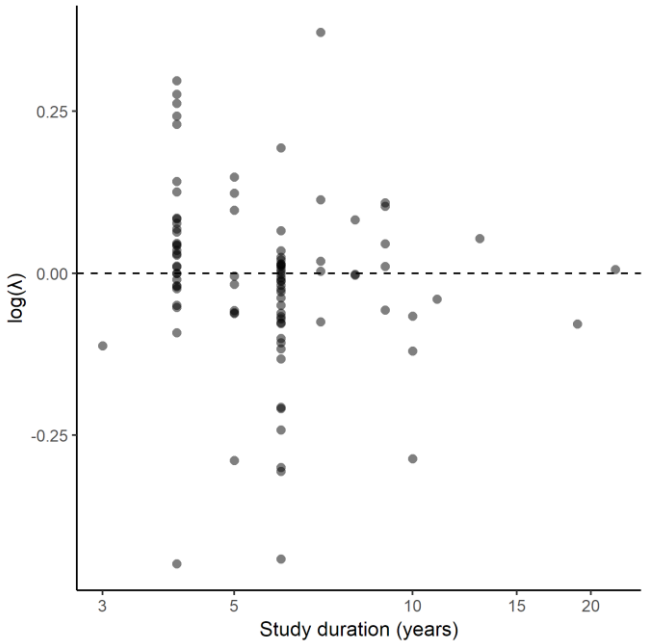


**Figure 2.1: Evidence to suggest that matrix populations constructed from demographic data with a longer study period have a log(λ) closer to zero.** The COMPADRE Plant Matrix Database is a repository for published matrix population models (MPMs) for plants. MPMs are constructed from a number of annual transitions. The longer the study duration, the more annual transitions can be used to construct a temporal mean. Each point represents the temporal mean MPM calculated from the element-wise mean of all MPMs constructed for all years. λ is calculated from the temporal mean MPM as the dominant eigenvalue and represents the predicted asymptotic growth rate.

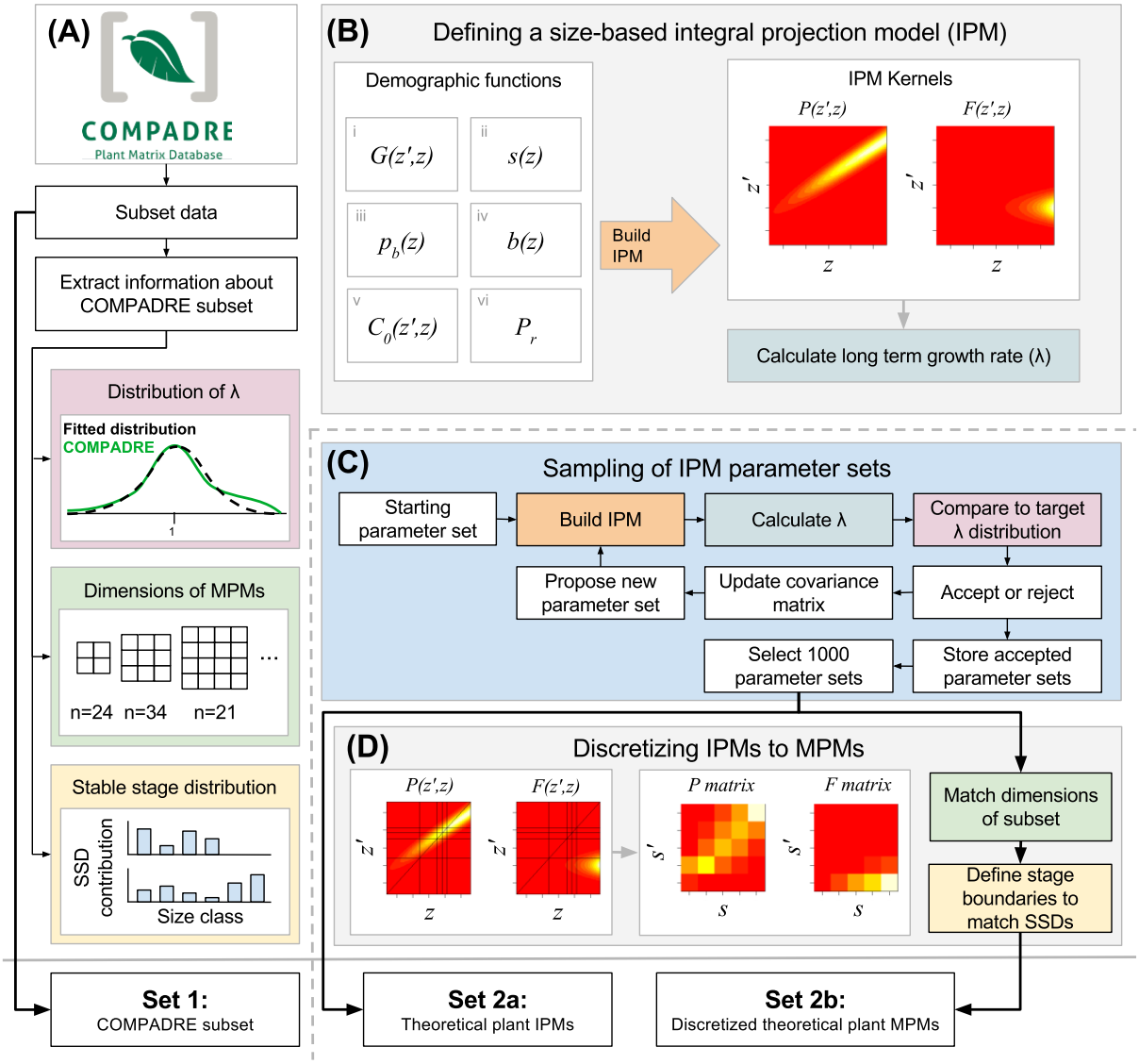


**Figure 2.2: Overview of methods for simulating plausible plant life history strategies with integral projection models (IPMs) discretised to matrix population models (MPMs).** Shared coloured boxes indicate when information from a subset of the COMPADRE plant matrix database (A) and IPM methods (B) are used in the sampling of IPM parameter sets (C) and discretization to MPMs (D). The distribution of long-term growth rate values log(λ) (pink box), the frequencies of dimensions of MPMs (green box) and the stable stage distributions (SSDs) (yellow box) are extracted from the COMPADRE subset. A size-based integral projection model (IPM) is defined (B) with demographic functions of size z; growth (i), survival (ii), flowering probability (iii), seed production (iv), size at birth (v) and recruitment probability (vi). These functions are used to construct a survival kernel *P(z',z)* and a fecundity kernel *F(z',z)* which can be used to calculate log(λ) (pink box). An adaptive Metropolis (AM)

algorithm with delayed rejection was used to sample IPM parameter sets to match a Gaussian distribution fitted to the log(λ) distribution of the COMPADRE subset (C). Set 1 is the COMPADRE MPM subset. Set 2a is the sampled IPM parameter sets, set 2b is the IPMs from set 2a discretized to MPMs with survival matrix (*P*) and fecundity matrix (*F*) with states *s* where frequencies of matrix dimension and SSD match set 1.

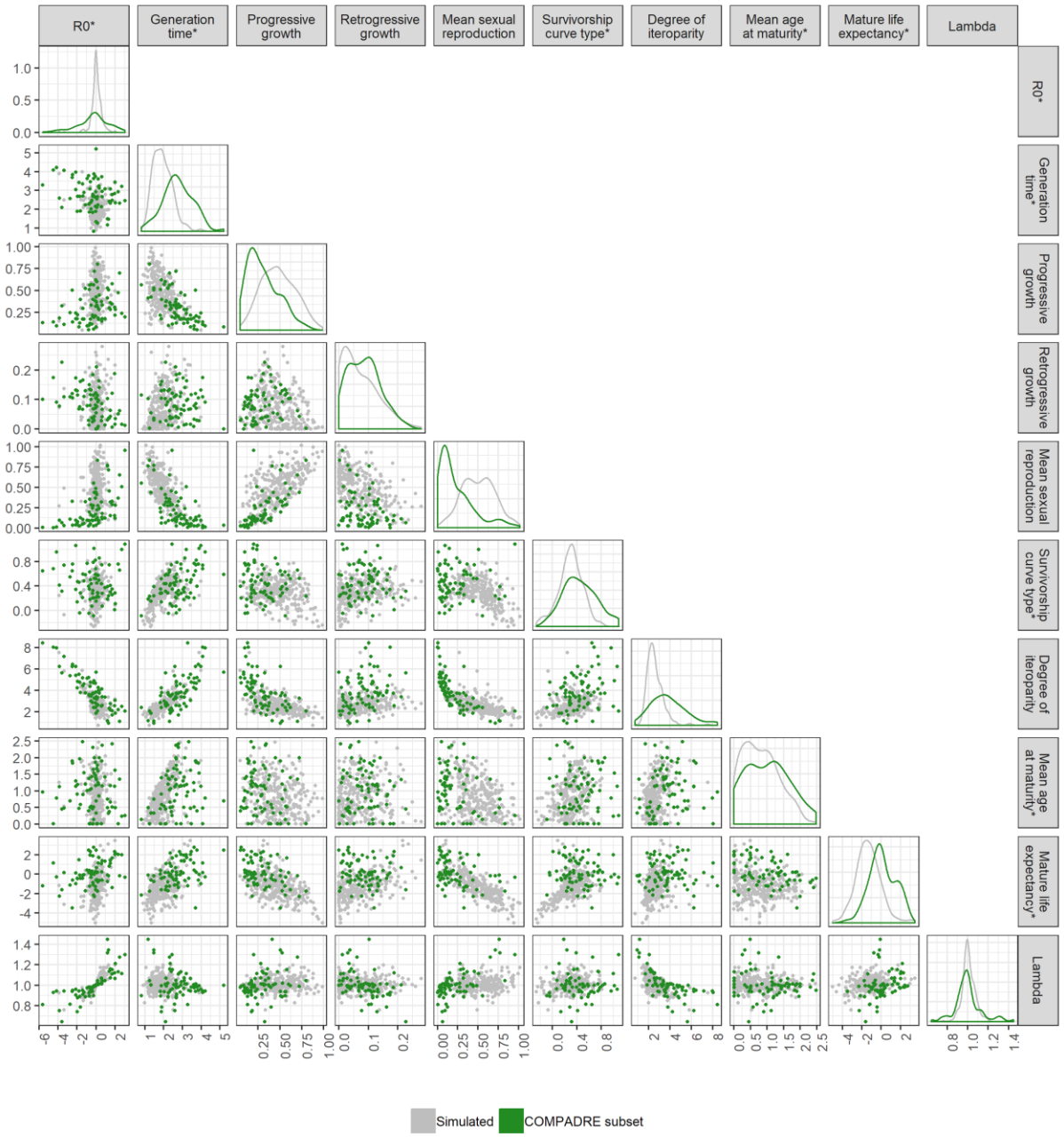


**Figure 2.3: overlap in (co)variance patterns of MPM-derived life history metrics from a subset of size-classified MPMs from the COMPADRE Plant Matrix Database compared to simulated MPMs.** Diagonal plots show the distribution of each metric and sub diagonal plots show the correlation between metrics. The final row shows the relationship between each life history metric and the long-term growth rate, lambda ($\lambda$). Life history metrics with a * next to their name (R0, survivorship curve type, mean age a maturity, mature life expectancy) have been $\log_{10}$ transformed.

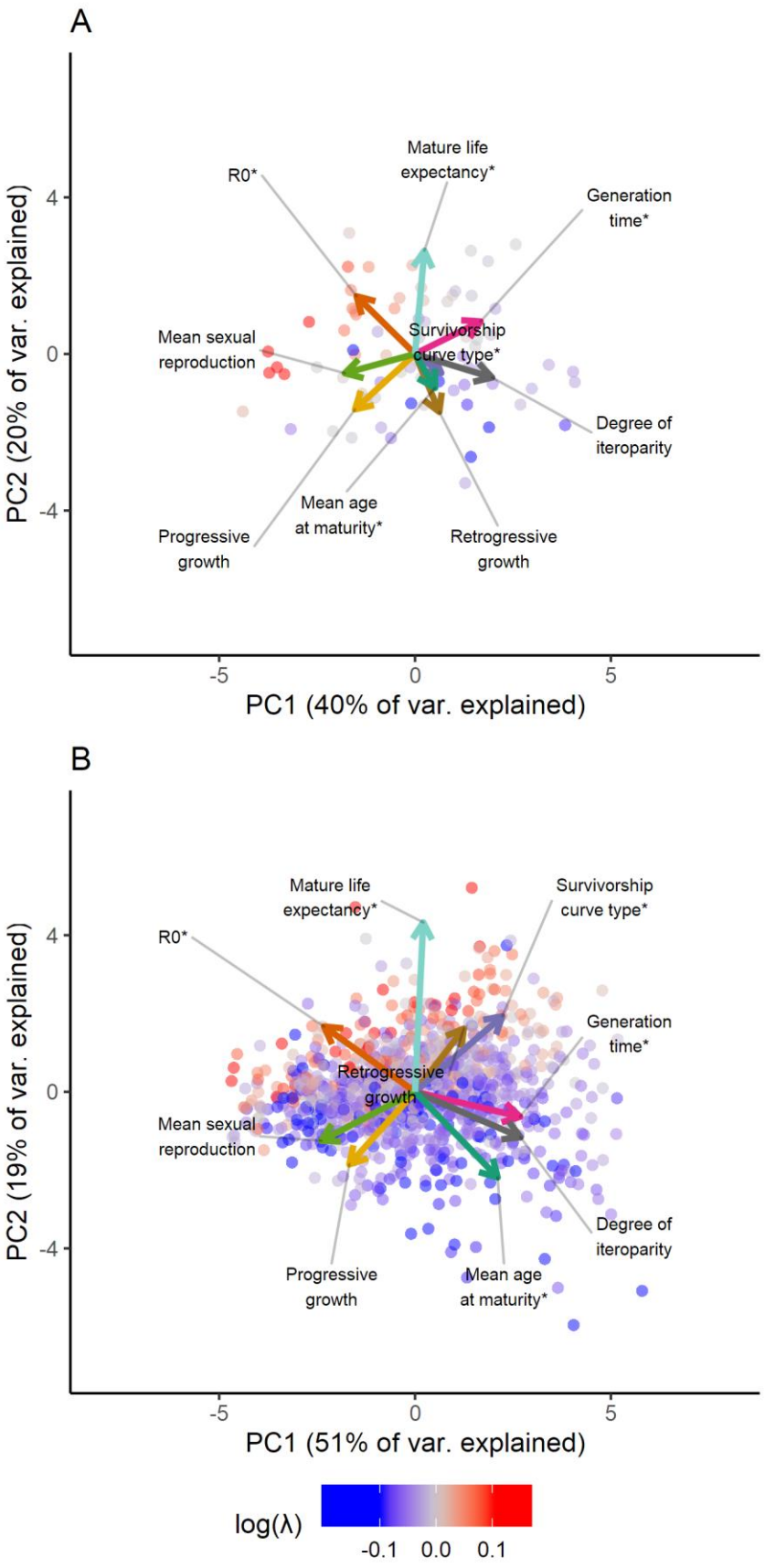
A
Mature life expectancy*
R0*
Generation time*
Mean sexual reproduction
Survivorship curve type*
Degree of iteroparity
Mean age at maturity*
Progressive growth
Retrogressive growth
PC2 (20% of var. explained)
PC1 (40% of var. explained)
B
Mature life expectancy*
Survivorship curve type*
R0*
Generation time*
Retrogressive growth
Mean sexual reproduction
Degree of iteroparity
Progressive growth
Mean age at maturity*
PC2 (19% of var. explained)
PC1 (51% of var. explained)
log(λ)
-0.1 0.0 0.1

**Figure 2.4: Principal component axes from a PCA of life history traits derived from simulated population models compared to a PCA of COMPADRE Plant Matrix Database.** This PCA was carried out on nine life history metrics derived from two sets of matrix population models (MPMs). The first set of MPMs (A) is a subset of 95 MPMs from the COMPADRE Plant Matrix Database. The second set of MPMs (B) is simulated population models sampled from a log(λ) distribution that closely resembles the log(λ) distribution of the COMPADRE subset in A. Arrow length and direction indicates the loading of each life history metric onto the PCA axes. Points represent the position of individual MPMs along the first and second principal components. Colour represents the log(λ) value of each MPM.

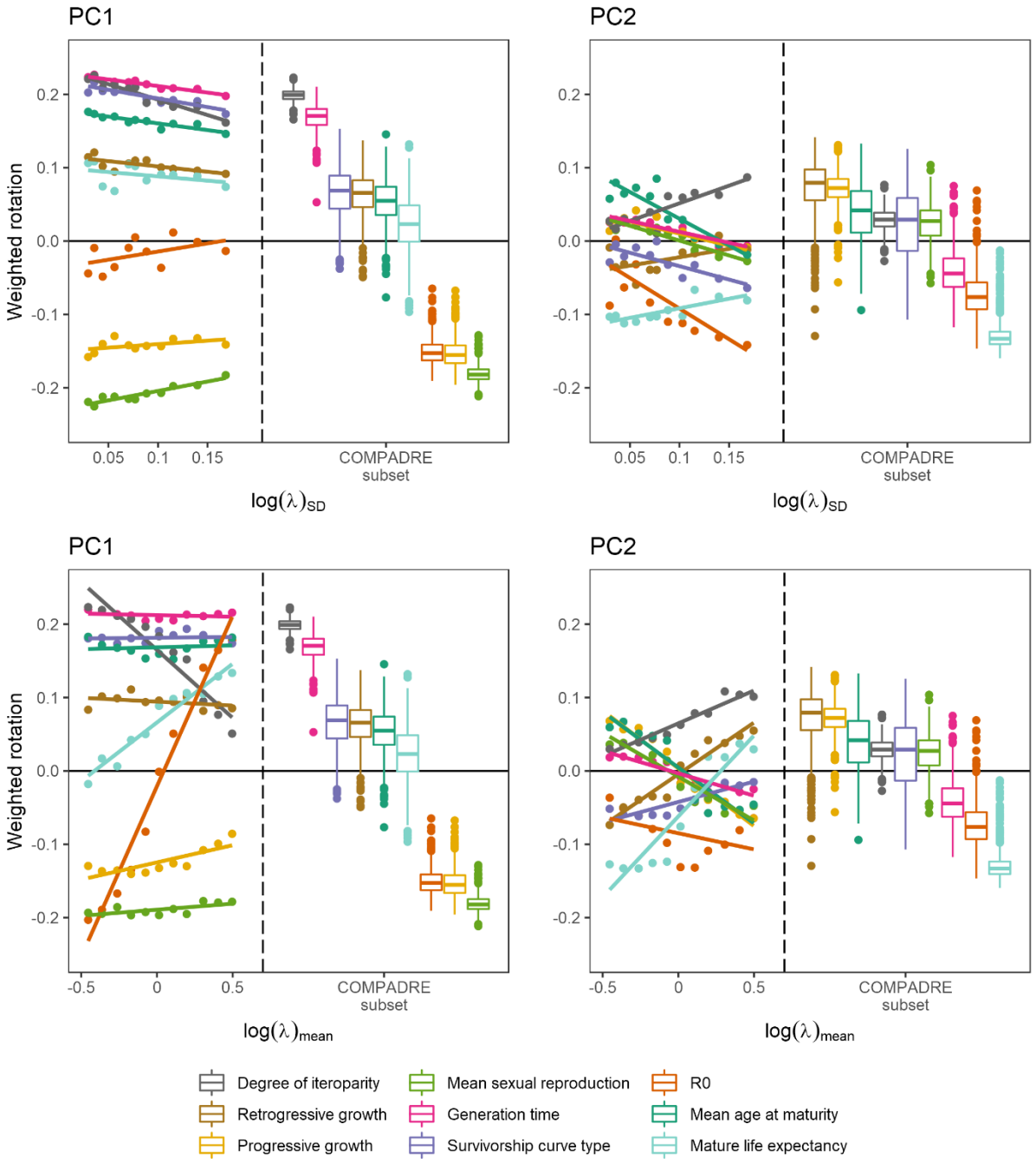


**Figure 2.5: The variance and mean of the log(λ) distribution of simulated population models affects the composition of principal components resulting from a principal component analysis (PCA) of 9 derived life history metrics.** A PCA was carried out on nine life history metrics derived from multiple sets of simulated population models in the form of matrix population models (MPMs). The first set of simulated MPMs (first row) was sampled from Gaussian log(λ) distributions with a mean of one and standard deviations from 0.01 to 0.1. The second set of simulated MPMs (second row) was sampled from Gaussian log(λ) distributions with a standard deviation of 0.1 and means from -0.5 to 0.5.

From each PCA result, we extracted the weighted rotation of each life history metric: the rotation towards a principal component (values ranging from -1 to 1) multiplied by the proportion of variance explained by the corresponding principal component (values ranging from 0 to 1). To the right hand of each plot we have included the full-sample bootstrapped (n=1000) weighted rotations from a PCA of life history metrics derived from a subset of the COMPADRE Plant Matrix Database.

# Tables

**Table 2.1:** Functional forms of the demographic processes in the integral projection model (IPM) used to simulate plausible plant life history strategies. The growth function is a probability density function with a linear function with normal densities. Survival probability and flowering probability are logistic functions, seed production is the exponential of a linear function, size at birth is a normal distribution with a mean of zero and recruitment probability is a constant. The parameter constraints are described in Table 2.2.

| Demographic function | Functional form |
|---|---|
| Growth | $G(z', z) = \frac{1}{\gamma_\sigma \sqrt{2\pi}} \exp\left(-\frac{(z' - (-\gamma_p\, z + (1 - \gamma_p)))^2}{2{\gamma_\sigma}^2}\right)$ |
| Survival probability | $s(z) = \frac{1}{1 + \exp\,(\tau_a + \tau_z(z - 0.5))}$ |
| Maturity probability | $m(z) = \frac{1}{1 + \exp\,(\varphi_a + \varphi_z(z - 0.5))}$ |
| Flowering probability | $p_b(z) = \frac{1}{1 + \exp\,(\beta_a + \beta_z(z - 0.5))}$ |
| Seed production | $b(z) = \exp\,(\omega_a + \omega_z(z - 0.5))$ |
| Size at birth | $c_0(z') = \frac{1}{\vartheta_\sigma \sqrt{2\pi}} \exp\left(-\frac{{z'}^2}{2{\vartheta_\sigma}^2}\right)$ |
| Recruitment probability | $p_r = \varepsilon$ |

**Table 2.2:** List of parameters used to parameterise an integral projection model (IPM), defined in Table 2.1, that can represent a range of plausible plant life history strategies. Parameters were constrained with an upper and/or lower limit to prevent the IPM from describing implausible plant life history strategies. When sampling life history strategies with an adaptive Metropolis (AM) algorithm, Gaussian (normally distributed) priors were placed on certain parameters to prevent the sampler from oversampling certain life history strategies. All other parameters were sampled from a uniform prior.

| Parameter | Symbol and constraint | Sampling prior distribution |
|---|---|---|
| Pace of growth | $0 < \gamma_p < 1$ | Uniform prior |
| Growth standard deviation | $0.01 < \gamma_\sigma < 0.5$ | Uniform prior |
| Survival function slope | $0 < \tau_z < 10$ | $\sigma_a \sim N(2, 2^2)$ |
| Survival function intercept at z = 0.5 | $-10 < \tau_a < 5$ | $\sigma_b \sim N(0, 2^2)$ |
| Probability of maturation slope | $0 < \varphi_z < 10$ | Uniform prior |
| Probability of maturity size of p = 0.5 | $-10 < \varphi_a < 5$ | Uniform prior |
| Probability of flowering function slope | $0 < \beta_z < 10$ | Uniform prior |
| Probability of flowering function intercept at z = 0.5 | $-10 < \beta_a < 5$ | Uniform prior |
| Seed production slope | $0 < \omega_z$ | $\omega_a \sim N(2, 2^2)$ |
| Seed production function intercept at z = 0.5 | $0 < \omega_a$ | $\omega_b \sim N(2, 2^2)$ |
| Size at birth standard deviation | $0.01 < \vartheta_\sigma < 0.5$ | Uniform prior |
| Recruitment probability | $0 < \varepsilon < 1$ | Uniform prior |

**Table 2.3:** Nine life history metrics that can be derived from matrix population models (MPMs), as used in Salguero-Gómez et al. (2016b) for classifying life history strategies using the COMPADRE Plant Matrix Database.

| Life history metric | Symbol | Definition from Salguero-Gómez et al. (2016b) |
|---|---|---|
| Generation time | T | Number of years necessary for the individuals of a population to be fully replaced by new ones |
| Survivorship curve type | H | Shape of the age-specific survivorship curve $l_x$ as quantified by Keyfitz' entropy (H). H >1, = 1, <1 correspond to survivorship curves types I, II, and III, respectively |
| Progressive growth | $\gamma$ | Mean probability of transitioning to a larger/more developed stage in the life cycle of the species, weighted by the stable stage distribution (SSD) |
| Retrogressive growth | $\rho$ | Mean probability of transitioning to a smaller/less developed stage in the life cycle of the species, SSD-weighted. |
| Mean sexual reproduction | $\Phi$ | Mean per-capita number of sexual recruits across stages in the life cycle of the species, SSD-weighted |
| Degree of iteroparity | S | Spread of reproduction throughout the lifespan of the individual as quantified by Demetrius' entropy (S). High/low S values correspond to iteroparous/semelparous populations |
| Net reproductive rate | $R_0$ | Mean number of recruits produced during the mean life expectancy of an individual in the population |

| | | |
|---|---|---|
| Age at maturity | $L_\alpha$ | Number of years that it takes an average individual in the population to become sexually reproductive |
| Mature life expectancy | $L_w$ | Log ratio of mean age at sexual maturity ($L_\alpha$) until the mean life expectancy ($\eta e$) of an individual in the population |

# Chapter 3

# Linking life history to transient dynamics via population models

Simon Rolph[1]*, Roberto Salguero-Gómez[2], Robert Freckleton[1], Jonathan Potts[3], Dylan Childs[1].

[1] Department of Animal & Plant Sciences, University of Sheffield, Alfred Denny Building, Western Bank, Sheffield, S10 2TN, UK.

[2] Department of Zoology, University of Oxford, Zoology Research and Administration Building, 11a Mansfield Road, Oxford, OX1 3SZ, UK.

[3] School of Mathematics and Statistics, University of Sheffield, Hicks Building, Hounsfield Road, Sheffield, S3 7RH, UK.

*Contact author: srolph1@sheffield.ac.uk

# Summary

1. Transient dynamics describe short-term dynamics that can behave distinctly from asymptotic dynamics and constitute an important, and historically underexamined, component of population dynamics. Reliable estimates of transient dynamics typically require constructing data-intensive population models.
2. A general understanding of transient dynamics would enable us to use more-easily measured traits, such as life history traits, to predict transient dynamics. Population models provide a tool to link life history to transients because they can be used to calculate both life history traits and indices of the transient potential. These indices quantify the upper and lower bounds of potential transient responses.
3. We used an integral projection model (IPM) framework to simulate demographic population models under the assumption that density dependence constrains growth rates. We used these simulated population models to derive life history traits and indices of transient dynamics. We used partial least squares, or projection to latent structures, (PLS) regression, a linear multivariate approach, to analyse links between life history traits and indices of transient dynamics. We compared our results to comparative studies that used published matrix population models (MPMs).
4. Variance and covariance patterns within transient indices showed two main axes: magnitude of response and tendency towards amplification as opposed to attenuation. The most important axis of variation in life history traits and transient indices emerged as a prototypical fast-slow continuum from short-lived, highly reproductive populations to long-lived, less reproductive populations. This axis explained 50% of the magnitude of transient potential but subsequent latent variables were needed to improve predictions.
5. Non-adaptive constraints, such as density dependence, explained much of the (co)variance patterns in life history and transients which improved predictions of transient potential. Non-linear patterns in life history traits suggest that statistical approaches with assumptions of linearity

such as PLS and PCA might not perform optimally. This work shows that using simulated population models can be used to ask the same questions as published MPMs.

**Keywords:** Transient dynamics, life history, comparative demography, density-dependence, matrix population model, integral projection model.

# Introduction

By studying transient dynamics, defined as dynamics that are distinct from a system's asymptotic behaviour, we can build a more complete understanding of population dynamics (Hastings, 2001). Theoretical and empirical research aims to determine what proportion of observed population dynamics can be attributed to ongoing transient processes (Hastings, 2004; Hastings et al., 2018). Transient processes mediate species' responses to variable environments and may impact species co-existence (Noonburg & Abrams, 2005) and life history evolution (Gamelon et al., 2014). A first step towards understanding transients in varying environments examines population-level responses to discrete disturbances or perturbations (Stott, 2016). Transient responses to discrete perturbations from extreme climatic events or anthropogenic impacts may also be important in a management setting (Ezard et al., 2010).

Unfortunately, modelling complex transient dynamics is difficult. Developing a detailed and robust demographic model from which to predict transient population dynamics, even for a single population, requires data for multiple years over hundreds of individuals (Crone et al., 2011; Kendall et al., 2019). Moreover, transient responses to novel and/or extreme perturbations may be outside of the realised transient responses we have observed in an established population. Therefore, it would be useful to identify traits that correlate with transient behaviour. One way to quantify this would be to calculate estimates of the upper and lower bound of the potential transient response. We would expect life history traits to correlate with transients because transient dynamics are a result of the population-level processes of survival, growth, and reproduction, which are shaped by individual-level life history traits. Potential transient responses to perturbation have shown to be linked to a species' life history (Gamelon et al., 2014; Iles et al., 2016; Koons et al., 2005; Stott et al., 2010). Life history traits such as the number of offspring and life expectancy are more easily measured than transient dynamics and are available in open-access trait databases with much greater species coverage than demographic databases (e.g. Jones et al., 2009; Kleyer et al., 2008). By linking transient responses to life history traits, we could reveal generalities and be able to predict transient responses from life history traits.

The ability to derive measures of both life history and transient bounds makes structured population models an ideal sandbox to examine links between these measures. Structured population modelling tools such as matrix population models (MPMs) and integral projection models (IPMs) describe transitions between discrete stages or continuous domains over a discrete time interval. Indices of life history (Cochran & Ellner, 1992; Salguero-Gómez et al., 2016b) and transient population dynamics (Stott, 2016) can readily be derived from these transition rates. Age-specific trajectories can be calculated from MPMs and IPMs, even if the model does not explicitly incorporate age structure. From these trajectories, we can calculate averages and variances of the timing of key life history events such as age at maturity and life expectancy (Caswell, 2001). There are diverse methods for analysing transient dynamics (reviewed in Stott, 2016) including stochastic simulations (Haridas et al., 2009), transfer function analysis (Stott et al., 2012) and differentiation (Yearsley, 2004).

The versatility and ubiquity of the MPM in population biology has led to over 2000 MPMs published in the scientific literature, presenting an opportunity for comparative work. The COMPADRE Plant Matrix Database (Salguero-Gómez et al., 2015) and COMADRE Animal Matrix Database (Salguero-Gómez et al., 2016a) are repositories for published MPMs. The comparative analysis of life history traits derived from MPMs has been used to classify life histories at the species level. Previous research has classified life histories via a framework that identified major axes of covariation within MPM-derived life history traits via principal component analysis (PCA) using demographic models from COMPADRE and COMADRE (Healy et al., 2019; Paniw et al., 2018; Salguero-Gómez, 2017; Salguero-Gómez et al., 2016b). This work has shown that 50-60% of covariation within life history traits could be captured with two main principal component axes, although each study used a different set of MPM-derived life history traits. The first axis was interpreted as ‘pace-of-life’, while the second axis correlated with reproductive strategy from iteroparity to semelparity. These two axes have been shown to be associated with variation in population growth rate (Salguero-Gómez, 2017), conservation status (Salguero-Gómez, 2017) and sensitivity to environmental temporal autocorrelation (Paniw et al., 2018). However, these analyses are exploratory rather than hypothesis oriented so it can difficult be to determine the mechanisms that underpin these axes. Suggested drivers included environmental variation

and trade-offs in the investment of energy into survival/growth/reproduction (Salguero-Gómez et al., 2016b).

The comparative analysis of demographic data has also been used to investigate patterns in transient dynamics across species. Out of the methods for quantifying transient behaviours in populations, one of the most widely adopted (e.g. Ellis & Crone, 2013; Gamelon et al., 2014; Mcdonald et al., 2016; Nicol-Harper et al., 2018; Stott et al., 2010) is a set of six transient indices (Stott et al., 2011). These indices are calculated by projecting from a perturbed population structure and observing how this diverges from a projection initialised at the asymptotic population structure. In a density-independent population model, a perturbed population will asymptotically return to the stable population structure. Within this transient period, we can calculate three indices of transient amplification and three indices of transient attenuation. Applying a PCA approach to the six indices of transient potential of plant populations, Stott et al. (2010) found that >90% of covariation could be captured by two principal components. The first represented the magnitude of transient potential, while the second axis represented a tendency to have greater potential to amplify relative to attenuate and vice versa.

Several studies have linked life history to transient dynamics. Position within the two-axis life history framework correlates with damping ratio (Salguero-Gómez, 2017), a transient measure of how quickly a density-independent population projection returns to stability after a disturbance. Stott et al. (2010) found that short-lived, semelparous plants and long-lived plants, representing life history extremes, exhibited the greatest transient potential, whereas intermediate life histories such as herbaceous perennials exhibited the least transient potential. Research using mammalian MPMs by Gamelon et al. (2014) suggested that the 'speed' of the life cycle, quantified by generation time, correlated with the tendency to amplify or attenuate. Whilst it has been ascertained that there is a link between life history and transient dynamics we do not know if these associations are general, and if so, whether using life history is a viable shortcut for predicting transient behaviours in populations. Furthermore, it is not known which life history traits are associated with which aspects of transient behaviours and the mechanism behind any associations.

It is important to interpret comparative analyses of demographic data in the context of different constraints. Given a set of variables, such as life history traits, a constraint is a mechanism that excludes some combinations of those variables and may be classed as adaptive or non-adaptive. An example of an adaptive constraint is a budgetary trade-off: an organism's finite energy budget induces a trade-off between the investment into survival, growth, or reproduction. Budgetary trade-offs are predicted to induce negative correlations among life history traits. A non-adaptive constraint is a constraint that is not under selection and is unrelated to the biology of the species. Density dependence is one such constraint. Negative density dependence ultimately limits population growth rate via its impact on survival and reproductive rates, causing population density to fluctuate around a carrying capacity and constraining long term growth rate. I showed that when population models without any form of energy budget were simulated under the simple constraint that population growth rate ($\lambda$) $\approx 1$, the emergent life history trait (co)variance patterns were consistent with patterns seen in a PCA of published MPMs (Rolph et al., 2021). Thus, the patterns previously attributed to budgetary life history trade-offs or environmental effects were also consistent with non-adaptive constraints imposed by density dependence. Prior work (Stott et al., 2010) has shown that transient indices are highly correlated, yet we do not know the significance of these correlations. It is not known whether these correlations are due to adaptive constraints such as environmental pressures selecting for combinations of life history traits that produce constrained transient dynamics, or non-adaptive constraints such as density dependence.

Another consideration when interpreting results of comparative analysis of MPMs is how factors relating to model construction, unrelated to the population's biology, affect MPM-derived outputs. It has been shown that outputs from MPMs, including indices of transient amplification and attenuation, are influenced by the discrete class structure of MPMs (Salguero-Gómez & Plotkin, 2010; Stott et al., 2010). Very few MPMs are constructed with the same class structure; the number of classes and how the classes are defined (by age, function, size etc.) differs among studies. The number of classes chosen is influenced by a range of factors such as lifecycle complexity, chosen modelling framework, data availability and author preference. This variation in class structure has been recognised as likely to affect the results of comparative analyses (Kendall et al., 2019; Ramula & Lehtilä, 2005; Salguero-

Gómez & Plotkin, 2010; Stott et al., 2010), but the effect of biases in a comparative setting is still uncertain. A proposed solution is the standardisation to a fixed four-class MPM, as utilised by Gamelon et al. (2014), which may ameliorate this issue; however, use of smaller MPMs has already been shown to dampen transient dynamics (Tenhumberg et al., 2009). It would be desirable to understand how discretisation and inconsistency in class structure affects the results of comparative analysis.

Here, we use the simulated population model framework outlined in Rolph et al. (2021) to simulate continuous state population models under the assumption that density dependence creates asymptotically stable populations. Using simulated demographic data allows us to treat the underlying IPM as 'reality' and the derived MPMs as discretised models such as those found in COMPADRE. We discretise these population models to MPMs with different configurations of discrete classes. For each derived MPM, we calculate an IPM-compatible version of the transient indices described in Stott et al. (2011) and we also calculate life history metrics used in (Healy et al., 2019). We refer to these measures of life history as life history metrics as opposed to life history traits. Traits are traditionally interpreted as being genetically determined; however, these life history metrics are derived from population models which are a composite of life history and population-level processes therefore inheritance cannot be assumed. Building upon the previous methods used to examine links between life history and transient potential using MPMs, our approach is to use partial least squares regression, or projection to latent structures (PLS), to derive a common latent space that simultaneously maximises covariance between life history traits and transient indices. We have three key aims in the use of this framework. Firstly, to determine whether the demographic constraint found in Rolph et al. (2021) explains previously published associations between transient indices. Secondly, to investigate the strength and direction of any associations between life history and transient indices. Finally, to determine how matrix discretisation biases this association between transient potential and life history.

# Methods

## Simulating population models

To explore the linkage between life history and transient dynamics, we used simulated population models under the assumption that density dependence constrains asymptotic growth rate. We defined a flexible IPM that could express a diversity of plant-like life histories. To ensure that these life histories were plausible we incorporated the key processes of survival, growth, maturity, flowering probability, number of offspring and the first-year survival of offspring. We sampled parameter sets for this IPM with a log long term growth rate, $log(\lambda)$, of 0, under the assumption that density dependence constrains growth rates to approximately 1. The underlying IPM was a size-structured, post-reproductive census model with a projection interval of one year. This IPM had two stages: immature non-reproductive class and mature reproductive class. The full IPM kernel, $K$, describes the transitions between two size distributions, immature, $n_I(z,t)$, and mature, $n_M(z,t)$, and from size $z$ to size $z'$ over a discrete time interval. The transitions for the immature plants take the form

$$n_I(z',t+1) = \int_L^U s(z)(1-m(z))G(z',z)n_I(z,t)dz + \int_L^U p_b(z)b(z)p_r(1-m(z'))c_0(z')\ n_M(z,t)dz \tag{3.1}$$

and the transitions for the mature plants take the form

$$n_M(z',t+1) = \int_L^U s(z)G(z',z)n_M(z,t)dz + \int_L^U s(z)m(z)G(z',z)n_{\mathrm{I}}(z,t)dz + \int_L^U p_b(z)b(z)p_r m(z')c_0(z')n_M(z,t)dz \tag{3.2}$$

where $n_M(z,t)$ is the size distribution of mature individuals at time $t$, $n_I(z,t)$ is the size distribution of immature individuals at time t, $s(z)$ is the size-dependent survival function, $G(z',z)$ is the size-dependent growth kernel, $m(z)$ is size-dependent maturity, $p_b(z)$ is size-dependent flowering probability, $b(z)$

is size-dependent number of offspring, $p_r$ is first year survival rate, $c_0(z')$ is size at birth and $p_r$ is probability of survival and recruitment from seed to seedling. $U$ and $L$ denote the upper and lower size limits of the kernel, respectively.

We used an adaptive Metropolis (AM) algorithm (Haario et al., 2001) with delayed rejection to sampled IPM parameters that result in an asymptotic growth rate $log(\lambda) \sim 0$. Metropolis algorithms are a Markov chain Monte Carlo (MCMC) method for generating random samples from a probability distribution for which direct sampling is difficult. The algorithm involves updating a proposal distribution which is used to generate candidate parameter sets. At each iteration, the corresponding IPM kernel was constructed from the candidate parameter set, and $log(\lambda)$ was calculated from the dominant eigenvalue of the kernel. The parameter set was accepted or rejected based on the $log(\lambda)$ value. We used the 'modMCMC' function from R package 'FME' (Soetaert & Petzoldt, 2010) to implement the AM algorithm in the R programming language (Core R Team, 2019). The parameter covariance matrix was re-evaluated every 500 iterations to improve the acceptance rate of proposed parameter sets. The chain ran for 200,000 iterations. The first 25,000 parameter sets were discarded as burn-in to allow the adaptation of the covariance matrix to occur. The remaining parameter sets were thinned to 1000 parameter sets to remove autocorrelation.

We constructed size and maturity structured MPMs from each IPM to explore the consequences of imposing a discrete stage structure on continuously structured populations. Discretisation of the state distribution preserved log(λ). To construct an MPM, the continuous size domain was divided into contiguous discrete intervals. The intervals were chosen by first calculating the stable state distribution of the IPM then splitting the stable state distribution into equal quantiles based on the number of size classes in the target MPM. The mean rates of growth-survival and reproduction for each interval were then derived by calculating the expectation with respect to the normalised stable size distribution over each interval. The derived MPM comprised of two matrices, $F_{mat}$ and $P_{mat}$, which describe fecundity and survival/growth transitions, respectively. The derived MPMs include the demographic process of stasis which is not present in continuously structured populations because there is no probability of remaining in the same life stage when there are no discrete life stages.

# Calculating life history metrics

For each simulated population, we calculated a set of six life history metrics selected to capture different facets of life history (Healy et al., 2019). These metrics represent the spread of reproduction, age at first reproduction, distribution of mortality, reproductive rate, mature life expectancy and generation time. The methods for calculating these metrics were originally intended for MPMs in which a single life stage, such as a seedling, represented the start of the life cycle. These methods could not be applied to our simulated IPMs because the start of the lifecycle was represented as a size distribution, rather than a discrete stage, meaning that the first life stage of our discretised simulated population models did not uniquely represent the start of the lifecycle. To overcome this difference, we adapted the calculations to accommodate an initial state distribution, $c(z)$, which represents the size class distribution of a new cohort of a population at its asymptotic stable stage distribution. $c(z)$ is defined as

$$c(z) = \mathrm{F}(\mathrm{z}', \mathrm{z})\omega \tag{3.3}$$

where ω is the stable state distribution, calculated as the dominant right eigenvector of $K$. For the MPMs that we derived from IPMs, the calculation is notated as

$$c = F_{mat}\ \omega \tag{3.4}$$

Some of the following life history metrics are derived from the age-specific survivorship curve $l_a$ and the age-specific fertility trajectory $f_a$, where the $a$ subscript denotes age in years (Caswell, 2001). $l_a$ and $f_a$ are calculated under the assumption that a single matrix class represents the size/state at birth. Therefore, we calculated an equivalent of $l_a\ f_a$ but for a cohort of individuals from the $c(z)$, notated as $\widetilde{l_a}\widetilde{f_a}$, and calculated as

$$\widetilde{l_a} = \langle l_a, c\rangle = \int_L^U l_a(z)c(z)dz \tag{3.5}$$

$$\widetilde{f_a} = \frac{1}{\widetilde{l_a}}\int_L^U \int_L^U FP^a\left(z', z\right)c(z)dz\ dz'$$

Because $c$ is a probability distribution (by assumption), $\langle l_a, c \rangle$ denotes an average value with respect to the distribution.

Demographic vital rates summarise population-level transitions between life stages whilst a population remains in a stable stage distribution. Mean sexual reproduction, $\emptyset$, describes the mean year to year per-capita number of sexual offspring once the population has converged to the stable stage distribution and is calculated as

$$\emptyset = \sum_{1}^{m} \mathrm{F}_{\mathrm{mat}}\, \omega \tag{3.6}$$

where F is the fecundity matrix or kernel, and ω is the stable stage distribution and $m$ is the number of life stages in the derived MPM.

Generation time is a measure of population turn-over: the number of years necessary for the individuals of a population to be fully replaced by new ones. Generation time ($T$) is calculated from reproductive rate ($R_0$) and asymptotic growth rate ($\lambda$) as

$$T = \frac{\log(R_0)}{\log(\lambda)} \tag{3.7}$$

where $R_0$ is defined as

$$R_0 = \int_0^\infty \tilde{l_a} \tilde{f_a} dz\,. \tag{3.8}$$

Age at maturity, $\mathrm{L}_{\alpha,}$ is the number of years that it takes an average individual in the population to enter a mature life stage, defined as a stage in which an individual can potentially reproduce. This is calculated by decomposing the MPM into $F_{mat}$ and $P_{mat}$ and using them to define a Markov chain with absorbing states for entering a potentially reproductive class and mortality. Markov chain theory can then be used to calculate the mean age of first reproduction, conditional on reaching maturity and this approach is outlined in (Caswell, 2001).

Mature life expectancy as calculated in (Healy et al., 2019; Salguero-Gómez et al., 2016b), $L_{w,}$ is the log ratio of mean age at sexual maturity, $L_\alpha$, until the mean life expectancy, $\eta_e$, of an individual in the

population and is calculated as $L_w = \log(\eta_e) - \log(L_\alpha)$. Healy et al. (2019) describe their metric for mature life expectancy to be conditional on reaching maturity in their methods. In fact, the function they used from the Rage R package (https://github.com/jonesor/Rage) calculated this metric using the log ratio calculation. For this study, we used a Markov chain approach to calculate the average age of mortality, conditional on reaching maturity as described in Ellner et al. (2016).

The final two metrics capture the spread of reproduction and mortality across age. To measure the spread of reproduction across the life course (G), we calculated the Gini index of the age-specific fecundity curves, $\widetilde{f_a}$using the Gini function of the ineq package (Zeileis, 2015). The resulting values go from 0, describing iteroparous strategies which reproduce across their lifespan, to 1, describing semelparous strategies with one large reproductive event. We calculated the distribution of mortality risk by calculating the standard deviation of the age-specific distribution of mortality derived from the age-specific survivorship curve $\widetilde{l_a}$. We used linear interpolation to standardise age-specific curves for comparing metrics derived from MPMs/IPMs with different matrix dimensions / kernel resolution. We calculated the mortality rate from each interpolated point on the standardised age-specific survival curves and calculated the standard deviation of the resulting sequence.

## Deriving indices of transient dynamics

To quantify transient dynamics, we calculated six indices of transient dynamics based on the indices described in detail in Stott et al (2010). Each index either quantifies amplification or attenuation. Each of these indices can be calculated as a case-specific projection from a predefined population structure or as a transient bound, i.e. the greatest possible magnitude amplification or attenuation. We used the transient bound because it doesn't require knowledge of the existing population structure. Indices for first-step amplification and first-step attenuation capture the biggest possible population increase or decrease after a single time step, relative to the asymptotic growth rate. Indices for maximum amplification or maximum attenuation calculate the greatest possible deviation, across all time steps, from what would have been projected if the population had started at the stable size/stage distribution. Indices for amplified and attenuated inertia calculate the greatest deviation from the long-term stable population

projection once the transient dynamics have reached their stable stage distribution, relative to the asymptotic projection.

The original calculation of the indices of transient potential (Stott et al., 2011) was not an appropriate method for directly applying to our simulated IPMs because these calculations determined the transient potential by projecting from an initial population vector with all individuals placed in a single discrete class. Conceptually, this wasn't appropriate for IPMs because IPMs are based on a continuous state variable. This calculation also wasn't appropriate for the MPMs derived from these IPMs because the measures of transient potential defined in Stott et al. (2011) were highly sensitive to the upper size limit of the final size class. This upper size limit was defined to minimise eviction (Williams et al., 2012), was not a biologically relevant parameter and was not consistent for each MPM/IPM. A greater upper size limit always resulted in greater transient amplification because in our simulated population models the vital rates of survival and fecundity increased with size.

Our modified transient indices were based on the transient amplification or attenuation from a standardised reference stage–size distribution. To calculate the three indices of transient amplification we projected from a cohort of mature-class projections and to calculate the three indices of transient attenuation we projected from a cohort of new recruits (Fig. 3.1). For measures of transient amplification, we used a starting Gaussian distribution with a mean of $z = 1$ and a standard deviation of 0.2. The value of 0.2 was chosen arbitrarily but our analyses were not sensitive to the value chosen for the standard deviation. For measures of transient attenuation, we used a starting Gaussian distribution with a mean of 0 and the standard deviation of the size at birth distribution. To translate these case-specific projections to the discretised MPM of each IPM, the continuous state starting distribution described above was 'cut' into the discrete size classes to derive an initial population vector (Fig. 3.1, second row).

## Linking life histories and transient potential

We generated a set of 1000 simulated integral projection models using the two-stage, size-classified IPM and the Metropolis algorithm sampling technique. From these simulated population models, we calculated the six life history traits and six transient indices described in the previous sections. We used

principal component analysis (PCA) to explore the main axes of (co)variation of transient indices and life history metrics separately, using R function 'prcomp' from base R package 'stats' (Core R Team, 2019). Life history metrics were all log transformed, as in Healy et al. (2019), and transient indices of transient amplification were log transformed due to right skew but indices of transient attenuation did not require log transformation. Life history metrics and transient indices were scaled and centred before carrying out the PCA.

We used partial least squares regression, also known as projection to latent structures, (PLS) to reveal associations between both life history metrics and transient indices derived from population models. PLS determined a linear regression model by projecting the predicted variables and the observable variables to a new space thus deriving latent variables that maximise (co)variance with both life history traits and transient indices. Life history metrics and transient indices were scaled and centred before carrying out PLS. To avoid confusion, components from PCA are referred to as principal components (PCs) and components from PLS are referred to as latent variables (LVs) throughout this manuscript. PLS was implemented using the R package 'pls' (Liland, 2013). We used 10-fold cross-validation to evaluate how many latent variables to retain. Cross-validation determined the proportion of variance explained in life history traits and transient indices as the number of LVs was increased. PLS also produced weightings for how each life history metric and transient index is weighted towards each LV. We used these weights, in addition to cross validation results, to determine the composition of each LV and how many LVs should be retained to quantify the link between life history and transient potential.

We used PLS to predict transient indices from life history metrics to test the viability of PLS as a predictive tool. We used the calculated life history metrics for each population model to predict values for each of the six transient indices using the PLS regression models (Fig. 3.2). We then projected each population model onto the major axes of transient response, representing the magnitude of transient response and the tendency to have greater amplification than attenuation. We projected into this PCA space using the transformations specified by the PCA fitted to the simulated IPMs. To assess the accuracy of prediction we compared the predicted transient indices or PCs to the observed transient indices or PCs and calculated the coefficient of determination (R-squared) and root mean squared error of

prediction (RMSEP). We made this comparison for transient indices predicted using PLS with an increasing number of LVs from one to six.

To determine how discretisation to MPMs might affect predictions of transient indices we derived two sets of MPMs for each set of 1000 simulated IPMs. Firstly, we derived a set of MPMs where the continuous size domain was discretised to four size classes with uniform stable size class distributions. Each of these size classes was also subclassified as immature or mature, reflecting the same size by maturity structure of the IPM. This meant that the MPMs had eight discrete life stages. These standardised eight class MPMs, referred herein as the 'fixed dimensions' set of MPMs, is analogous to the approach employed by Gamelon et al. (2014), whereby they standardised published MPMs from COMADRE to have the same number of classes. Secondly, from the same set of IPMs, we derived a second set of MPMs discretised to a range of different dimension. Each of these MPMs were randomly allocated to have 1,4 or 8 size classes, resulting in MPMs with 2, 8 or 16 discrete life stages. This diversity in matrix dimension aimed to replicate the diversity of matrix dimensions in databases such as COMPADRE, as such this set is termed 'COMPADRE analogue'. From these two sets of MPMs, we repeated the analysis conducted for IPMs and compared the PLS-predicted transient indices to the measured transient indices of the original IPM (Fig. 3.2).

# Results

There were clear (co)variance patterns between the six transient indices derived from simulated IPMs (Supplementary fig. S3.1). The principal component analysis (PCA) of the six transient indices showed that 91.5% of the variance in the six transient indices could be explained by two principal components (Fig. 3.3). When interpreting these axes, it is important to note that larger values for amplification indices represent large transient potential whereas for attenuation indices the opposite is true and large transient potential is represented by smaller values. PC1 described the amplitude of transient responses and accounted for 72.1% of (co)variance. Increasing values on PC1 were associated with large transient

bounds: larger values for transient amplification and smaller values for transient attenuation. PC2 described a tendency to amplify as opposed to attenuate and accounted for 19.4% of (co)variance. Increasing values on PC2 were associated with a tendency towards amplification: larger values for transient amplification and larger values for transient attenuation. Populations were not normally distributed within the PCA space and the positions of simulated population models within these two PCA axes exhibited non-linear patterns (Fig. 3.3). For example, we observed few population models with a small magnitude of transient potential (negative values on PC1) and a tendency towards attenuation (negative values on PC2). We didn't find evidence of an inherent link between the transient magnitude or tendency of a population model and its long-term growth rate. For our simulated population models, there was no clear relationship between the position on these PCA axes and asymptotic long term growth rate, $\lambda$ (Fig. 3.3).

Similarly, we observed very strong covariance patterns in the life histories of simulated population models. Life history, as quantified by the six life history metrics, could be organised in a two-axis life history space which explained 98% of life history variation (Fig. 3.4). The first PC accounted for 90.0% of the variance in the life history metrics and the second PC accounted for 8.0%. The position within this PCA space was primarily informed by measures of longevity: generation time, life expectancy post maturity and mean age at maturity. This implies that the other metrics covaried so strongly with these three metrics that they didn't provide any new information. When we looked for covariance patterns across both transient dynamics and life history simultaneously using PLS, we identified a six-dimensional latent space in which we refer to each axis as latent variables (LVs) 1-6. Using cross-validation, we determined that LV 1 explained 73% of (co)variance in life history metrics and LV 2 explained 12% (Table 3.1). Thus, we could explain 85% of the variance in life history traits with two LVs, compared to 98% explained by the first two PCA-derived components. We also saw that spread of reproduction, mean sexual reproduction and distribution of mortality risk were important for positioning a population in the PLS latent space, unlike in PCA space. LV 4 explained the third most variance, accounting for 9.3% of variance compared to only 2.7% of variance explained by LV3.

Whilst the first LV resembled a fast-slow continuum similar to the life history PC1, subsequent axes/LVs deviated from the definitions of the PCA axes (Fig. 3.5, Table 3.2). LV1 captured variation in mean measures of life history, such as mean sexual reproduction and mean age at maturity, but also captured variation in the spread of reproduction and mortality. Increasing values for LV1 were associated with population models with iteroparous reproductive strategies and life histories where mortality is concentrated at particular parts of the life course rather than spread equally throughout the life course. LV1 was negatively correlated with life history metrics associated with a slower population turnover: longer generation times, later age at maturity and longer mature life expectancy. LV 2 (9.3% variance explained) accounted for some remaining (co)variances and negatively correlated with all life history metrics except for the spread of reproduction. LV 3 (2.7% variance explained) described an axis from early maturing, semelparous life histories to life histories with unequally spread mortality, longer mature life expectancy and longer generation times.

For indices of transient amplification, increasing from one to two to three LVs produced consistent increases in the proportion of variance explained, but subsequent LVs produced negligible further increases (Fig. 3.6). Contrastingly, for indices of attenuation, we didn't see substantial increases in variance explained beyond using 2 LVs and we saw much greater variation in variance explained by LV1 for each attenuation index. Variance explained by LV 1 for amplified inertia, maximum amplitude and maximum attenuation was between 30-32% (Table 3.1). Using only the first LV very poorly explained variance in attenuated inertia, with only 9.0% of variance explained. However, variance explained for attenuated inertia increased to 62.7% when two LVs were used. Using LV 2 increased variances explained for attenuation indices: we observed increases of 19.0%, 52.9%, 53.8% for first step attenuation, maximum attenuation, attenuated inertia, respectively. This was compared to 16.3%, 14.9% and 11.5% for the respective amplification indices.

The relationship between transient indices and each LV translated into the relationship between each LV and the transient PCA axes: magnitude and tendency to amplify. The first LV captured the magnitude of transient dynamics, LV2 captured variation in both magnitude and tendency, LV3 captured variation in tendency (Fig. 3.6). As quantified by $R^2$, one LV explained 45.1% of variance in the

magnitude of transient potential (PCA axis 1) and two LVs explained 79.1% of variance, however, the variance explained increased only marginally to 82.2% when three LVs were used. Contrastingly, LV 1 essentially described none of the variance (0.001%) in the transient PCA axis 2: the tendency for a population to amplify as opposed to attenuate. Two LVs still explained only 14.9% of variance; however, when three LVs were used, 53.1% of variance was explained. Increasing the number of LVs to 4, 5 or 6 led to only very marginal increases in the proportion of variance explained in the transient indices, and therefore in the PCA axes for magnitude and tendency.

The link between life history and transient indices was weaker for indices that describe transient response at longer timescales from the initial perturbation. The first step amplification/attenuation was directly linked to the reproductive capacity or survival rate of the initial cohort, whereas amplified/attenuated inertia was more poorly predicted by position on a fast-slow continuum due to being calculated a greater number of time steps from the initial perturbation. LV1+2+3 explained 71.3%, 65.6% and 59.1% for first step amplification, maximum amplification, and amplified inertia, respectively (Fig. 3.6, Table 3.1). LV1+2 explained 86.3%, 83.3% and 62.8% for first step attenuation, maximum attenuation, and attenuated inertia, respectively (Fig. 3.6, Table 3.1). Calculating these metrics further from the initial perturbation meant that the projection had cycled through the life cycle multiple times and therefore the inertia indices were a result of more complex pathways through each population model.

Using demographic data with discretised structuring of a continuous state variable, as found in databases such as COMPADRE, affected predictions of transient potential. The discretisation of the continuous state variable affected the values of derived life history metrics and transient indices (Supplementary fig. S3.3). Therefore, when compared to a PLS fitted to our simulated IPMs, PLS models fitted to MPM-derived metrics provided an altered link between life history and transients. Surprisingly, we found that when only one LV was used to predict transient indices using our two MPM-fitted PLSs, the predicted transient indices were more similar to the actual values than the values predicted by the IPM-fitted PLS (Fig. 3.6, Supplementary fig. S3.2). Despite this apparent improvement by discretising the demographic data, we saw evidence that the PLS model had been degraded by fitting to discretised data; when increasing from one to two latent variables, which should improve prediction, the proportion

of variance explained decreased for all measures of transient amplification (Fig. 3.6). The predictions of both transient magnitude (PC1) and the tendency towards amplification/attenuation (PC2) were degraded by using a discretised version of the population models. Predictions for PC1 using MPM-fitted PLSs only explained 55% to 60% of variance when any number of LVs were used, whereas predictions from continuously structured models using two LVs explained 79.1% of variance (Fig. 3.6). PC2 was even more poorly predicted; 25% of variance explained was barely exceeded by a PLS using 4 LVs fitted to fixed dimension MPMs (Fig. 3.6). Compared to the effect of using discretised models versus continuously structured models, whether the models were discretised to fixed dimension or the 'COMPADRE analogue' made a relatively small difference. For indices of transient amplification, predictions using the PLS fitted to fixed dimension MPMs scored better than the COMPADRE analogue MPMs, as measured by $R^2$; however, for indices of transient attenuation, the opposite was true. Differences in the ability to predict transient PC1 was negligible between fixed dimension MPMs and the COMPADRE analogue MPMs.

# Discussion

Our simulated population models are sampled under the assumption that density dependence means populations fluctuate around a carrying capacity and therefore growth rates are constrained. As a result, the emerging patterns can be attributed in part to non-adaptive constraints: a factor not typically considered when interpreting these analyses. We found multivariate associations in covariance patterns in metrics of life history and transient potential. However, there are still significant proportions of variance in transient indices that remained unexplained by life history metrics when using PLS. Our PCAs showed that the six transient indices and life histories were highly constrained. If a population has a large potential for transient amplification, then it will have a large potential for transient attenuation: we described this as the magnitude of transient potential. The first latent variable in life history and transient indices resembled the familiar but imprecisely defined fast-slow continuum, explaining over 70% of variance in life history traits and 50% of variance in the magnitude of transient potential. This shows a clear link between life history and transients. However, our results agree with prior research that showed additional axes of variation are required to usefully classify life histories (Healy et al., 2019; Paniw et al., 2018; Salguero-Gómez et al., 2016b). In our work, using two LVs explained 75% of the magnitude of transient potential and three LVs were needed to explain 50% of variation in a population's tendency towards amplification or attenuation. Finally, we found that the relationship between life history metrics and the transient potential can be obscured when predictions are made using discretised population models. A population's tendency towards transient amplification/attenuation couldn't be reliably determined via a comparative approach using discrete class population models.

Non-adaptive constraints shape covariance patterns in transient indices and understanding the role of non-adaptive constraints provides context for interpreting empirical analyses. When observing covariance patterns in empirical data, it can be hard to determine whether the patterns arise from adaptive constraints, where certain combinations of traits are selected through evolution, or from non-adaptive constraints such as density dependence. In the case of transient indices, the covariance patterns previously observed in empirical research (Gamelon et al., 2014; Stott et al., 2010, 2011) are non-adaptive;

the (co)variance patterns within life history metrics and transient indices that we observed reflect those found in our simulated population models so are due to a combination of density dependent constraint of log(λ) ~ 0 and mathematical constraints. An example of a mathematical constraint is that the maximum amplitude must be greater than or equal to the first-step amplification. We do not explore mathematical constraints in-depth and a future direction to explore mathematical constraints from MPMs might be to investigate the properties by random matrices (Grela, 2017), since MPMs are just matrices of transition rates. Stott et al. (2010) and Gamelon et al. (2014) showed a positive correlation between the magnitude of transient potential and asymptotic growth rate (Fig. 3.3). We can better contextualise this correlation because we did not identify the same relationship in simulated populations; their findings imply that in real-world populations transient potential may be associated with population persistence. However, another explanation is that this result may be due to biases in published MPMs. For example, invasive and endangered species are overrepresented in the scientific literature (Crone et al., 2011). Invasive species tend to have a greater amplitude of transient potential (Jelbert et al., 2019) and they are also more likely to be studied when they are not at carrying capacity or under density-dependent pressures, therefore a model of these populations may have a growth rate > 1. The presence of non-adaptive constraints does not affect our ability to use this framework as a predictive tool and we can exploit non-adaptive constraints to reduce uncertainty in mapping the association between life history and transient dynamics.

In general, the position along a fast-slow continuum provides some insight into a population's transient potential, however, it still leaves critical unexplained variance in transient behaviour, especially in the second axis: the tendency towards amplification or attenuation. We found ~50% of the variance in the magnitude of transient potential is explained by our fast-slow axis, LV1. Reproduction is a requirement for amplification and mortality is a requirement for attenuation therefore an association was expected of life histories being structured from 'fast' high reproduction, high mortality life histories to 'slow' low reproduction, low mortality life histories. Furthermore, due to demographic constraints attributed to density dependence which constrains $\lambda \sim 1$, life histories with higher reproduction must, on average, exhibit lower survival across some or all parts of the lifecycle (Rolph et al., 2021). This means that less

reproductive populations exhibit higher survival rates, therefore living longer and having longer generation times which leads to a smaller transient potential. At first glance, these findings seem to counter the research suggesting that species with a longer generation time have a greater extinction risk because they struggle to recover from disturbances (Hutchings et al., 2012). When interpreting the strength and direction of the association between life history and transient dynamics we have to be precise about what aspect of transient dynamics is being captured by the transient indices used in this analysis. Slow life histories have been found to take longer to recover from disturbance than fast life histories because their population growth rate is restricted by a lower reproductive rate and a later age at maturity. For example, previous comparative work showed that 'slower' life histories had a smaller damping ratio meaning that they took longer to return to their asymptotic state (Salguero-Gómez, 2017). However, the transient indices used in our analysis do not quantify time taken to recover from a perturbation, therefore our finding that slower life histories have a smaller magnitude of transient potential is not counter to existing evidence.

Our findings regarding the association of life history and transient dynamics differ from comparative work by Stott et al. (2010) which found that life history extremes exhibited a larger transient potential. Life history was classified by Stott et al. (2010) in terms of ecological succession from annuals to perennials to late succession rather than on a fast-slow continuum. It may be that our underlying IPM is not flexible enough to describe tree-like life histories with long lifespans but high early-life mortality. Another possible explanation for these differences is that late succession life histories in Stott et al. (2010) included species like trees which are typically modelled with large matrices comprising many size classes (Zuidema et al., 2010) and we found, reflecting existing evidence (Stott et al., 2010; Tenhumberg et al., 2009), that MPMs with more size classes can express larger transient bounds. Demographically, to express the combination of long generation times but high early-life mortality a life history needs slow growth and low survival. These types of life history can be expressed through our IPM in terms of vital rates with large numbers of offspring, $b(z)$, but low first year survival of offspring, $p_r$, but do not manifest in the annual transition rates because the 'trade-off' between adult survival and offspring survival occurs in the within-year processes. Secondly, depending on census timing

(Okuyama, 2019) or MPM construction methods (Kendall et al., 2019), a seed stage may appear in the matrix structure of published tree MPMs providing a low survival class from which a population can be projected to exhibit large attenuations in transient response. Similarly, production of seeds means that a population has a large capacity for transient amplification (Ezard et al., 2010).

Previous comparative analyses have identified a 'reproductive strategies' axis as important for structuring life histories, however, none of the axes emerging from either our PCA or PLS can be clearly labelled as reproductive strategies. The reproductive strategies axis is typically associated with the metric for the spread of reproduction (Healy et al., 2019) or Demetrius' entropy (Salguero-Gómez et al., 2016b) or iteroparity (Paniw et al., 2018). The life history axes exhibited by our PCA of six life history metrics differed from previous studies in two key ways and highlights very strong covariance patterns. Firstly, three of the six life history metrics hardly contributed to PC1 and PC2. Secondly, the percentage of variance explained by the first axis increased considerably to 90%, compared to previous empirical analyses which presented second axes explaining 40-60% of variation. This percentage of variance explained is greater than in the PCA of 9 metrics from simulated MPMs in Rolph et al. (2021), indicating that these six metrics are more highly constrained than the nine used previously, and that noise introduced by discretisation to MPMs weakens covariance patterns. Instead of a 2-axis framework, we find that three LVs are required to link life history to transients, especially in predicting a population's tendency to amplify instead of attenuate. We found that whether a population had a tendency for amplification or attenuation was linked most strongly to metrics of mortality: distribution of mortality and mature life expectancy, whereas Gamelon et al., (2014) found a link between generation time and the tendency to attenuate. Populations with a long mature life expectancy and semelparous strategies had a greater tendency for attenuation. This 'tendency' axis may be more pertinent to determining the 'resilience' of populations than the magnitude of transient response.

Artefacts arising from discretisation of continuous state variables impacted the association between life history and transient dynamics, but we have shown that simulated population models provide a toolkit for diagnosing how this discretisation process affects comparative analyses. Our results support a growing body of evidence that modelling decisions in MPM construction affect the reliability and robustness

of their predictions (Kendall et al., 2019; Salguero-Gómez & Plotkin, 2010; Stott et al., 2010). Our findings corroborate with work by Tenhumberg et al. (2009) that discretisation of continuous state variables allows organisms to move through the state space faster. Discretisation also artificially induced the demographic processes of stasis, remaining at the same size across the projection interval, which does not mathematically exist in a continuous structured population. This analysis showed that these discretisation effects meant that the transient dynamics of discretised population models were of lesser magnitude than those of their parent IPM. These effects also extended to life history metrics; however, the effects were less unidirectional, often introducing noise instead of bias. These results are concerning because our exploration of discretisation was somewhat limited; investigating the use of discrete class models derived from a continuously structured model. Many other factors that may also affect the association between life history and transient indices, including the existence of multiple state variables (e.g. sex and size), what type of MPM structure was used (Carslake et al., 2009) and the presence or exclusion of cryptic life stages (Kendall et al., 2019). We showed that standardising published MPMs (e.g. Gamelon et al., 2014) to a fixed set of life stages before analyses only marginally improved the accuracy of our comparative analysis. We would expect to see a similar effect in other comparative analyses. We echo calls to always review the associated publication for an MPM before inclusion in comparative analyses (Kendall et al., 2019) to check MPM construction methods. Another consideration is that non-adaptive constraints and matrix discretisation may interact. Whilst our discretisation process impacted measures of life history and transient dynamics, it did not alter asymptotic growth rate, $\lambda$, and so the $\lambda \approx 1$ non-adaptive constraint is still in force. Therefore, we might expect that the overall covariance patterns, constrained by $\lambda \approx 1$, would hold true and any latent space derived by PCA or PLS would be less affected by use of discretised population models. This may falsely give the impression that discretisation is having a negligible effect on comparative analyses, however the position of a population within this latent space could be affected considerably.

This work was motivated to build a more general understanding of transient dynamics and aimed to answer three questions; what explains covariance patterns in transient indices, what is the strength and direction of any association between life history and transient dynamics, and how does MPM

discretisation affect this association. Firstly, we showed that covariance patterns in transient indices for published MPMs conform to patterns attributed to non-adaptive constraints. This reiterates an important consideration when interpreting these analyses: dimension reduction techniques such as PCA and PLS will always find axes and we must be careful not to ascribe our preferred explanation to these patterns. Secondly, we've shown that life history links to transient dynamics, and generally, the expectation that fast life histories have greater potential for transient amplification and attenuation holds. However, we need subsequent LVs to explain more variance, especially in a population with a tendency towards amplification or attenuation, and there remains a proportion of variance that we cannot explain using our PLS approach. However, to generalise this finding, we have to critically consider how well the covariance patterns from population models relate to measurements from real populations. Thirdly, our ability to discern this association would have been weakened if we had used published discretely structured demographic data. Overall, this work makes a useful step towards a more general understanding of the link between life history and transient dynamics.

# Acknowledgements

This research was supported by the Centre for Advanced Biological Modelling funded by the Leverhulme Trust. We thank the COMPADRE Plant Matrix Database team, supported by the Max Planck Institute for Demographic Research (MPIDR), for data digitalization and error-checking.

# References

Carslake, D., Townley, S., & Hodgson, D. J. (2009). Patterns and rules for sensitivity and elasticity in population projection matrices. *Ecology*, *90*(11), 3258–3267.

Caswell, H. (2001). *Matrix population models*. (L. John Wiley & Sons, Ed.).

Cochran, M. E., & Ellner, S. (1992). Simple methods for calculating age-based life history parameters for stage-structured populations. *Ecological Monographs*, *62*(3), 345–364.

Core R Team. (2019). A Language and Environment for Statistical Computing. *R Foundation for Statistical Computing*. Vienna: R Foundation for Statistical Computing.

Crone, E. E., Menges, E. S., Ellis, M. M., Bell, T., Bierzychudek, P., Ehrlén, J., … Williams, J. L. (2011). How do plant ecologists use matrix population models? *Ecology Letters*, *14*(1), 1–8.

Ellis, M. M., & Crone, E. E. (2013). The role of transient dynamics in stochastic population growth for nine perennial plants. *Ecology*, *94*(8), 1681–1686.

Ellner, S. P., Childs, D. Z., & Rees, M. (2016). Basic Analyses 1: Demographic Measures and Events in the Life Cycle. In *Data-driven Modelling of Structured Populations: A Practical Guide to the Integral Projection Model* (pp. 57–85).

Ezard, T. H. G., Bullock, J. M., Dalgleish, H. J., Millon, A., Pelletier, F., Ozgul, A., & Koons, D. N. (2010). Matrix models for a changeable world: The importance of transient dynamics in population management. *Journal of Applied Ecology*, *47*(3), 515–523.

Gamelon, M., Gimenez, O., Baubet, E., Coulson, T., Tuljapurkar, S., & Gaillard, J.-M. M. (2014). Influence of life-history tactics on transient dynamics: A comparative analysis across mammalian populations. *American Naturalist*, *184*(5), 673–683.

Grela, J. (2017). What drives transient behavior in complex systems? *Physical Review E*, *96*(2), 022316.

Haario, H., Saksman, E., & Tamminen, J. (2001). An adaptive Metropolis algorithm. *Bernoulli*, *7*(2), 223.

Haridas, C. V., Tuljapurkar, S., & Coulson, T. (2009). Estimating stochastic elasticities directly from longitudinal data. *Ecology Letters*, *12*(8), 806–812.

Hastings, A. (2001). Transient dynamics and persistence of ecological systems. *Ecology Letters*, *4*(3), 215–220.

Hastings, A. (2004, January 1). Transients: The key to long-term ecological understanding? *Trends in Ecology and Evolution*. Elsevier Ltd.

Hastings, A., Abbott, K. C., Cuddington, K., Francis, T., Gellner, G., Lai, Y. C., … Zeeman, M. Lou. (2018). Transient phenomena in ecology. *Science*, *361*(6406).

Healy, K., Ezard, T. H. G., Jones, O. R., Salguero-Gómez, R., & Buckley, Y. M. (2019). Animal life history is shaped by the pace of life and the distribution of age-specific mortality and reproduction. *Nature Ecology and Evolution*, *3*(8), 1217–1224.

Hutchings, J. A., Myers, R. A., García, V. B., Lucifora, L. O., & Kuparinen, A. (2012). Life-history correlates of extinction risk and recovery potential. *Ecological Applications*, *22*(4), 1061–1067.

Iles, D. T., Salguero-Gómez, R., Adler, P. B., & Koons, D. N. (2016). Linking transient dynamics and life history to biological invasion success. *Journal of Ecology*, *104*(2), 399–408.

Jelbert, K., Buss, D., McDonald, J., Townley, S., Franco, M., Stott, I., … Hodgson, D. (2019). Demographic amplification is a predictor of invasiveness among plants. *Nature Communications*, *10*(1), 1–6.

Jones, K. E., Bielby, J., Cardillo, M., Fritz, S. A., O'Dell, J., Orme, C. D. L., … Purvis, A. (2009). PanTHERIA: a species-level database of life history, ecology, and geography of extant and recently extinct mammals. *Ecology*, *90*(9), 2648–2648.

Kendall, B. E., Fujiwara, M., Diaz-Lopez, J., Schneider, S., Voigt, J., & Wiesner, S. (2019). Persistent problems in the construction of matrix population models. *Ecological Modelling*, *406*(June), 33–43.

Kleyer, M., Bekker, R. M., Knevel, I. C., Bakker, J. P., Thompson, K., Sonnenschein, M., … Peco, B. (2008, November 1). The LEDA Traitbase: A database of life-history traits of the Northwest European flora. *Journal of Ecology*. Blackwell Publishing Ltd.

Koons, D. N., Grand, J. B., Zinner, B., & Rockwell, R. F. (2005). Transient population dynamics: Relations to life history and initial population state. *Ecological Modelling*, *185*, 283–297.

Liland, B.-H. M. and R. W. and K. H. (2013). {pls}: Partial Least Squares and Principal Component regression. Comprehensive R Archive Network (CRAN).

Mcdonald, J. L., Stott, I., Townley, S., & Hodgson, D. J. (2016). Transients drive the demographic dynamics of plant populations in variable environments. *Journal of Ecology*, *104*(2), 306–314.

Nicol-Harper, A., Dooley, C., Packman, D., Mueller, M., Bijak, J., Hodgson, D., … Ezard, T. (2018). Inferring transient dynamics of human populations from matrix non-normality. *Population Ecology*, *60*(1–2), 185–196.

Noonburg, E. G., & Abrams, P. A. (2005). Transient Dynamics Limit the Effectiveness of Keystone Predation in Bringing about Coexistence. *The American Naturalist*, *165*(3), 322–335.

Okuyama, T. (2019). Census timing alters stage duration distributions in matrix population models. *Ecology and Evolution*, *9*(15), 8500–8508.

Paniw, M., Ozgul, A., & Salguero-Gómez, R. (2018). Interactive life-history traits predict sensitivity of plants and animals to temporal autocorrelation. *Ecology Letters*, *21*(2), 275–286.

Ramula, S., & Lehtilä, K. (2005). Matrix dimensionality in demographic analyses of plants: When to use smaller matrices? *Oikos*, *111*(3), 563–573.

Rolph, S., Childs, D. Z., & Salguero-Gómez, R. (2021). Density-dependence limits the comaprative analysis of demographic data. *PhD Thesis*.

Salguero-Gómez, R. (2017). Applications of the fast-slow continuum and reproductive strategy framework of plant life histories. *New Phytologist*, *213*(4), 1618–1624.

Salguero-Gómez, R., Jones, O. R., Archer, C. R., Bein, C., de Buhr, H., Farack, C., … Vaupel, J. W. (2016a). COMADRE: A global data base of animal demography. *Journal of Animal Ecology*, *85*(2), 371–384.

Salguero-Gómez, R., Jones, O. R., Archer, C. R., Buckley, Y. M., Che-Castaldo, J., Caswell, H., … Vaupel, J. W. (2015). The compadre Plant Matrix Database: An open online repository for plant demography. *Journal of Ecology*, *103*(1), 202–218.

Salguero-Gómez, R., Jones, O. R., Jongejans, E., Blomberg, S. P., Hodgson, D. J., Mbeau-Ache, C., …

Buckley, Y. M. (2016b). Fast-slow continuum and reproductive strategies structure plant life-history variation worldwide. *Proceedings of the National Academy of Sciences of the United States of America*, *113*(1), 230–235.

Salguero-Gómez, R., & Plotkin, J. B. (2010). Matrix dimensions bias demographic inferences: Implications for comparative plant demography. *The American Naturalist*, *176*(6), 710–722.

Soetaert, K., & Petzoldt, T. (2010). Inverse modelling, sensitivity and Monte Carlo analysis in R using package FME. *Journal of Statistical Software*, *33*(3), 1–28.

Stott, I. (2016). Perturbation analysis of transient population dynamics using matrix projection models. *Methods in Ecology and Evolution*, *7*(6), 666–678.

Stott, I., Franco, M., Carslake, D., Townley, S., & Hodgson, D. (2010). Boom or bust? A comparative analysis of transient population dynamics in plants. *Journal of Ecology*, *98*(2), 302–311.

Stott, I., Hodgson, D. J., & Townley, S. (2012). Beyond sensitivity: Nonlinear perturbation analysis of transient dynamics. *Methods in Ecology and Evolution*, *3*(4), 673–684.

Stott, I., Townley, S., & Hodgson, D. J. (2011). A framework for studying transient dynamics of population projection matrix models. *Ecology Letters*, *14*(9), 959–970.

Tenhumberg, B., Tyre, A. J., & Rebarber, R. (2009). Model complexity affects transient population dynamics following a dispersal event: A case study with pea aphids. *Ecology*, *90*(7), 1878–1890.

Williams, J. L., Miller, T. E. X., Ellner, S. P., & Doak, D. F. (2012). Avoiding unintentional eviction from integral projection models. *Ecology*, *93*(9), 2008–2014.

Yearsley, J. M. (2004). Transient population dynamics and short-term sensitivity analysis of matrix population models. *Ecological Modelling*, *177*(3–4), 245–258.

Zeileis, A. (2015). Measuring Inequality, Concentration, and Poverty [R package ineq version 0.2-13].

Zuidema, P., Jongejans, E., Chien, P. D., During, H. J., & Schieving, F. (2010). Integral Projection Models for trees: a new parameterization method and a validation of model output. *Journal of*

*Ecology*, *98*(2), 345–355.

# Figures

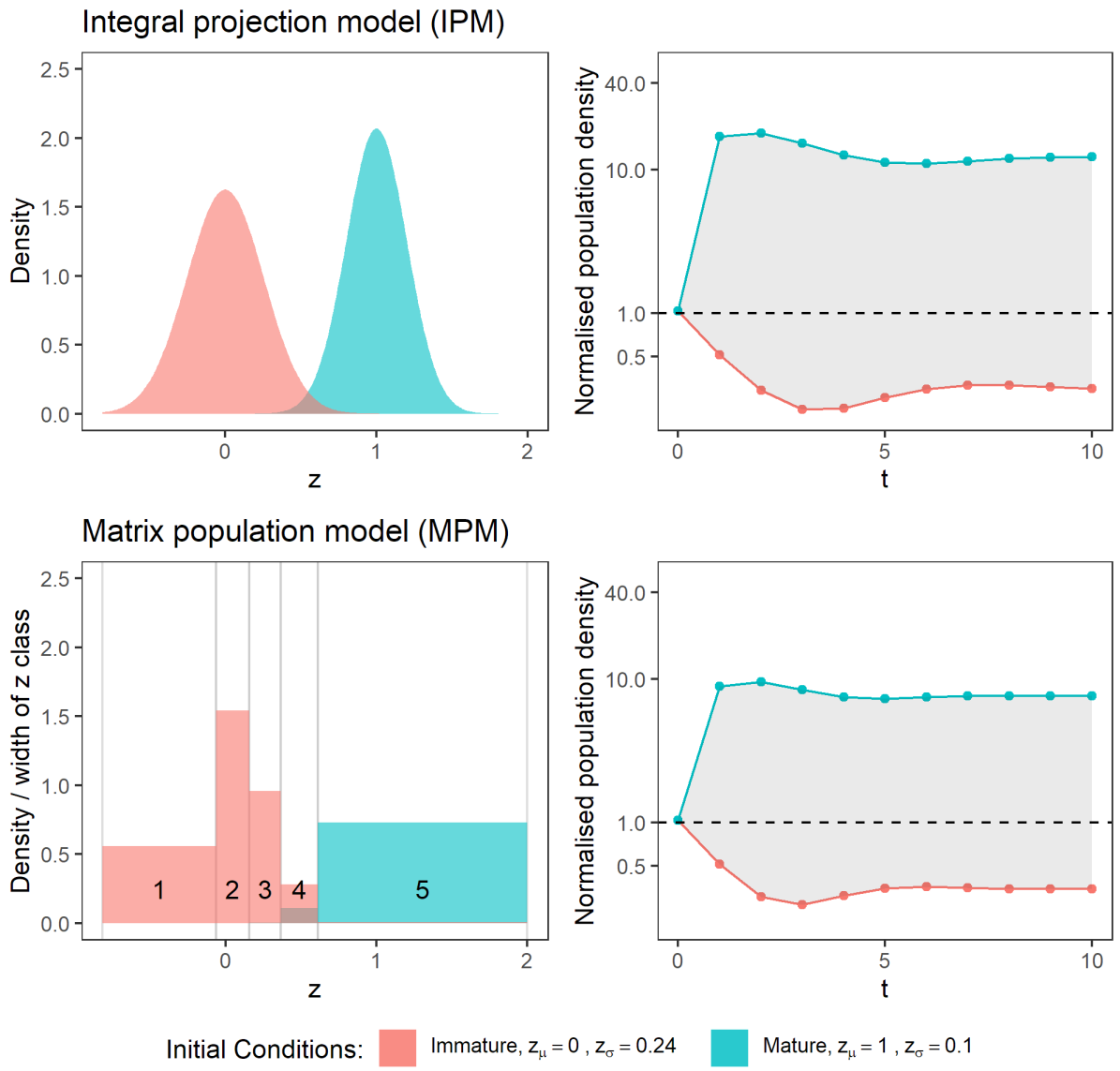


**Figure 3.1: Standardised case-specific projection method used to quantify transient amplification and attenuation for integral projection models (IPM) and matrix population models (MPMs).** The figures in the first column show the initial population distribution for each case-specific projection. Each colour represents two cases of initial conditions. Red is an immature cohort with a Gaussian size distribution centred on z = 0 and standard deviation corresponding to the size at birth parameter of that parameter set. Blue is a mature cohort with a Gaussian distribution centred on z = 1 and a standard deviation of 0.1. For the matrix population models (row 2), the continuous size distribution is split into discrete size classes. The discrete size classes are numbered with vertical lines indicating the upper and

lower bounds of each class. The area of each bar represents the population density in each size class. The figures in the second column show population projections over 10 time-steps from each of the initial distributions, normalised by the asymptotic growth rate.

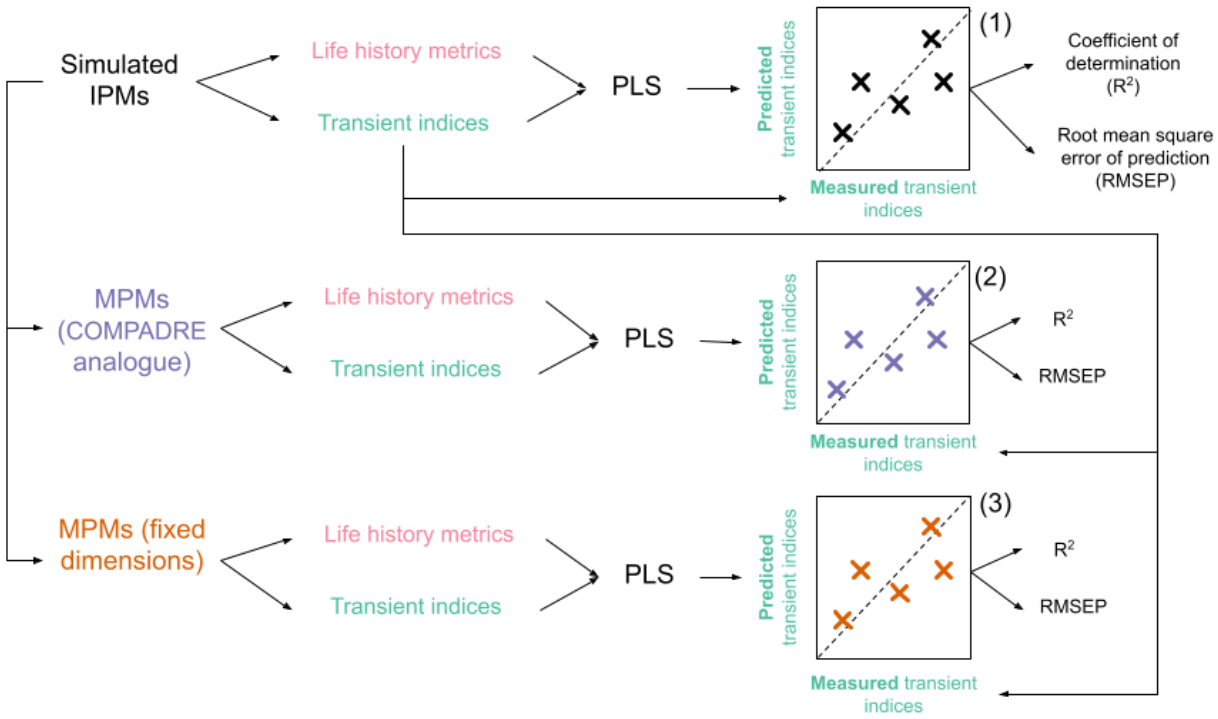


**Figure 3.2: Outline for analysis designed to determine: (1) the predictive performance of a PLS fitted to metrics derived from IPMs, (2) whether these predictions are affected by using COMPADRE analogue MPMs, (3) whether standardising MPMs to fixed dimensions improves predictions compared to the COMPADRE analogue.** A set of 1000 simulated integral projection models (IPMs), sampled to $\lambda \sim 1$, are also discretised to two sets of matrix population models. The first set is discretised to MPMs with 1,2 or 4 size classes. The second set is discretised to two size classes with a uniform stable stage distribution. Each set of M/IPMs are used to derive six life history metrics and six indices of transient dynamics and are used to fit three separate partial least squares regressions (PLS). Each of these models is used to predict transient indices from life history metrics derived from their respective set of M/IPMs. These predictions are made using an increasing number of latent variables from 1-6. These predicted transient indices are then compared to the measured transient indices derived from the original IPM (before discretisation, if applicable). Each comparison is used to calculate $R^2$ and the root mean square error of prediction (RMSEP) to determine the accuracy of prediction.

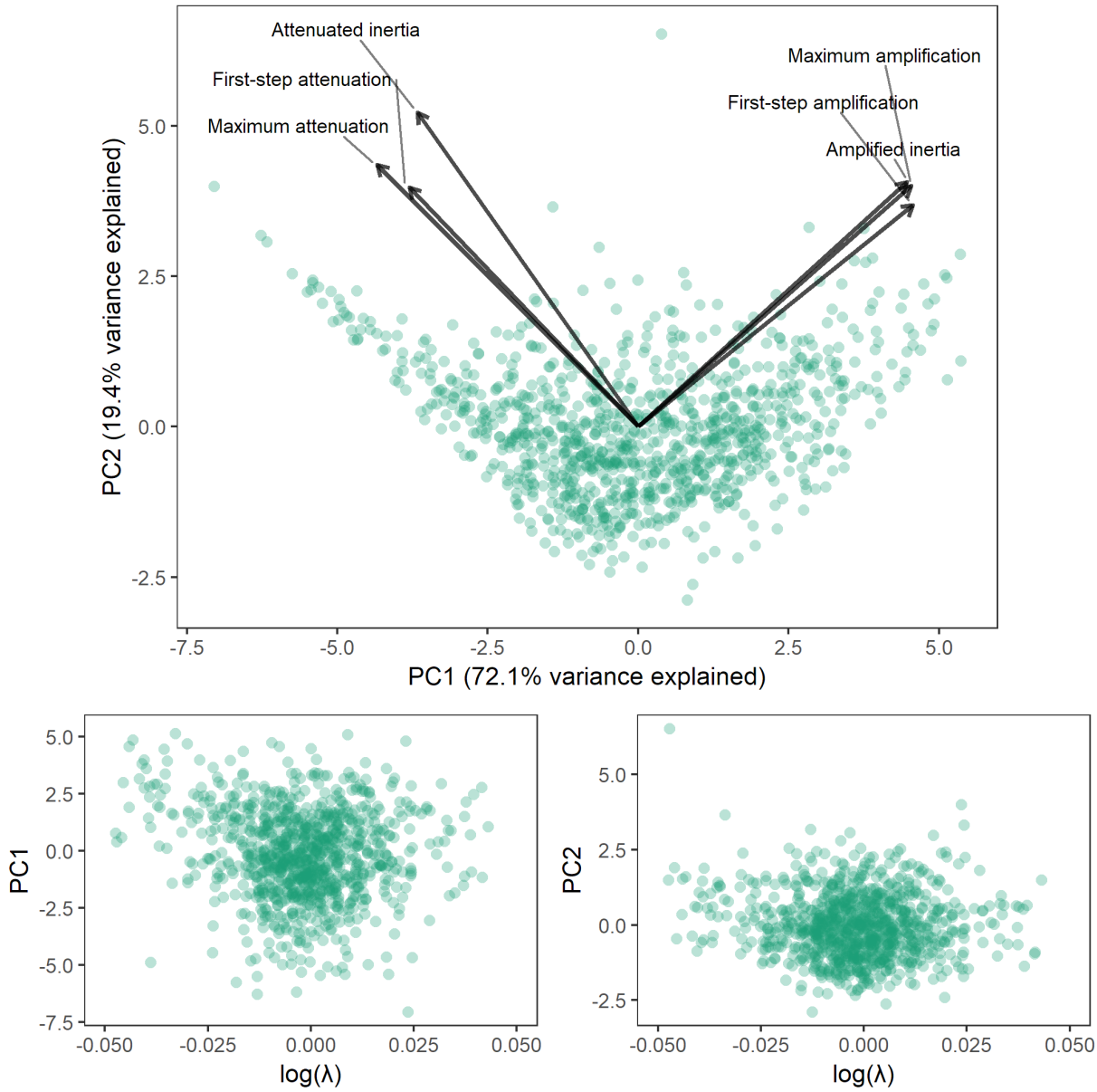


**Figure 3.3: > 90% of (co)variance in six indices of transient dynamics derived from simulated integral projection models (IPMs) can be accounted for by two components derived from a principal component analysis.** The size and direction of arrows indicate loadings of the transient indices towards PC1+2. Each point represents an IPM and its position in the PC1+2 space. Subplots show the relationship between PC1+2 and log long-term asymptotic growth rate ($\lambda$).

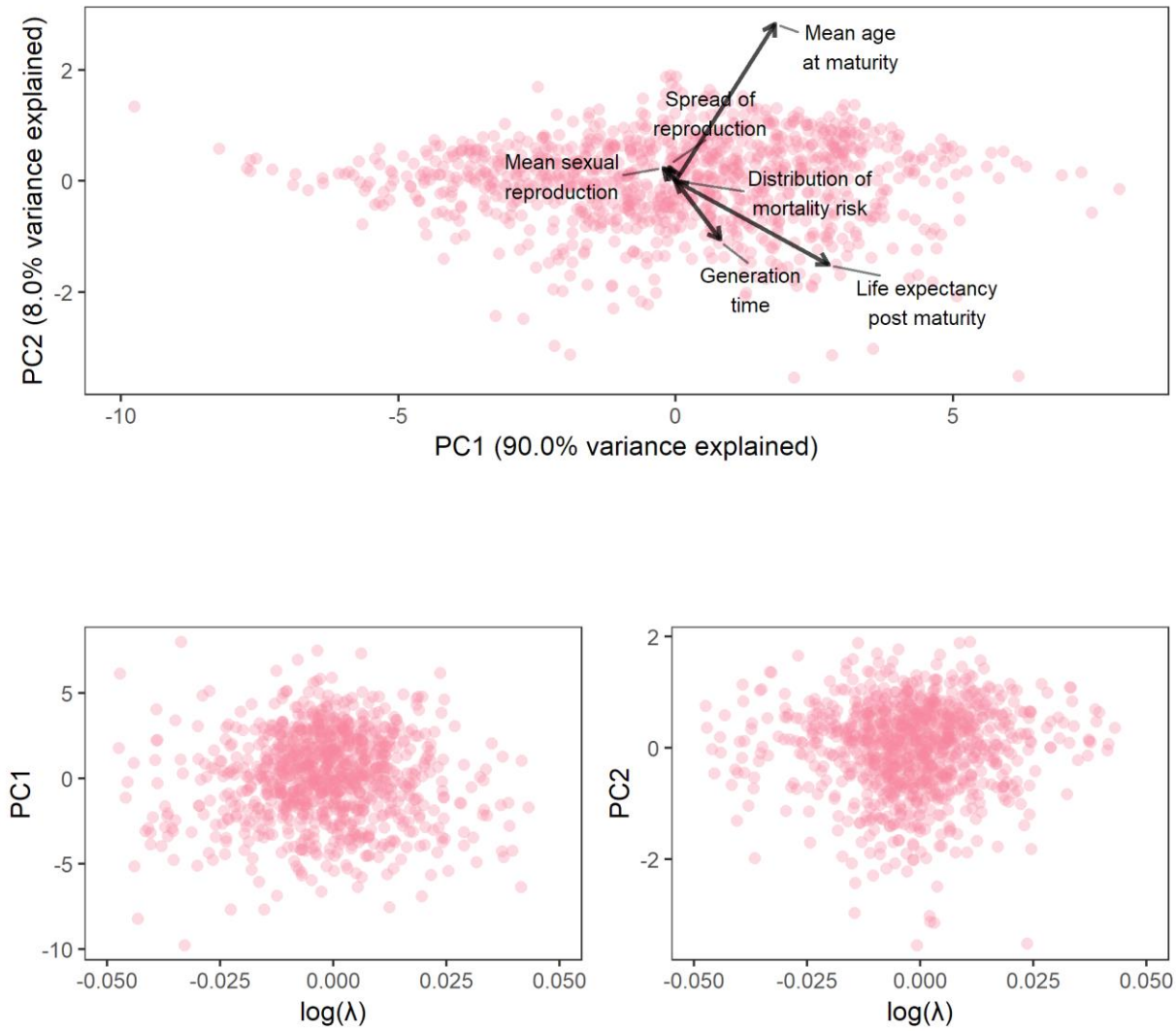


**Figure 3.4: ~98% of (co)variance in six life history metrics derived from simulated integral projection models (IPMs) can be accounted for by two components derived from a principal component analysis.** Size and direction of arrows indicate loadings of the life history metrics towards PC1+2. Each point represents an IPM and its position in the PC1+2 space. Subplots show the relationship between PC1+2 and log long-term asymptotic growth rate ($\lambda$).

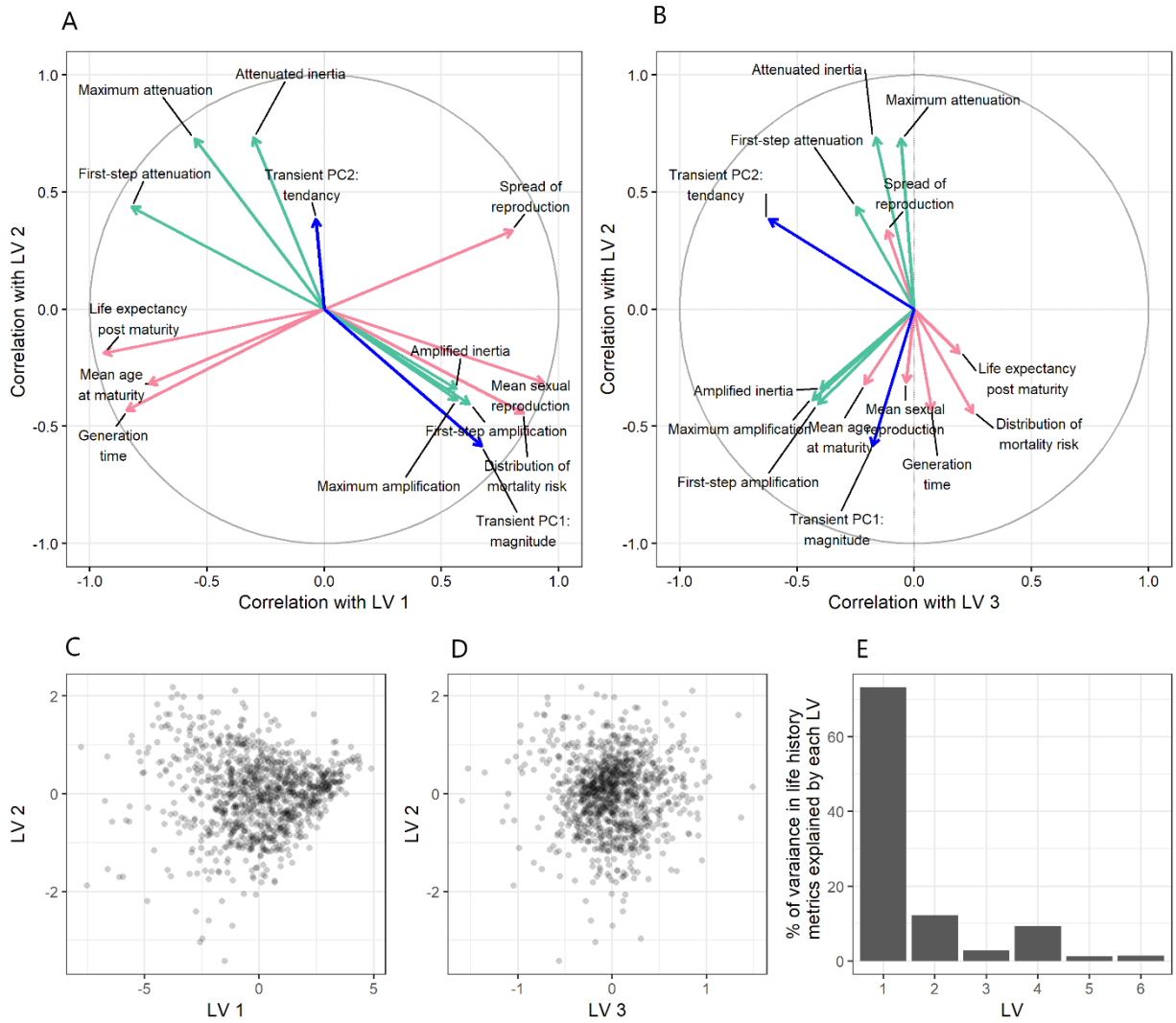


**Figure 3.5: Correlation between the partial least squares regression (PLS) derived latent variables (LVs) 1+2 (A), 2+3 (B) and the life history trait predictor variables (pink), and between LVs and the transient indices (green).** The direction of arrows indicate the variable's correlation with the first two LVs, therefore similar variables are grouped, and variables positioned on opposite sides of the plot origin are negatively correlated. Distance between the origin and the variables represents the strength of correlation to the first two components as calculated by Pearson's correlation coefficient. The axes labels indicate the proportion of variance in life history metrics explained by each LV. The percentage of variance in life history metrics explained by the other LVs is shown in panel E. Panel C and D shows the position of the simulated IPMs on the first three LVs.

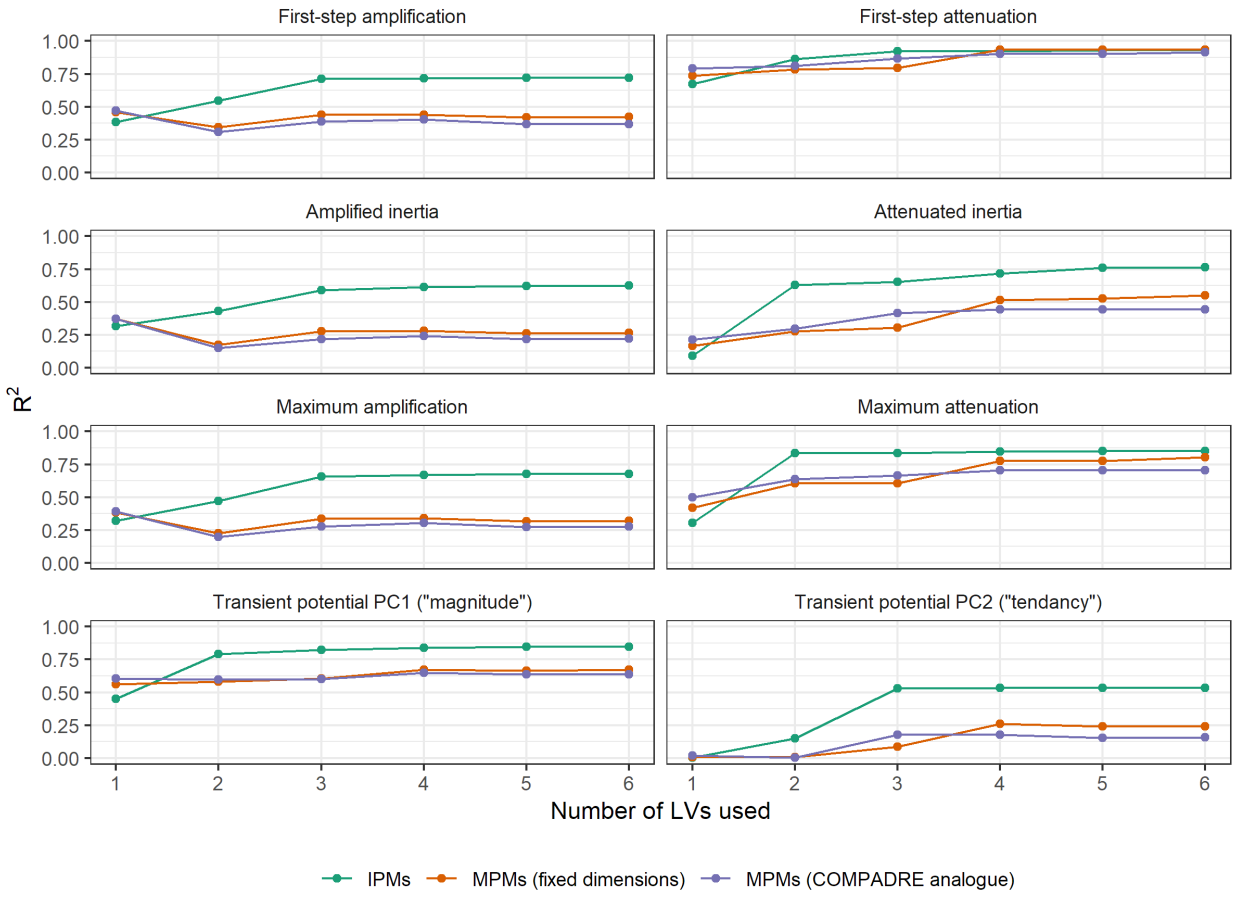


**Figure 3.6: Proportion of variance explained, $R^2$, of partial least squares regressions with increasing numbers of latent variables fitted to three sets of population models each predicting six transient indices from nine life history traits.** An $R^2$ value equalling 1 would represent an exact match between measured and predicted values. The $R^2$ values are calculated by comparing the PLS predicted values to the 'true' measured values derived from an original set of simulated IPMs (Fig. 2). PLSs were fitted to three different sets of population models: IPMs, MPMs with a fixed dimension discretised from the IPMs and COMPADRE analogue MPMs discretised from the IPMs.

# Tables

**Table 3.1:** Cumulative percentage of variance explained by using increasing number of PLS latent variables

| | Number of latent variables | | | | | |
|---|---|---|---|---|---|---|
| | 1 | 2 | 3 | 4 | 5 | 6 |
| Life history metrics | 73.3 | 85.4 | 88.1 | 97.4 | 98.6 | 100.0 |
| First step amplification | 38.3 | 54.6 | 71.3 | 71.5 | 71.9 | 71.9 |
| First step attenuation | 67.3 | 86.3 | 92.3 | 92.4 | 93.0 | 93.0 |
| Amplified inertia | 31.6 | 43.1 | 59.1 | 61.5 | 62.2 | 62.5 |
| Attenuated inertia | 9.0 | 62.8 | 65.4 | 71.5 | 76.1 | 76.2 |
| Maximum amplitude | 32.0 | 46.9 | 65.7 | 66.7 | 67.5 | 67.6 |
| Maximum attenuation | 30.5 | 83.4 | 83.7 | 84.6 | 85.0 | 85.1 |

**Table 3.2:** Life history loadings describing the transformation from each life history metric onto each of the six latent variables.

| | Latent variable | | | | | |
|---|---|---|---|---|---|---|
| | 1 | 2 | 3 | 4 | 5 | 6 |
| Spread of reproduction | 0.394 | 0.44 | -0.316 | -0.589 | -0.499 | 0.624 |
| Age at sexual maturity | -0.367 | -0.417 | -0.576 | -0.741 | -0.157 | -0.251 |
| Distribution of mortality | 0.417 | -0.582 | 0.684 | | -0.43 | -0.161 |
| Mean sexual reproduction | 0.459 | -0.41 | | | 0.635 | 0.13 |
| Mature life expectancy | -0.462 | -0.245 | 0.528 | -0.261 | 0.331 | |
| Generation time | -0.414 | -0.565 | 0.202 | 0.292 | -0.433 | 0.706 |

**Table 3.3:** Transient loadings describing the transformation from each of the six latent variables onto transient indices.

| | Latent variable | | | | | |
|---|---|---|---|---|---|---|
| | 1 | 2 | 3 | 4 | 5 | 6 |
| First step amplification | 0.389 | -0.677 | -1.433 | | -0.313 | |
| First step attenuation | | 0.111 | -0.131 | | | |
| Amplified inertia | 0.339 | -0.547 | -1.342 | 0.264 | -0.419 | -0.223 |
| Attenuated inertia | | 0.115 | | | 0.102 | |
| Maximum amplitude | 0.364 | -0.664 | -1.551 | 0.189 | -0.454 | -0.104 |
| Maximum attenuation | | 0.124 | | | | |

**Table 3.4:** Life history metrics, their description, and the interpretation of large/small values.

| Metric | Description | Smaller value means | Larger value means |
|---|---|---|---|
| Mean sexual reproduction | The mean year to year per-capita number of sexual offspring once the population has converged the stable stage distribution | Low average annual reproduction | High average annual reproduction |
| Generation time | The mean time between two consecutive generations | Short generation time | Long generation time |
| Age at maturity | Age at first reproduction is the age when individuals reach sexual maturity | Early maturation | Late maturation |
| Mature life expectancy | Log ratio of mean age at sexual maturity | Fewer years spent alive and mature | More years spent alive and mature |
| Spread of reproduction | Describes the range between iteroparous and semelparous on a scale of 0 to 1 using the Gini index | Semelparous; few reproductive events | Iteroparous; many reproductive events |
| Distribution of mortality | The standard deviation of the age distribution of mortality | Constant mortality throughout the life cycle | Mortality concentrated at particular parts of the lifecycle |

# Supplementary figures

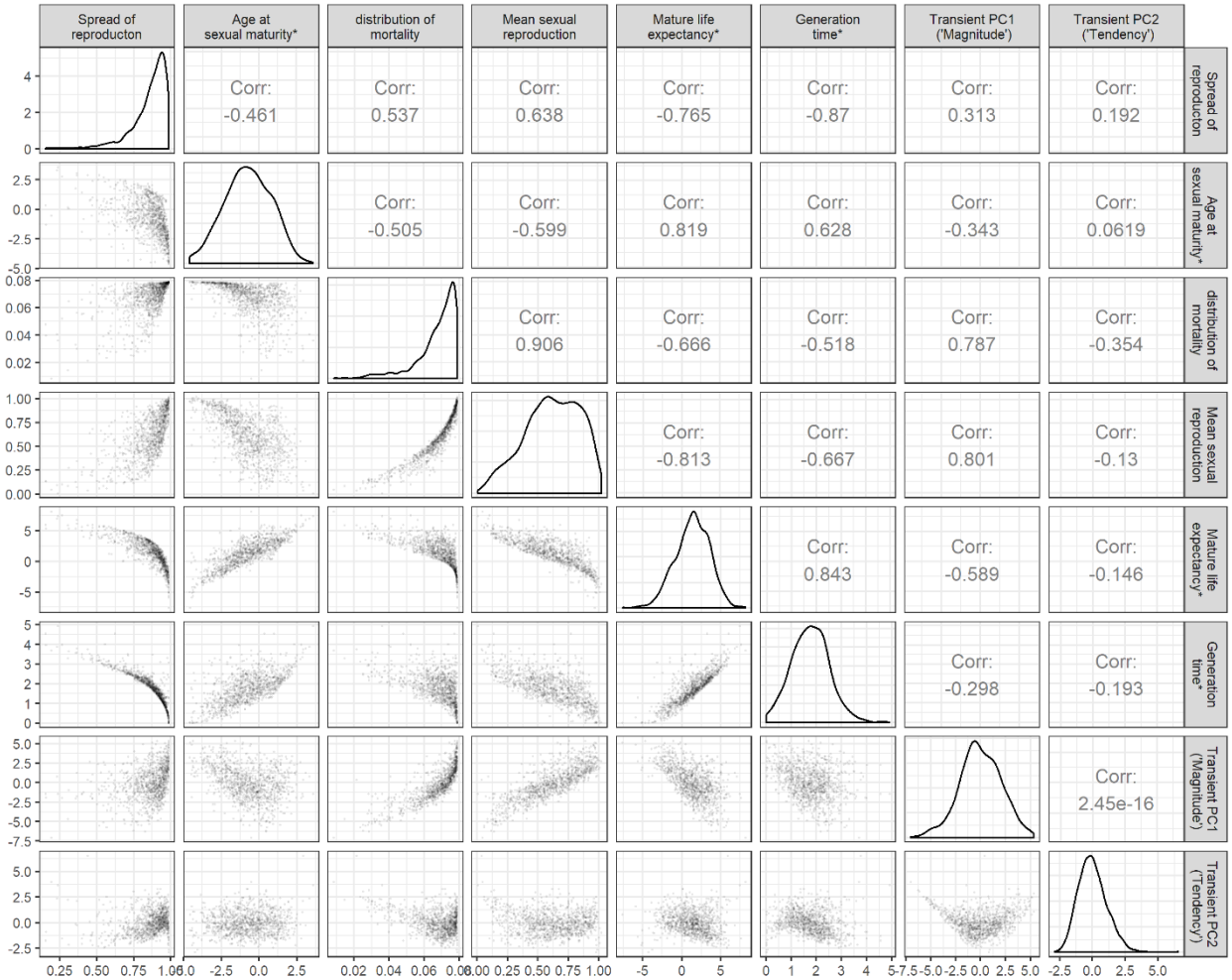


**Supplementary figure S3.1: Non-linear covariance patterns between life history metrics and major axes of transient dynamics.** Pairwise correlations between each of the life history metrics (after transformation) and the first and second principal components derived from a PCA of the 6 transient indices. Transient indices denoted with a * have been $\log_{10}$ transformed. Plots on the diagonal are density plots. Plots on the sub diagonal are pairwise scatter plots. Values on the above diagonals are correlation coefficients where a value of 0 represents no correlation, a value of 1 represents a perfect positive correlation and a value of -1 represents a perfect negative correlation.

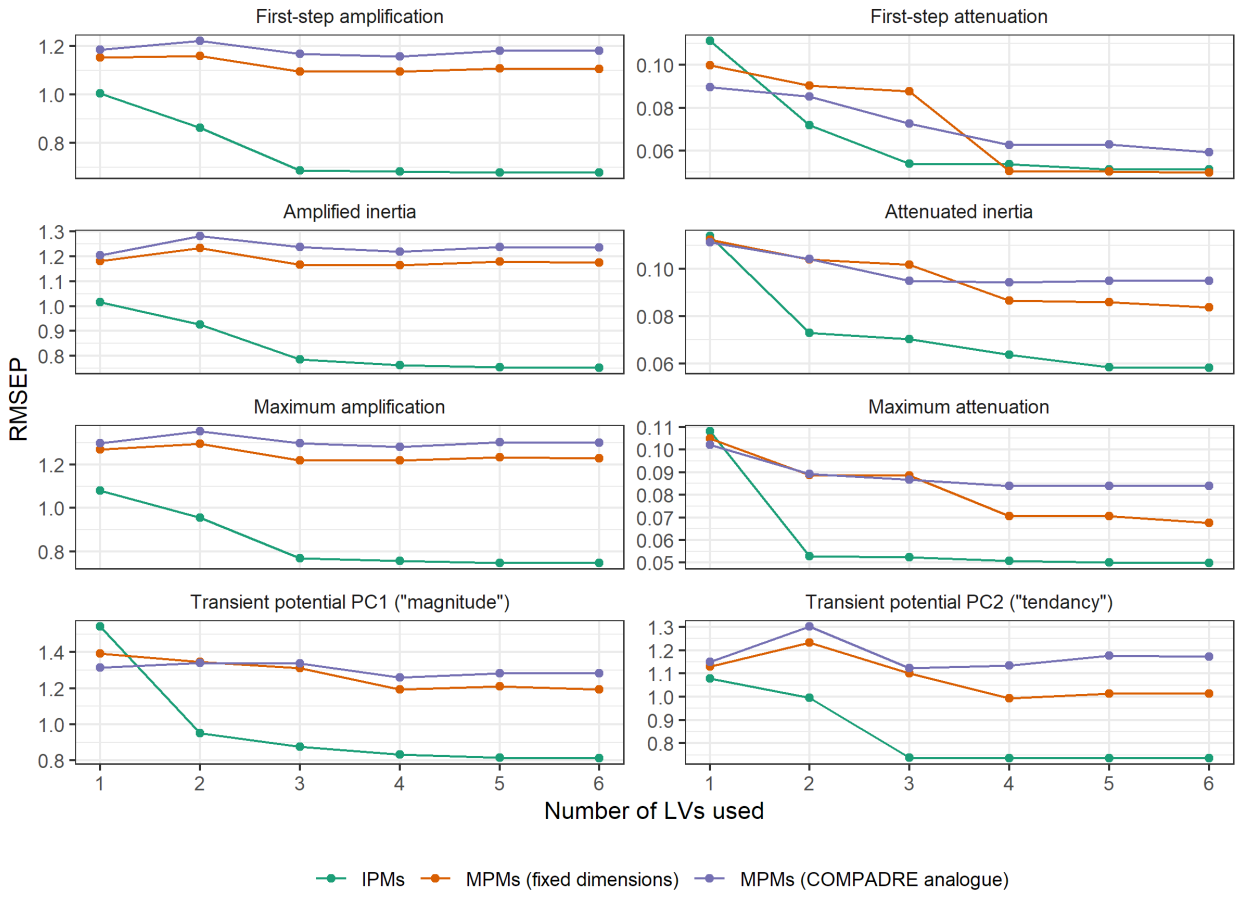


**Supplementary figure S3.2: Root mean squared error of prediction (RMSEP) of partial least squares regressions with increasing numbers of latent variables fitted to three sets of population models each predicting six transient indices from nine life history traits.** The RMSEP values are calculated by comparing the PLS predicted values to the 'true' measured values derived from an original set of simulated IPMs (Fig. 2). PLSs were fitted to three different sets of population models: IPMs, MPMs with a fixed dimension discretised from the IPMs and COMPADRE analogue MPMs discretised from the IPMs.

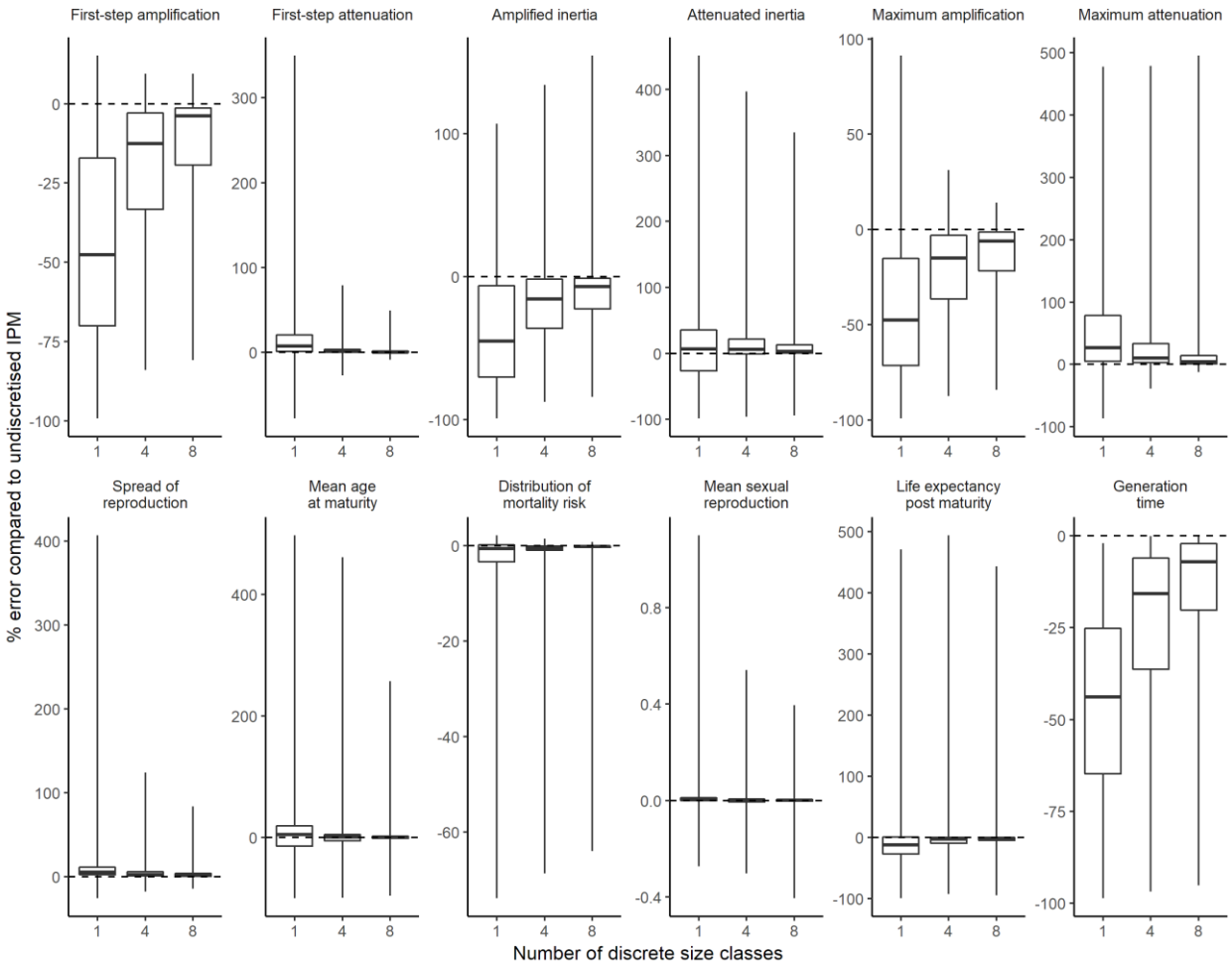


**Supplementary figure S3.3: Discretisation from IPMs to MPMs biases metrics of life history and indices of transient dynamics.** The discretisation of integral projection models (IPMs) to matrix population models (MPMs) affected the value of derived transient indices. The values on the y axis are the percentage error when the MPM derived metrics is compared to the value of the metric calculated from the original IPM. The values on the x-axis are the number of size classes of each MPM. The boxplots represent the median, interquartile range (IQR) and maximum/minimum values.

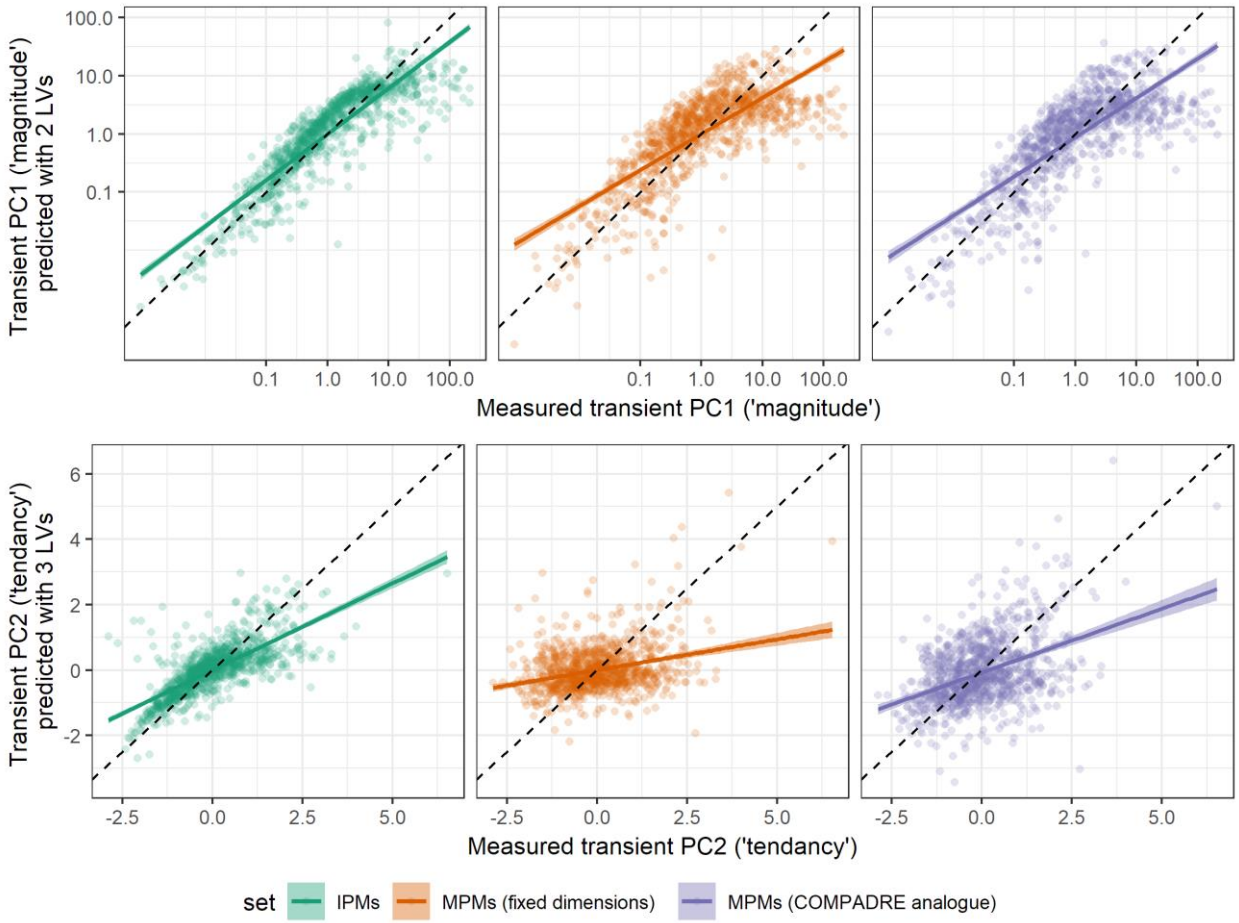


**Supplementary figure S3.4: Major axes of transient dynamics, the magnitude of response and tendency to amplify, can be predicted from life history traits using partial least squares regression (PLS); however, using metrics derived from discretised versions of the population models affects the accuracy of prediction.** Based on a set of simulated IPMs, this plot shows the predicted values for transient PC1 and transient PC2 from a PLS fitted on the IPMs, from a PLS fitted on MPMs with a fixed dimension discretised from the IPMs and a PLS fitted to COMPADRE analogue MPMs. These predicted values are plotted against the values for transient PC1 and PC2 derived from the original IPMs. The dashed line indicates the 1:1 line for perfect prediction. Lines added to highlight bias in the prediction linear model with a 95% confidence interval for the mean value.

# Chapter 4

# Time-varying vital rates for population modelling: how flexible do we need to be?

Simon Rolph[1]*, Roberto Salguero-Gómez[2], Robert Freckleton[1], Jonathan Potts[3], Dylan Childs[1].

[1] Department of Animal & Plant Sciences, University of Sheffield, Alfred Denny Building, Western Bank, Sheffield, S10 2TN, UK.

[2] Department of Zoology, University of Oxford, Zoology Research and Administration Building, 11a Mansfield Road, Oxford, OX1 3SZ, UK.

[3] School of Mathematics and Statistics, University of Sheffield, Hicks Building, Hounsfield Road, Sheffield, S3 7RH, UK.

*Contact author: srolph1@sheffield.ac.uk

# Summary

1. Populations of plants, animals and other organisms show interannual variability in the vital rates of survival, growth, and reproduction. Stochastic population models are a key tool for predicting how temporal variation affects measures of population performance and life history. How we model between-year variability in regression relationships may affect the interpretation of population models and our understanding of population dynamics.
2. Integral projection models (IPMs) enable the use of continuous state structure and parsimonious modelling of trait-fate relationships. Ecologists modelling interannual variability in vital rates for constructing IPMs typically use generalised linear mixed-effects models (GLMMs) with year as a random effect. The use of hierarchical general additive models (HGAMs) provides an alternative, more flexible, approach to modelling interannual variability.
3. We test how different functional approaches to modelling interannual variation affects the outputs of IPMs using 27 years of data from the Soay sheep population on the Scottish island of St. Kilda as a case study.
4. HGAMs scored better in model comparisons and the choice to use HGAMs or GLMMs had some effect on prospective projections and measures of life history. Differences in functional expressions of vital rates resulted in the average size distribution of HGAM-fitted IPMs to have smaller sheep than GLMM-fitted IPMs. This size change is reflected in perturbation analyses: HGAM-fitted IPMs showed that the stochastic long-term growth rate was more sensitive to changes in the vital rates of smaller sheep.
5. This work shows that how model time-variant vital rates do matter for our understanding of ecological systems. However, this work does not invalidate results from previous Soay sheep IPMs. HGAMs provide a robust approach for fitting non-linear time-varying vital rate models and might be especially useful in cases where there are hidden state variables.

# Introduction

Understanding the drivers of population dynamics is a key challenge in ecology (Sutherland et al., 2013). In an evolutionary context, maximising population growth rate is equivalent to maximising fitness (Metcalf & Pavard, 2007). In an applied context, understanding the drivers of population growth rate can aid conservation actions by predicting population viability (Menges, 2000) given sufficient data (Coulson et al., 2001b). Within populations, we observe substantial interannual variability in the vital rates of survival, growth, and reproduction. In turn, among-individual variation in these vital rates is driven by variability in individual-level traits such as size or age. To understand these relationships between traits, vital rates and population dynamics, ecologists typically fit models parametrised by field data to build demographic models such as matrix population models (MPMs) (Caswell, 2001) and integral projection models (IPMs) (Merow et al., 2014). M/IPMs take statistical models of individual trait-fate relationships and use these to infer population-level processes. To ensure reliable inference of population-level processes, is it crucial that the underlying statistical models accurately capture the trait-fate relationships of the study system.

IPMs, and many MPMs, are parametrised using mainstream regression tools that capture the functional form of the trait-fate relationships (Ellner et al., 2016d; Merow et al., 2014). MPMs discretise the fitted regression model into discrete classes whereas IPMs retain the continuous nature of this relationship. As a result, it has been argued that IPMs produce better predictions of population dynamics with fewer data (Ramula et al., 2009) and are not biased from discretising a continuously size-structured population (Picard & Liang, 2014). However, MPMs have considerable flexibility to describe complex demography with any number of life stages and any combination of transition rates between them. A potential limitation of IPMs is that they are over-constrained; the functional expression of vital rates must come from a universe of alternatives and a choice of modelling framework may constrain the range of possible functional forms. These constraints might not be appropriate; for example, assuming linearity when there is no evidence of a linear relationship in the natural system (Dahlgren et al., 2011). This may mean that vital rates models underpinning IPMs are susceptible to biases when the model fails to capture the

relevant relationship between predictors and outputs. That is, when one or more vital rate models underfits the data. The bias-variance trade-off describes the conflict in any model fitting scenario between minimising both bias and variance. This trade-off is important to consider when fitting vital rate models because how adequately the models capture vital rates might affect results from population models, and therefore our understanding of populations.

Long-term studies have enabled researchers to examine stochastic, non-equilibrium population dynamics. For example transient dynamics (Ezard et al., 2010) and incorporating variable environments (e.g. Rees & Ellner, 2009) building on pioneering work by Tuljapurkar & Orzack (1980). It is recognised that incorporating environmental stochasticity (Fieberg & Ellner, 2001) and individual stochasticity (Caswell, 2009) improves population predictions. Modelling vital rates in a variable environment is a key focus of ecological modelling and affects the projected population dynamics and thus our ecological inference. The need to incorporate time-variant processes in population models has implications on the methods used to model vital rates.

There are a multitude of options in how we can model vital rates, any tool that translates predictor variables to response variables can be used, however, only a small subset of these tools is typically used. Generalised linear models (GLMs) are usually the most basic appropriate modelling tool, the generalisation facilitated by link functions is required because vital rates such as survival probability violate the normality assumption. There are a few examples where more flexible, non-linear models such as restrictive cubic splines (Dahlgren et al., 2011) or generalised additive models (GAMs) (González et al., 2013) have been used. With multiple years of data, there are an even greater variety of options to model time-variant vital rates. It is well-known that partial pooling of information using hierarchical models improves inferences (Schaub & Kéry, 2012). This makes intuitive sense for time-variant vital rates: it might be expected that the vital rate function of one year will resemble vital rate functions of other years. For example, the survival probability might increase with size for all years, however, the rate of increase or the overall survival rate may be different for different years. Time-variant, stochastic IPMs can be constructed from vital rate models where a year can be fitted in a GLM as a fixed effect, however, this assumes that the year effect is constant across individuals, which may not be appropriate. An

alternative approach uses generalised linear mixed-effects models (GLMMs) with year as a random effect (Rees & Ellner, 2009). Both GLMs and GLMMs are constrained to have a linear and/or polynomial underlying relationship (on the scale of the link function) and simple parametric forms are typically used which may underfit the data and induce the bias error. Fitting generalised additive mixed models (GAMMs) with year as a random effect is a non-linear approach for modelling time-varying processes however the smoothness of the modelled vital rates must be consistent across years.

An alternative tool for modelling vital rates, currently unused in IPMs, is hierarchical generalised additive models (HGAMs). HGAMs are a natural extension of the GAM framework and allow smooth functional relationships between traits and vital rates to vary between groups (e.g. years) but with pooling towards a common shape. HGAMs can model relationships with five alternative assumptions of interannual variability in functional response (Pedersen et al., 2019). Therefore, HGAMs provide a framework for testing assumptions about the between year variability of the function's smoothness and/or average trends across years. HGAMs provide the strengths of GAMs, the ability to fit non-linear vital rate relationships, but also the strengths of the hierarchical structure of GLMMs, whilst making parsimonious use of data.

Estimates of life history metrics and perturbation analyses might be improved by using more flexible HGAMs for capturing interannual fluctuations in vital rates because they minimise bias whilst not overfitting variance. Demographic models such as MPMs and IPMs can be used to proliferate an initial cohort of individuals through time to visualise survivorship and fecundity across age, even if the models themselves were not age-structured. From these trajectories, life history metrics such as mean life expectancy and age at maturation can be derived (Ellner et al., 2016a). These life history metrics have already been shown to be sensitive to how vital rates are modelled in time-invariant IPMs (Dahlgren et al., 2011; González et al., 2013). Perturbation analyses, or sensitivity analyses, identify the relative importance of different demographic processes for maintaining long term population growth rate (Ellner et al., 2016b). These analyses are used to identify the relative evolutionary importance of particular demographic transitions and are used to target population management actions. Thus, our understanding

of ecological systems, as attained through life history analyses and sensitivity analyses, may be affected by how we model time-varying vital rates.

Using St Kilda's Soay sheep population as a case study we aim to determine if using more flexible models to capture vital rate relationships, traversing the variance-bias trade-off, can improve estimates of life history and demographic outputs. Using 27 years of data from the Soay sheep population, we model vital rates with GLMMs and five forms of HGAM. The Soay Sheep make an ideal case study because individual-based demographic data has been collected since 1985 from annual censuses. There are well-documented differences in environmental sensitivity for sheep at different stages of the life cycle and can be structured by differences in vital rates explained by age and size. We define two IPM structures: a simple one-state IPM for all sheep and a two-state IPM with discrete classes for lambs and adult sheep. We construct four stochastic, time-varying, density-independent IPMs from the combinations of the two IPM structures with vital rates modelled either by GLMMs or the best scoring HGAMs. With these IPMs we implement a suite of routine analyses: calculating population growth rate, calculating life history metrics and perturbation analyses. From these analyses, we aim to determine how our understanding of a population's dynamics and life history is affected decisions regarding modelling vital rates could affect in a variable environment. We test this by looking for differences in life history trajectories and the relative importance of different demographic processes for maintaining long term population growth rate. Ultimately, this work aims to determine whether using more flexible vital rate models should be considered when constructing IPM and provide novel insights into the role of inter-annual variation of vital rates of the Soay sheep in St Kilda.

# Methods

## Field Data

The motivation for developing powerful approaches for modelling vital rates was to then fit these models to real systems to gain a better understanding of that system. An ideal system to test how we model vital rates affects results is the semi-feral population of Soay Sheep on the island of Hirta (Pemberton & Clutton-Brock, 2004). The data used in this analysis were collected from a population of unmanaged Soay sheep (*Ovis aries*) found on the 100-hectare island of Hirta in the St Kilda Archipelago (54°49'N 08°34'W) located 65km offshore from the Outer Hebrides, Scotland. Humans left the island of Hirta in 1930 but established a population of sheep to maintain the grazed pasture (Pemberton & Clutton-Brock, 2004). The island of Hirta has exposed oceanic conditions and its weather system, and sheep population, is highly influenced by the North Atlantic Oscillation (NAO) (Coulson et al., 2001a; Hurrell, 1995). A major cause of mortality in Soay sheep is overwintering conditions (Pemberton & Clutton-Brock, 2004). Lambs are born in March-May and are weaned in August. The population has been studied since the 1950s and a longitudinal individual-based study began in 1985. Since being studied, the population has fluctuated between 600 to 2000 individuals. The subset (approximately 30%) of the population live around the Village Bay area where these individuals are more reliably recorded.

Because we had a good understanding of the basic facets of the study system and because they are a self-contained population with no immigration or emigration, this Soay Sheep population provided a good foundation for testing methodological approaches. We can compare the results of this work to previous research, for example, a time-variant IPM has been constructed with vital areas fitted using GLMMs by Simmonds & Coulson (2015). The Soay sheep have also been used as a model system for several research areas including parasitology (Leivesley et al., 2019), selection (Ozgul et al., 2009) and population ecology (Hindle et al., 2019).

The data chosen for this study include annual census data from 1990 to 2017; years prior to 1990 had insufficient census records for fitting the required statistical models and 2017 was the latest year of data

available to the authors at the time of analysis. Each summer census record contained information about a sheep's capture weight (kg), age (years), whether it survived to the following year (true/false) and whether it reproduced (true/false). Additionally, data was collected on the mothering and fate of lambs: the number of lambs (integer), survival of lambs to the lamb's first census (true/false), size of lamb at the lamb's first census (kg).

## Functional expression of vital rates

Six vital rates were modelled from the Soay sheep data: the probability of survival from t to t+1, size at t+1, probability of reproducing between t and t+1, number of offspring produced, survival of offspring to t+1, size of offspring at t+1. Vital rates were fitted to data for all sheep, data for lambs, and data for adult sheep. These vital rates were first modelled as generalized linear mixed-effects models (GLMMs). The suitably transformed output was modelled as a function of size (kg) with time (year) as a random effect. We used R package mgcv (Simon Wood, 2016) to fit GLMMs. The R function calls for fitting these models are presented in supplementary table 4.1.

Vital rates were also modelled as hierarchical generalised additive models (HGAMs) which are an extension of generalised additive models (GAMs). HGAMs facilitate modelling of nonlinear functional relationships between explanatory factors and response where the shape of the function itself can vary between different grouping levels. We fitted five types of HGAM models based on the families of HGAMs outlined in Pedersen et al. (2019) and can be summarised as follows; model G: A single common smoother for all observations, model GS: a global smoother plus group-level smoothers that have the same wiggliness, model GI: A global smoother plus group-level smoothers with differing wiggliness, model S: group-specific smoothers without a global smoother, but with all smoothers having the same wiggliness, model I: group-specific smoothers with different wiggliness (Fig. 1). 'Wiggliness' is a term introduced in Pedersen et al. (2019) and I use it here for consistency. HGAMs were fitted using R package mgcv (Simon Wood, 2016) using restricted maximum likelihood (REML). The R function calls for fitting these models are presented in supplementary materials.

# Integral projection model

In this study, we used integral projection models (IPMs) to model the age and size-structured population dynamics. The IPM was introduced to ecology by Easterling et al. (2000) and describes transitions over a discrete-time interval between continuous state, with discrete categories. Mathematically an IPM is described as

$$n_{t+1}(z') = \int_L^U K(z', z) n_t(x) \tag{4.1}$$

where z is size at year t and z' is size at year t+1 and n is the size distribution of individuals. The K kernel comprises functions describing the processes of survival, growth, and reproduction.

For our Soay Sheep IPM, we constructed post-reproductive summer census IPMs with a projection interval of one year. We defined a simple one-state IPM definition where individuals were classified by size (capture weight, kg) and no other discrete factor where the population dynamics are described as

$$n(z, t+1) = \int_L^U K(z', z) n(z, t) dz \tag{4.2}$$

The full IPM kernel, $K(z', z)$ was composed of a survival/growth component $\mathrm{P}(\mathrm{z}', \mathrm{z})$ and a reproductive/recruitment component $\mathrm{F}(\mathrm{z}', \mathrm{z})$ which were comprised of functions describing demographic processes, in full:

$$K(z', z) = \mathrm{P}(\mathrm{z}', \mathrm{z})\ \mathrm{F}(\mathrm{z}', \mathrm{z}) = s(z)G(z', z) + \frac{1}{2} s(z) p_b(z) b(z) p_r(z) C_0(z', z) \tag{4.3}$$

where $s(z)$ was survival, $G(z', z)$ was growth, $p_b(z)$ was probability of reproducing, $b(z)$ was the number of offspring, $p_r(z)$ was the probability of a lamb surviving to its first census and $C_0(z', z)$ was the size of lamb at its first census in the summer after birth. The 1/2 was because we were only modelling the females in the population and assumed a 50/50 gender ratio at birth.

To explore how explicitly incorporating structure into the IPM affected demographic outputs we defined a second IPM formulation. By defining IPMs with different complexities, we could determine how fitting vital rates with GLMMs or HGAMs interacted with different IPM structures. Due to known

differences in vital rates, we separated sheep into lambs (L), defined as individuals between the age of 0 and their second summer census, and adult sheep, ewes (E). This produced the second IPM formulation and the population dynamics for this model were described as

$$n_L(z,t+1) = \int_L^U K_{LL}(z',z)n_L(z,t)dz + \int_L^U K_{LE}(z',z)n_E(z,t)dz \tag{4.4}$$

$$n_E(z,t+1) = \int_L^U K_{EE}(z',z)n_L(z,t)dz + \int_L^U K_{EL}(z',z)n_L(z,t)dz$$

where the E and L subscript denotes the life stage of the individual (following similar notation to Childs et al., (2011). $K_{LL}(z',z)$ and $K_{LE}(z',z)$ were recruitment kernels. $K_{EE}(z',z)$ was a survival/growth kernel of adult ewes and $K_{EL}(z',z)$ was a survival/growth kernel describing transitions from summer lambs to adult ewes. These kernels were written out as:

$$K_{LL}(z',z) = \frac{1}{2}\, s_L(z)p_{b,L}(z)b_L(z)p_{r,L}(z)C_{0,\mathrm{L}}(z',z) \tag{4.5}$$

$$K_{LE}(z',z) = \frac{1}{2}\, s_E(z)p_{b,E}(z)b_E(z)p_{r,E}(z)C_{0,\mathrm{E}}(z',z)$$

$$K_{EE}(z',z) = s_E(z)G_E(z',z)$$

$$K_{EL}(z',z) = s_L(z)G_L(z',z)$$

For each of the two types of IPM structures, one-state and two-state, we constructed two different IPMs from the fitted vital rate models. One IPM was constructed from vital rates fitted with GLMMs and the other IPM was constructed using the best fitting HGAM model for each vital rate, as quantified by the lowest Akaike information criterion (AIC) score. Overall, this meant we had constructed four IPMs.

The age structuring in this study was simpler than in other studies which classify individuals as lambs, yearlings, or adults (Hindle et al., 2019). However, by using two IPM class structures, this was sufficient to show that adding more model structure minimised differences arising from whether vital rates were fitted using HGAMs or GLMMs. Another simplification was that vital rates were fitted independently, for example, the size and survival of offspring were independent of the number of offspring, whereas,

in reality, twins are lighter at birth than singletons and size (Wilson et al., 2005). An implementation of modelling reproductive allocation strategies is outlined in Childs et al. (2011).

From each kernel, an iteration matrix was derived for the computational implementation of the IPM. An iteration matrix is a discretised approximation of the continuous kernel at a sufficiently high resolution that the kernel resolution has a negligible effect on outputs such as growth rate. The upper and lower size limit of the kernels were set to 0kg and 50kg respectively to prevent eviction; eviction describes cases where individuals fated for a size outside the size limits are lost (Williams et al., 2012).

## Stochastic IPM

We incorporated environmental stochasticity to improve our estimates of life history metrics, perturbation analyses and long-term growth rate. There are two main approaches to incorporating environmental stochasticity into an IPM: kernel selection and parameter selection (see Ellner et al., 2016). We implemented density-independent environmental stochasticity using kernel selection by constructing a set of kernels using the year-specific sets of parameters. We generated sets of kernels for both IPM structures (1-state and 2-state), for each model-fitting method (GLMM and HGAM) and for every interannual transition. This resulted in four sets of kernels corresponding to the four different IPMs. We generated the kernel for each year by using the predict.gam function from R package mgcv (Simon Wood, 2016) to calculate the response at points across the size domain by midpoint approximation. For all our simulations of stochastic environments, we assumed an identical independent distribution (i.i.d.) where every annual transition kernel has an equal probability of being sampled at each time-step.

## Calculating life history traits

We calculated a set of life history traits from our IPMs by using methods from Ellner et al. (2016a) based on Markov chain theory. These methods were extended for use with a stochastic environment by constructing megakernels where individuals are now cross-classified by the environment in addition to being classified into adults or lambs. This is an analogous approach to using megamatrices for cross classifying MPMs (e.g. Tuljapurkar & Horvitz, 2006). To construct megakernels, we generated kernels whose dimensions are given by the product of the dimension of the discretised size kernel with the

number of age classes with the number of temporal variants of the environment. One megakernel was produced for each of the four IPMs, $K_{mega}$, which was split into the fecundity megakernel, $F_{mega}$ and survival megakernel $P_{mega}$. From these megakernels we calculated the main results of analyses of individual life trajectories outlined in table 3.3 of Ellner et al. (2016a).

To investigate how life history trajectories were affected by size at birth, metrics were calculated as a function of initial size, z0. We calculated the survival probability to age a, $l_a(z_0)$, and average per capita fecundity at age a conditional on survival to age a, $f_a(z_0)$. To visualise the survivorship and fecundity curves we fitted a Gaussian distribution to a dataset of the size of lambs at first census to define a starting cohort c(z). From this starting cohort, we calculated $l_a(z_0)$ and $f_a(z_0)$. We calculated the fundamental matrix, $N_0$, of the megakernels to calculate mean and variance in lifespan, probability of reproducing at least once, mean size at death and mean age at first breeding.

## Perturbation analyses

We used prospective perturbation analyses to identify how changes to vital rates at different sizes affected stochastic population growth rate, $\lambda_s$. Prospective perturbation analyses determine which vital rates are most important to the population's survival and at that stage/size these vital rates are most sensitive. Perturbations can be applied at different levels of the IPM's structure: kernel, vital rate function, or parameter (Ellner et al., 2016b). Parameter level perturbations did not have a useful ecological interpretation for HGAMs, nor could we have made an equal comparison between parameter perturbations for GLMMs and HGAMs because different model-fitting methods had different parameter structures. Kernel-level perturbations would have identified the effect of changes to a composite of different vital rate functions and so were less insightful. Therefore, for this analysis, we focussed on function-level perturbations. For these perturbation analyses, we did not need to take a mega kernel approach. We followed the overall perturbation methods from Ellner et al., (2016b, page 93) with the methods for perturbation analyses with environmental stochasticity (Ellner et al., 2016c, page 211) but adapted for a 2-state model. A perturbation to the standard deviation (SD) of a vital rate represented a test of how

long-term stochastic growth was affected by the result of an increase in the year-to-year variability of the vital rate: did a population respond to a more variable environment?

We chose to calculate elasticities and sensitivities analytically as opposed to numerically because numerical calculations were more computationally intensive. Sensitivity was defined as a partial derivative: we calculated the partial derivative of stochastic growth rate $\lambda_s$ with respect to a vital rate which we have perturbed by a very small value $\epsilon$ and can be expressed, using Tuljapurkar's small fluctuation approximation (SFA) (Tuljapurkar & Haridas, 2006) as

$$\frac{\partial log \lambda_s}{\partial \epsilon} = \frac{1}{\lambda_s}\frac{\partial \lambda_s}{\partial \epsilon} = E\left[\frac{\langle v_{t+1}, C_t w_t\rangle}{\langle v_{t+1}, K_t w_t\rangle}\right] \tag{4.6}$$

where $C_t$ is a perturbation kernel that in the format of perturbing $K_t$ to $K_t + \epsilon C_t$. The time-varying population structure $w_t$ and reproductive value $v_t$ were calculated from these formulas

$$\widetilde{w}_{t+1} = K_t w_t, \qquad w_{t+1} = \widetilde{w}_{t+1} \,/\, \int_L^U \widetilde{w}_{t+1}(z)dz \tag{4.7}$$

$$\tilde{v}_{t-1} = v_t K_{t-1} = \int_L^U v_t(z')K_t(z', z)dz', \quad v_{t-1} = \tilde{v}_{t-1} \,/\, \int_L^U \tilde{v}_{t-1}(z)dz$$

where $K_t$ was the full kernel $K$ for year $t$ and U and L were the lower and upper size limits, respectively. For constructing $C_t$ for vital rate perturbation, we applied perturbations to mean vital rate and variance with the coefficient of variance = σ/μ which is represented as

$$p_t \rightarrow p_t + \epsilon p_t \tag{4.8}$$

where $p_t$ is the vital rate function for a given year t and $\epsilon$ represents the very small value. We applied this perturbation by using a direc, δ, function. A δ function can be thought of as a gaussian distribution with a variance that is shrunk to zero and was used to describe how we perturbed a vital rate around a particular size $z$. δ functions are explained in Ellner et al. (2016b, Page 91). For example, a perturbation to the probability of survival vital rate looks like

$$s(z, \theta(t)) \rightarrow s(z, \theta(t)) + \epsilon s(z, \theta(t))\, \delta_{z_0}(z) \tag{4.9}$$

and substituting this into the full kernel (Eqtn. 4.3) and collecting the $\epsilon$ terms produced a perturbation kernel $C_t$. The survival function is part of both the survival/growth component $\mathrm{P}(\mathrm{z}', \mathrm{z})$ and the fecundity component $\mathrm{F}(\mathrm{z}', \mathrm{z})$ so the perturbation kernel is defined as such:

$$C_t(z, z') = s\big(z, \theta(\mathrm{t})\big)G\big(z', z, \theta(\mathrm{t})\big)\delta_{z_0}(z) + \frac{1}{2}s(z, \theta(\mathrm{t}))p_b(z, \theta(\mathrm{t}))p_r(z, \theta(\mathrm{t}))C_0(z', z, \theta(\mathrm{t}))\delta_{z_0}(z) \tag{4.10}$$

The perturbation kernel $C_t$ can be substituted into the sensitivity equation (4.5) and can be calculated as

$$\frac{1}{\lambda_s}\frac{\partial \lambda_s}{\partial \epsilon} = E\left[\frac{\langle v_{t+1}, C_t w_t\rangle}{\langle v_{t+1}, K_t w_t\rangle}\right] = \int\int E\left[\frac{v_{t+1}(z')w_t(z)C_t(z', z)}{\langle v_{t+1}, K_t w_t\rangle}\right] dz\, dz' \tag{4.11}$$

For the two-state model, the perturbation is applied slightly differently. Instead of just $C_t$ we have $C_{tLL}$, $C_{tLE}$ for perturbations to recruitment transitions, $C_{tEE}$ for perturbations to adult survival and $C_{tEL}$ for perturbations transitions from lambs to adult sheep. We used survival as an example again and by substituting equation 4.8 into the two-state model (Eqtn. 4.4) gives us

$$\begin{aligned} C_{tLL}(z, z') &= \frac{1}{2}\, s_L(z, \theta(\mathrm{t}))p_{b,L}(z, \theta(\mathrm{t}))b_L(z, \theta(\mathrm{t}))p_{r,L}(z, \theta(\mathrm{t}))C_{0,\mathrm{L}}(z', z, \theta(\mathrm{t}))\delta_{z_0}(z) \\ C_{tLE}(z, z') &= \frac{1}{2}\, s_E(z, \theta(\mathrm{t}))p_{b,E}(z, \theta(\mathrm{t}))b_E(z, \theta(\mathrm{t}))p_{r,E}(z, \theta(\mathrm{t}))C_{0,\mathrm{E}}(z', z, \theta(\mathrm{t}))\delta_{z_0}(z) \\ C_{tEE}(z, z') &= s_E\big(z, \theta(\mathrm{t})\big)G_E\big(z', z, \theta(\mathrm{t})\big)\delta_{z_0}(z) \\ C_{tEL}(z, z') &= s_L\big(z, \theta(\mathrm{t})\big)G_L\big(z', z, \theta(\mathrm{t})\big)\delta_{z_0}(z) \end{aligned} \tag{4.12}$$

and for the two-state IPM, equation 4.10 looks like

$$\begin{aligned} \frac{1}{\lambda_s}\frac{\partial \lambda_s}{\partial \epsilon} = {} & E\left[\frac{\langle v_{t+1,L}, C_{t,LL} w_{t,L}\rangle}{\langle v_{t+1,L}, K_{t,LL} w_{t,L}\rangle}\right] + E\left[\frac{\langle v_{t+1,L}, C_{t,LE} w_{t,E}\rangle}{\langle v_{t+1,L}, K_{t,LE} w_{t,E}\rangle}\right] \\ & + E\left[\frac{\langle v_{t+1,E}, C_{t,EE} w_{t,E}\rangle}{\langle v_{t+1,E}, K_{t,EE} w_{t,E}\rangle}\right] + E\left[\frac{\langle v_{t+1,E}, C_{tEL} w_{t,L}\rangle}{\langle v_{t+1,E}, K_{tEL} w_{t,L}\rangle}\right] \end{aligned} \tag{4.13}$$

and the equivalent integration equation 4.11 can be derived from equation 4.13.

The perturbation analysis was implemented by simulating a stochastic environment for 10,000 time-steps with a uniform starting distribution. To allow the simulation to progress from the uniform starting

distribution to a time-varying 'stable' size structure we excluded the values for the first 500 values. Each time-step we randomly chose a projection kernel for any of the 26 annual transitions and projected the population based on that kernel. Independent and identically distributed (i.i.d.) assumptions remain in place; all projection kernels were always as likely to occur as any other. For each of the four IPMs, the perturbation analyses were repeated for each vital rate: the probability of survival from t to t+1, size at t+1, probability of reproducing between t and t+1, number of offspring produced, survival of offspring to t+1, size of offspring at t+1. The same randomly generated sequence of years was used for the kernel selection step of the perturbation analyses for each of the vital rates of each of the IPMs.

# Results

Size and year were important predictors of an individual's vital rates, but more flexible functional forms were needed to capture state-fate relationships in the 1-state IPM structure because lambs and adult sheep were demographically distinct (Supplementary fig. S4.1-S4.2). In all vital rate models adding the year as an explanatory factor improved the model fit, as measured by AIC score (Tables 4.1-4.3) and global size-dependent trends were underlying the interannual fluctuations. This is evidenced by the fact that the best performing HGAM models for all vital rates had a global trend with either a group-level trend with the same wiggliness (GS) or differing wiggliness (GI) (Tables 4.1-4.3). The size was positively correlated with higher survival, more offspring, and larger offspring. However, this positive trend did not hold for some vital rates beyond a certain size; the probability of reproduction and the survival probability of offspring had a negative correlation with size after approximately 25kg (Supplementary fig. S4.1-S4.2). This negative correlation was captured more distinctly in HGAMs than GLMMs (S4.1-S4.2). It was more important that the modelling tool could capture this non-linear feature in the 1-state IPM than the 2-state IPM because modelling the vital rates separately in the 2-state model split the data; this, in effect, created a piecewise regression that could better accommodate the non-linear functional form. As a result, the vital rates of larger sheep (approximately >25kg) and smaller sheep (approximately <10kg) fitted with GLMMs, especially in the 1-state IPM structure, were inflated to be higher

than their HGAM equivalent. This was especially prominent in the probability of reproducing, probability of reproduction and size of offspring (Supplementary fig. S4.3). When comparing how the modelling approaches captured interannual variation, in our case study HGAMs fitted a more consistent functional form for each year, whereas GLMMs exhibited more variety in the strength and direction of the association between size and vital rate.

The four different IPMs produced generally consistent predictions about the long-term population dynamics, however, GLMM-fitted IPMs produced a population of larger individuals. All four models predicted a long-term population increase; stochastic long-term growth rates were between 1.051 and 1.062 with the 2-state IPMs predicting lower growth rates (Table 4.4). Across the survey period (1991 to 2017), the one-step growth rates of the 1-state IPM were more closely associated with the observed population and exhibited minimal difference between the GLMM-fitted IPM and HGAM-fitted IPM (Supplementary fig. 4.4). In contrast, the 2-stage IPMs had one-step growth rates a greater distance from the observed growth rates and were less consistent when comparing the GLMM-fitted IPM to the HGAM-IPM. The one-step growth rate for the year 1991 of the 2-state models showed a negative growth rate, whereas the observed data and GLMM-fitted IPMs showed a positive growth rate. Across all four IPMs, the stable size/state distributions (SSD) of stochastic population projections were bimodal: the majority of the female populations were comprised of adult sheep that were between 15 and 30 kg in weight with a smaller cohort of lambs that were between 8 and 17kg (Fig. 4.2). The bimodality of the SSDs of the 1-state IPMs was more pronounced when vital rates were fitted using HGAM. Across both 1-state and 2-state IPMs, the SSDs of GLMM-fitted IPMs consisted of larger sheep than the SSDs of HGAM-fitted IPMs (Fig. 4.2). This change in size was most apparent in adult sheep and the 2-state IPM, there was a negligible difference in the SSD of first-year individuals (Fig 4.2).

Differences in whether vital rates were modelled with HGAMs or GLMMs affected trajectories of life history, which in turn affected life history metrics. However, the effect of the modelling method on life history was contingent on whether a 1-state or 2-state IPM structure was used. All IPMs showed a type II survivorship curve with a low, but highly annually variable, lamb survival (Fig. 4.3, top row). There were fewer differences in survivorship curves between the GLMM-fitted IPM and the HGAM-fitted

IPM for the 2-state IPMs than the 1-state IPMs. Average per capita fecundity ($f_a$) of a surviving cohort of lambs for age ($a$) 0 to 8 showed differences due to whether the IPM's underlying vital rates were modelled with GLMMs or HGAMs (Fig. 4.3, bottom row). If vital rates were modelled with HGAMs, the per capita fecundity steeply increased as a sheep ages but then flattens by age 4 to a value of ~0.37. This trend is consistent for IPMs with HGAM-fitted vital rates for both 1-state model and 2-state models whereas for IPMs with GLMM-fitted vital rates the fecundity curve was steeper for the 2-state model than the 1-state model and did not flatten by age eight years. These differences were a consequence of the inflated vital rates for larger sheep that resulted from fitting vital rate using less flexible GLMMs. In terms of life history metrics, we found that GLMM-fitted 1-state IPM producing results least consistent with the other 3 IPMs. The 2-state IPM produced similar estimates for their mean life expectancy of 4.86 and 4.80 years for the GLMM-fitted and HGAM-fitted IPM, respectively (Table 4.4). However, the 1-state, GLMM-fitted IPM predicted longer lives sheep with a life expectancy of 5.32 years whereas the HGAM-fitted 1-state IPM was closer to the 2-state IPMs with a predicted life expectancy of 5.01 years. We saw a similar pattern for variance in life span, $\sigma_\eta^2$, with a value of 91.7 produced by the GLMM 1-state IPM but between 55-59 for the other three IPMs.

Out of the modelled vital rates, the stochastic population growth rate was most sensitive to perturbations of the survival and growth, and least sensitive to the reproductive rates of lamb (Fig. 4.4). The stochastic growth rate was not sensitive to perturbations to the reproductive vital rates of lambs. The shifts in SSD that we observed due to differences in model fit are reflected in the results of a perturbation to the vital rate function (Fig. 4.4); GLMM-fitted IPMs identified that sheep were more sensitive to vital rate perturbation at larger sizes than HGAM-fitted IPMs. The elasticity functions for the mean vital rates peak at a smaller size in the HGAM-fitted version of all models. Relative to GLMM-fitted IPMs, HGAM-fitted IPMs identified growth and survival to be less sensitive to perturbation and reproductive vital rates to be more sensitive (Fig. 4). There were two exceptions to this: for the 2-state IPM structure, the stochastic growth rate was more sensitive to perturbations to the probability of reproduction and survival probability of offspring when vital rates were fitted by HGAM rather than GLMMs (Fig. 4.4).

At any size, increases in the year-to-year variability of the vital rate of survival or growth negatively impacted long-term growth rate (Fig. 4.5), however, perturbations to the standard deviation (SD) of the size of offspring birthed by adult sheep at year t+1 always positively population growth rate (Fig. 4.5). For the other three vital rates, perturbations to the SD of the probability of reproduction, number of offspring and the survival probability of offspring had a relatively small effect, as indicated by the much smaller values for stochastic elasticity to standard deviation (Fig 4.5). These elasticities were less sensitive to perturbations but, depending on how vital rates were fitted, the elasticity for one IPM could exhibit both positive and negative effects of perturbation to SD for different sized individuals. Some vital rates were not affected; in the 2-state model, the vital rate for a lamb's size of offspring was not affected by perturbation to that standard deviation of that vital rate (Fig. 4.5). For the vital rates of survival, growth, and size of offspring, the three vital rates for which $\lambda_s$ was most sensitive to perturbations to, $\lambda_s$ was sensitive to perturbations at larger sizes for GLMM-fitted IPMs when compared to HGAM-fitted IPMs. Across these vital rates, HGAM-fitted IPMs produced results that suggested that $\lambda_s$ was more sensitive increases in the year-to-year variability than their GLMM-fitted counterpart with larger elasticity peaks. The other three vital rates, probability of reproduction, number of offspring, and survival of offspring, were even more affected by model fit and produced quite different results depending on model structure and model fit. For example, GLMM-fitted 1-state IPM predicted that $\lambda_s$ was negatively affected by increases in the variability of the survival probability of offspring from adult sheep (>24kg), however, the HGAM counterpart predicted that $\lambda_s$ was positively or not affected by the same perturbation. For survival and growth, across 1-state and 2-state IPMs, the HGAM-fitted IPMs produced generally more consistent results, whereas, across the other 4 vital rates, GLMMs produced more consistent results.

# Discussion

Previous IPMs have typically used less flexible models to minimise the risk of overfitting (eg. Childs et al., 2003; Kuss et al., 2008; Simmonds & Coulson, 2015) but in this work, we have shown that using more flexible HGAMs can improve predictions from stochastic IPMs. We tested this by constructing four different IPMs of the Soay Sheep of St Kilda using two model structures with time-variant vital rates models fitted by HGAMs or GLMMs. We found that using HGAMs was a natural extension to the existing repertoire of models used to fit vital rates for IPMs and better captured the vital rate relationships in our study; we found that HGAMs outperformed GLMMs when scored by AIC. The choice of vital rate model subtly impacts the model outputs and can affect our interpretation of the results. We found that IPMs with vital rates fitted with GLMMs had overinflated survival of large individuals which increased the average size of sheep in stochastic population simulations. This shift in stable stage distribution was reflected in the sizes that long term stochastic growth rate, $\lambda_s$, was sensitive to vital rates perturbations. When using HGAMs to model vital rates temporal variation manifested differently in each vital rate function. These differences affected how the long-term growth rate was sensitive to perturbations to the standard deviation of each vital rate. Model structure, whether lambs and adult sheep were modelled together or separately, affected life history trajectories and metrics of life history; however, model structure had a lesser effect if HGAMs were used to model vital rates.

The flexibility required for modelling vital rates depends on what outputs are to be calculated from an IPM. In our case study, GLMMs were flexible enough for calculating life history metrics which were mean measures such as mean life expectancy and mean size at death, and long-term growth rate. The measures derived from HGAM or GLMM fitted IPMs were not identical, but the differences would not substantially affect the interpretation of results. However, variance in lifespan, a life history metric that was a measure of variance, was much more affected by whether GLMMs or HGAMs were used to fit vital rates for a 1-state IPM. Again, we did see that incorporating an age structure produced more consistent measures of variance in lifespan across HGAM and GLMM-fitted IPMs but for the 1-state IPM, variance in lifespan derived from the HGAM-fitted IPM was much closer to the metrics derived from

the 2-state IPMs. This may be a general result that added flexibility in vital rate models improves estimates of metrics of variance, but we would need more examples of this across other case studies to confirm this generalisation. The shift in stable state distribution due to using HGAMs or GLMMs, and its subsequent effect on perturbation analyses, shows that the added flexibility is important if perturbation analyses is an output of the IPM.

More flexible vital rate models might be useful when there are hidden or unmeasured additional state variables. For example, age is often an unmeasured variable because an organism is hard to age (e.g. Brault & Caswell, 1993). The need to test more flexible models stems from a concern that IPMs are too constrained because, in contrast to MPMs, they must model vital rates from a universe of alternatives, of which only a subset of models is typically used. Whilst previous work has shown how using more flexible non-linear functional forms can better capture vital rate relationships (Dahlgren et al., 2011; González et al., 2013), our work shows that it is possible to extend this flexibility to how we capture time-varying vital rates. In practice, implementing a stochastic IPM with HGAMs is no more complex than using GLMMs. In our study HGAMs was a better fit for the data than GLMMs, this was especially apparent in a simpler model structure. Furthermore, this means that more flexible HGAMs might be an appropriate approach for modelling vital rates in high volume demographic data collected via image analysis (e.g. Bruijning et al., 2018) and/or remote sensing (e.g. Tredennick et al., 2016) because these methods focus on measuring continuous physical attributes. However, in our case study, the 'hidden' state variable was age, of which the two age classes of lambs and adults populated largely distinct size ranges. Therefore, a non-linear functional form could describe the distinct vital rates of these groups along a single axis. HGAMS might not provide the same improvements over GLMMs in cases where a hidden variable (e.g. age) does not correlate with the modelled continuous state variable.

Our results are broadly consistent with previous work on the Soay sheep population. Size was an important predictor of vital rates but lambs and adult sheep were demographically distinct (Catchpole et al., 2000), lamb survival was more temporally variable than adult survival (Hindle et al., 2019), and we observed cyclical patterns of population crashes (Coulson et al., 2001a). However, our results also provide some are new insights, particularly concerning the role of size-dependent variation on population

growth. For example, that increased variability in reproductive vital rates had negative or positive impacts on population growth rate depending on what size this increase in variability was acting, and whether we used HGAMs or GLMMs to those vital rates. This effect of changes in variability in vital rates is important to understand, especially as we expect greater variability in vital rates because climate change is predicted to affect the North Atlantic Oscillation (NAO) leading to more variability in the environment (Simmonds & Coulson, 2015). This is important to correctly model because research has shown that a changing climate is leading to smaller sheep (Ozgul et al., 2009), and so it's important to understand at which sizes selection is acting; however, in this case, the shrinking of sheep is primarily attributed to environmental effects despite the heritability of sheep size. In other settings, if a study's purpose is to advise on population management actions (e.g. Gerber & Heppell, 2004), a shift in the results in a sensitivity analysis could result in management actions being targeting inappropriately (Easterling et al., 2000). Despite some differences in our results from HGAM IPMs and GLMM IPMs, when age structuring was incorporated these differences were fairly minimal. Since previous studies on Soay sheep have incorporated age structuring (Catchpole et al., 2000; Hindle et al., 2019; Ozgul et al., 2009; Simmonds & Coulson, 2015), their results are unlikely to have been invalidated by our findings.

There are implications in how HGAM IPMs can be used because of the loss of interpretability of the model parameters. For example, in a typical GLMM-fitted vital rate model the parameters represent time-varying slopes and intercepts of each vital rate (Ellner et al., 2016c) whereas in HGAM the parameters refer to a series of smooth functions (Pedersen et al., 2019). In this work, we implemented stochasticity using kernel selection which generates a transition matrix for each year of data available and simulates a population by randomly selecting a kernel at each timestep. An alternative method of incorporating stochasticity in IPMs is to do parameter selection which generates a unique kernel for each time step by sampling the parameters of each vital rate model and constructing a transition matrix for each set of sampled parameters (Ellner et al., 2016c). Whilst technically possible, sampling HGAM parameters to generate unique kernels would be unlikely to produce realistic transition matrices. Nonetheless, implementing stochasticity via parameter selection is less common because it can negate important intra-annual correlations between vital rates which can be an important part of assessing

uncertainty in model prediction (Fieberg & Ellner, 2001). For the same reason as stochasticity cannot be implemented by parameter selection, HGAMs cannot be used to calculate the elasticity to perturbations to vital rate parameters and are restricted to elasticities to function perturbations and kernel perturbations. Another method that is limited by using HGAMs is state-space integral projection models (SSIPMs). This is an approach for estimating demographic parameters from time series of size-structured survey data using a Bayesian framework (White et al., 2016). However, parameters of HGAM IPMs would be harder to sample, as opposed to simple slope and intercepts, because of poorer parameter identifiability and a greater potential for biologically unrealistic parameter combinations. Similarly, HGAMs might not be optimal for the underlying IPM in the simulated population models approach outlined in Rolph et al. (2021) because it relies on sampling parameter sets of IPMs which produce IPMs with a long-term growth rate of 1.

Our findings provide direction for future research and opportunities for integrating HGAMs with other IPM methods. Because most demographic datasets do not have the detail and longitude of the Soay sheep dataset and typically span 5 or fewer years (Menges, 2000) the generalisation we can make from this case study is limited. Therefore, future research needs to assess whether using HGAMS with fewer years of data provides the same differences we observed, especially as to whether HGAMs are more likely to overfit when using fewer years of data. This could be assessed with the Soay sheep data by fitting vital rate models to a subset of years from the full demographic time series and comparing to the model fit to the full time series. An alternative approach might use simulated demographic data from which HGAM or GLMM vital rate models can be fitted to samples from this simulated data representing a wider range of life histories, to observe how sample size and longitude of the dataset affect model fit. A methods-focused area of research could investigate how HGAMs can be utilised effectively in other forms of IPMs such as dynamic energy budget (DEB) IPMs (Smallegange et al., 2017), integrated projection model integral projection models ($IPM^2$) (Plard et al., 2019) and density-dependent IPMs (Ellner & Rees, 2006). In terms of types of models, we constructed for comparison, an omission in this study is generalise additive mixed-effects models (GAMMs) with a random intercept (Wood, 2017).

Conceptually, GAMMs would provide a midpoint between GLMMs and HGAMs as it incorporates the additive features of HGAMS but not the pooled smoothing parameter.

In conclusion, we can use non-linear functional forms to model time-varying vital rates using HGAMs. We found that using HGAMs over GLMMs improved model fit, affected IPM outputs relating to life history and response to perturbations, and thus may affect our understanding of ecological systems. Hesitancy to using non-linear vital rates in IPMs may be due to the shortage of published examples or a concern that non-linear models may overfit the data. This work helps overcome these hurdles by providing another example of a non-linear IPM which shows that additional flexibility is possible to incorporate into IPMs, this flexibility improved the model fit and resulted in differences in predictions. Going forward, we recommend fitting HGAMs alongside GLMMs to check for any non-linear relationships so that time-variant vital rates are not inappropriately approximated by a linear constraint. This is especially appropriate in species where the demography of a system is poorly understood or data deficient so that the population may be structured by a single continuous variable. In cases like this, explicit demographic structuring is less important because non-linear splines can account for more complex demographic relationships and/or hidden state variables. Overall, HGAM IPMs are a promising extension to the stochastic IPM approach and should be considered when fitting vital rates.

# Acknowledgements

This research was supported by the Centre for Advanced Biological Modelling funded by the Leverhulme Trust. Thanks to the National Trust for Scotland and Scottish National Heritage for permission to work on St. Kilda and the Ministry of Defence, QinetiQ, Amey, and ESS staff on St. Kilda and Benbecula for logistical support. The collection of demographic data on St Kilda over the period on which this analysis was based was initiated and maintained for the first 10 years by Tim Clutton-Brock. JGP, Andrew MacColl, Tony Robertson, Richard Clarke, and Jerry Kinsley led field data collection assisted by many other project members and volunteers. We also thank Steve Albon, Mick Crawley, Tim Coulson, Alastair Wilson, and Loeske Kruuk for their contributions in running the project.

# References

Brault, S., & Caswell, H. (1993). Pod-specific demography of killer whales (Orcinus orca). *Ecology*, *74*(5), 1444–1454.

Bruijning, M., Visser, M. D., Hallmann, C. A., & Jongejans, E. (2018). trackdem: Automated particle tracking to obtain population counts and size distributions from videos in r. *Methods in Ecology and Evolution*, *9*(4), 965–973.

Caswell, H. (2001). *Matrix population models*. (L. John Wiley & Sons, Ed.).

Caswell, H. (2009). Stage, age and individual stochasticity in demography. *Oikos*, *118*(12), 1763–1782.

Catchpole, E. A., Morgan, B. J. T., Coulson, T. N., Freeman, S. N., & Albon, S. D. (2000). Factors influencing Soay sheep survival. *Applied Statistics*, *49*(4), 453–472.

Childs, D. Z., Coulson, T. N., Pemberton, J. M., Clutton-Brock, T. H., & Rees, M. (2011). Predicting trait values and measuring selection in complex life histories: Reproductive allocation decisions in Soay sheep. *Ecology Letters*, *14*(10), 985–992.

Childs, D. Z., Rees, M., Rose, K. E., Grubb, P. J., & Ellner, S. P. (2003). Evolution of complex flowering strategies: An age- and size-structured integral projection model. *Proceedings of the Royal Society B: Biological Sciences*, *270*(1526), 1829–1838.

Coulson, T., Catchpole, E. A., Albon, S. D., Morgan, B. J. T., Pemberton, J. M., Clutton-Brock, T. H., … Grenfell, B. T. (2001a). Age, sex, density, winter weather, and population crashes in Soay sheep. *Science*, *292*(5521), 1528–1531.

Coulson, T., Mace, G. M., Hudson, E., & Possingham, H. (2001b, May 1). The use and abuse of population viability analysis. *Trends in Ecology and Evolution*. Elsevier Current Trends.

Dahlgren, J. P., García, M. B. M. B., & Ehrlén, J. (2011). Nonlinear relationships between vital rates and state variables in demographic models. *Ecology*, *92*(5), 1181–1187.

Easterling, M. R., Ellner, S. P., & Dixon, P. M. (2000). Size-specific sensitivity: Applying a new structured population model. *Ecology*, *81*(3), 694–708.

Ellner, S. P., Childs, D. Z., & Rees, M. (2016a). Basic Analyses 1: Demographic Measures and Events in the Life Cycle. In *Data-driven Modelling of Structured Populations: A Practical Guide to the Integral Projection Model* (pp. 57–85).

Ellner, S. P., Childs, D. Z., & Rees, M. (2016b). Basic Analyses 2: Prospective Perturbation Analysis. In *Data-driven Modelling of Structured Populations: A Practical Guide to the Integral Projection Model* (pp. 87–109).

Ellner, S. P., Childs, D. Z., & Rees, M. (2016c). Environmental Stochasticity. In *Data-driven Modelling of Structured Populations: A Practical Guide to the Integral Projection Model* (pp. 187–227).

Ellner, S. P., Childs, D. Z., & Rees, M. (2016d). General Deterministic IPM. In *Data-driven Modelling of Structured Populations: A Practical Guide to the Integral Projection Model* (pp. 139–185).

Ellner, S. P., & Rees, M. (2006). Integral Projection Models for Species with Complex Demography. *The American Naturalist*, *167*(3), 410.

Ezard, T. H. G., Bullock, J. M., Dalgleish, H. J., Millon, A., Pelletier, F., Ozgul, A., & Koons, D. N. (2010). Matrix models for a changeable world: The importance of transient dynamics in population management. *Journal of Applied Ecology*, *47*(3), 515–523.

Fieberg, J., & Ellner, S. P. (2001). Stochastic matrix models for conservation and management: A comparative review of methods. *Ecology Letters*, *4*(3), 244–266.

Gerber, L. R., & Heppell, S. S. (2004). The use of demographic sensitivity analysis in marine species conservation planning. *Biological Conservation*, *120*(1), 121–128.

González, E. J., Rees, M., & Martorell, C. (2013). Identifying the demographic processes relevant for species conservation in human-impacted areas: does the model matter? *Oecologia*, *171*(2), 347–

356.

Hindle, B. J., Pilkington, J. G., Pemberton, J. M., & Childs, D. Z. (2019). Cumulative weather effects can impact across the whole life cycle. *Global Change Biology*, *25*(10), 3282–3293.

Hurrell, J. W. (1995). Decadal trends in the North Atlantic oscillation: Regional temperatures and precipitation. *Science*, *269*(5224), 676–679.

Kuss, P., Rees, M., Ægisdóttir, H. H., Ellner, S. P., & Stöcklin, J. (2008). Evolutionary demography of long-lived monocarpic perennials: A time-lagged integral projection model. *Journal of Ecology*, *96*(4), 821–832.

Leivesley, J. A., Bussière, L. F., Pemberton, J. M., Pilkington, J. G., Wilson, K., & Hayward, A. D. (2019, May 20). Survival costs of reproduction are mediated by parasite infection in wild Soay sheep. (J. Gaillard, Ed.), *Ecology Letters*. John Wiley & Sons, Ltd.

Menges, E. S. (2000). Population viability analyses in plants: Challenges and opportunities. *Trends in Ecology and Evolution*, *15*(2), 51–56.

Merow, C., Dahlgren, J. P., Metcalf, C. J. E., Childs, D. Z., Evans, M. E. K., Jongejans, E., … Mcmahon, S. M. (2014). Advancing population ecology with integral projection models: A practical guide. *Methods in Ecology and Evolution*, *5*(2), 99–110.

Metcalf, C. J. E., & Pavard, S. (2007). Why evolutionary biologists should be demographers. *Trends in Ecology and Evolution*, *22*(4), 205–212.

Ozgul, A., Tuljapurkar, S., Benton, T. G., Pemberton, J. M., Clutton-Brock, T. H., & Coulson, T. (2009). The dynamics of phenotypic change and the shrinking sheep of St. kilda. *Science*, *325*(5939), 464–467.

Pedersen, E. J., Miller, D. L., Simpson, G. L., & Ross, N. (2019). Hierarchical generalized additive models in ecology: An introduction with mgcv. *PeerJ*, *2019*(5), e6876.

Pemberton, J. M., & Clutton-Brock, T. H. (2004). *Soay Sheep: Dynamics and Selection in an Island*

*Population*. Cambridge University Press.

Picard, N., & Liang, J. (2014). Matrix models for size-structured populations: Unrealistic fast growth or simply diffusion? *PLoS ONE*, *9*(6), e98254.

Plard, F., Turek, D., Grüebler, M. U., & Schaub, M. (2019). IPM2: toward better understanding and forecasting of population dynamics. *Ecological Monographs*, *89*(3).

Ramula, S., Rees, M., & Buckley, Y. (2009). Integral projection models perform better for small demographic data sets than matrix population models: A case study of two perennial herbs. *Journal of Applied Ecology*, *46*(5), 1048–1053.

Rees, M., & Ellner, S. P. (2009). Integral projection models for populations in temporally varying environments. *Ecological Monographs*, *79*(4), 575–594.

Schaub, M., & Kéry, M. (2012, April 1). Combining information in hierarchical models improves inferences in population ecology and demographic population analyses. *Animal Conservation*. John Wiley & Sons, Ltd.

Simmonds, E. G., & Coulson, T. (2015). Analysis of phenotypic change in relation to climatic drivers in a population of Soay sheep Ovis aries. *Oikos*, *124*(5), 543–552.

Simon Wood. (2016). Package 'mgcv.' *CRAN*, 1–244.

Smallegange, I. M., Caswell, H., Toorians, M. E. M. M., Roos, A. M., & de Roos, A. M. (2017). Mechanistic description of population dynamics using dynamic energy budget theory incorporated into integral projection models. *Methods in Ecology and Evolution*, *8*(2), 146–154.

Sutherland, W. J., Freckleton, R. P., Godfray, H. C. J., Beissinger, S. R., Benton, T., Cameron, D. D., … Wiegand, T. (2013). Identification of 100 fundamental ecological questions. *Journal of Ecology*, *101*(1), 58–67.

Tredennick, A. T., Hooten, M. B., Aldridge, C. L., Homer, C. G., Kleinhesselink, A. R., & Adler, P. B. (2016). Forecasting climate change impacts on plant populations over large spatial extents.

*Ecosphere*, *7*(10), 1–16.

Tuljapurkar, S. D., & Orzack, S. H. (1980). Population dynamics in variable environments I. Long-run growth rates and extinction. *Theoretical Population Biology*, *18*(3), 314–342.

Tuljapurkar, S., & Haridas, C. V. (2006). Temporal autocorrelation and stochastic population growth. *Ecology Letters*, *9*(3), 327–337.

Tuljapurkar, S., & Horvitz, C. C. (2006). From stage to age in variable environments: Life expectancy and survivorship. *Ecology*, *87*(6), 1497–1509.

White, J. W., Nickols, K. J., Malone, D., Carr, M. H., Starr, R. M., Cordoleani, F., … Botsford, L. W. (2016). Fitting state-space integral projection models to size-structured time series data to estimate unknown parameters. *Ecological Applications*, *26*(8), 2675–2692.

Williams, J. L., Miller, T. E. X., Ellner, S. P., & Doak, D. F. (2012). Avoiding unintentional eviction from integral projection models. *Ecology*, *93*(9), 2008–2014.

Wilson, A. J., Pilkington, J. G., Pemberton, J. M., Coltman, D. W., Overall, A. D. J., Byrne, K. A., & Kruuk, L. E. B. (2005). Selection on mothers and offspring: Whose phenotype is it and does it matter? *Evolution*, *59*(2), 451–463.

Wood, S. N. (2017). *Generalized additive models: An introduction with R*. *Generalized Additive Models: An Introduction with R, Second Edition*. CRC Press.

# Figures

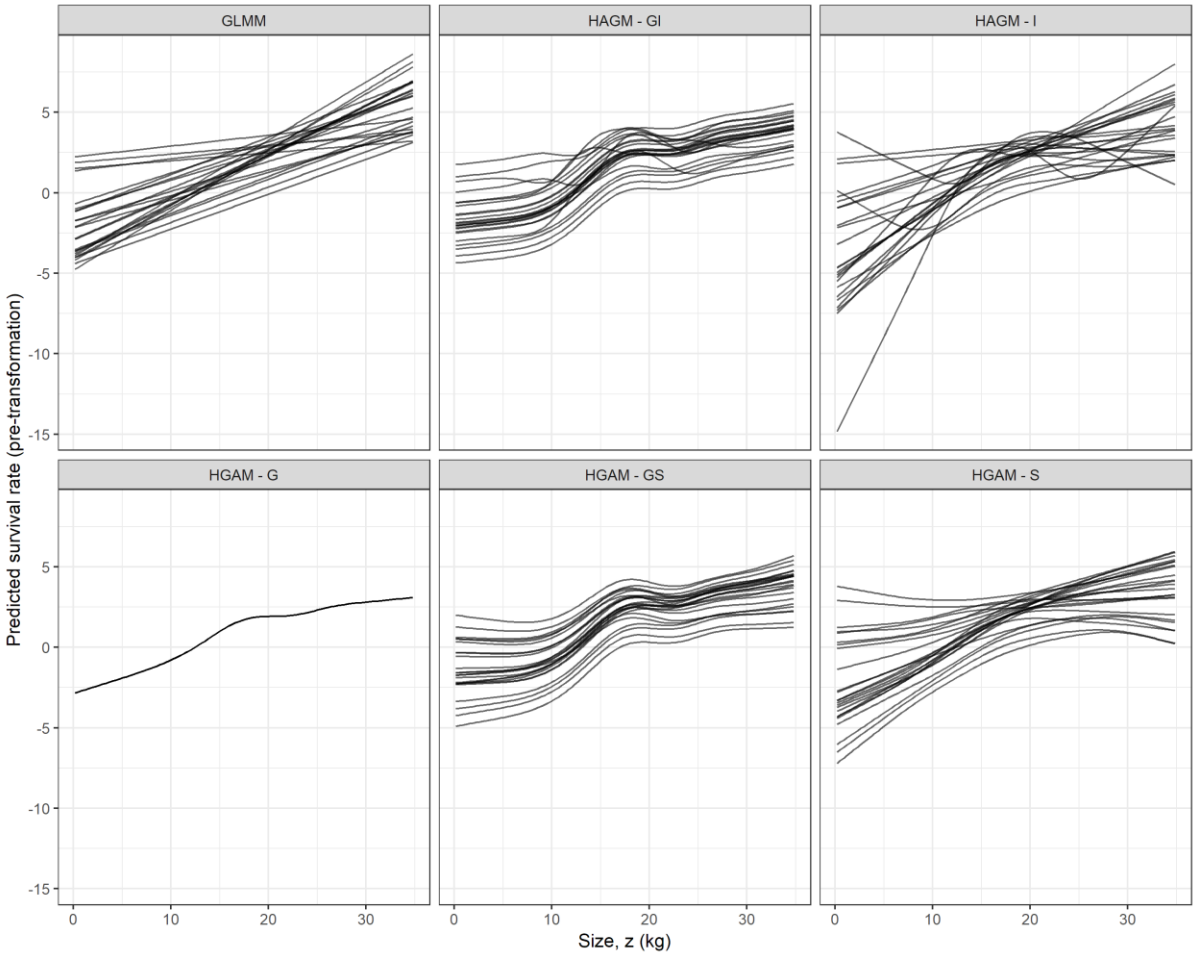


**Figure 4.1: Comparison of functional forms of models fitted to survival probability when lambs and adult are modelled together rather than separately.** The models fitted are a generalised linear mixed-effects model and five types of hierarchical generalised additive model (HGAM). The five types of HGAMs can be summarised as follows; model G: A single common smoother for all observations, model GS: a global smoother plus group-level smoothers that have the same wiggliness, model GI: A global smoother plus group-level smoothers with differing wiggliness, model S: group-specific smoothers without a global smoother, but with all smoothers having the same wiggliness, model I: group-specific smoothers with different wiggliness.

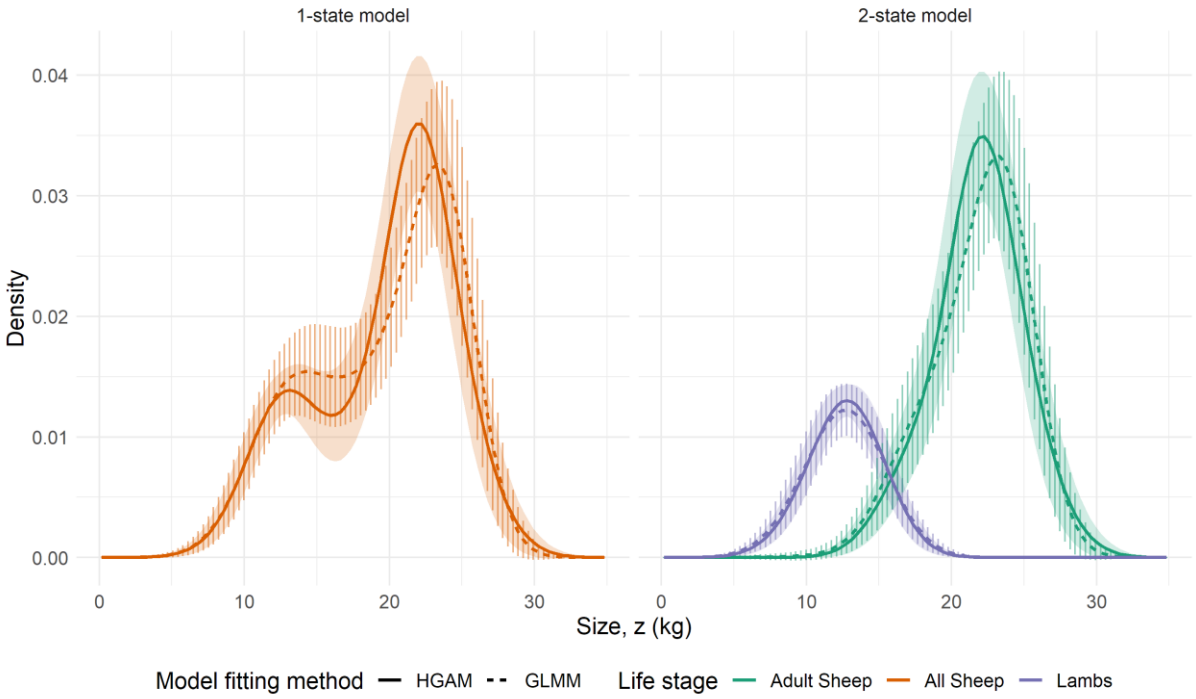


**Figure 4.2: The stochastically simulated stable state distributions of the study population of sheep.** Temporal mean average +- 1 standard deviation size distributions for four integral projection models fitted to Soay sheep data resulting from i.i.d. stochastic simulations of length 10,000 timesteps. Populations were projected for two model structures; a one-state model where all sheep were grouped and a two-state model where lambs and adult sheep were modelled separately where lambs transitioned to adult sheep after their first year. For each model structure, vital rates were fitted using two methods: hierarchical generalised additive models (HGAMs) and generalised linear mixed models (GLMM).

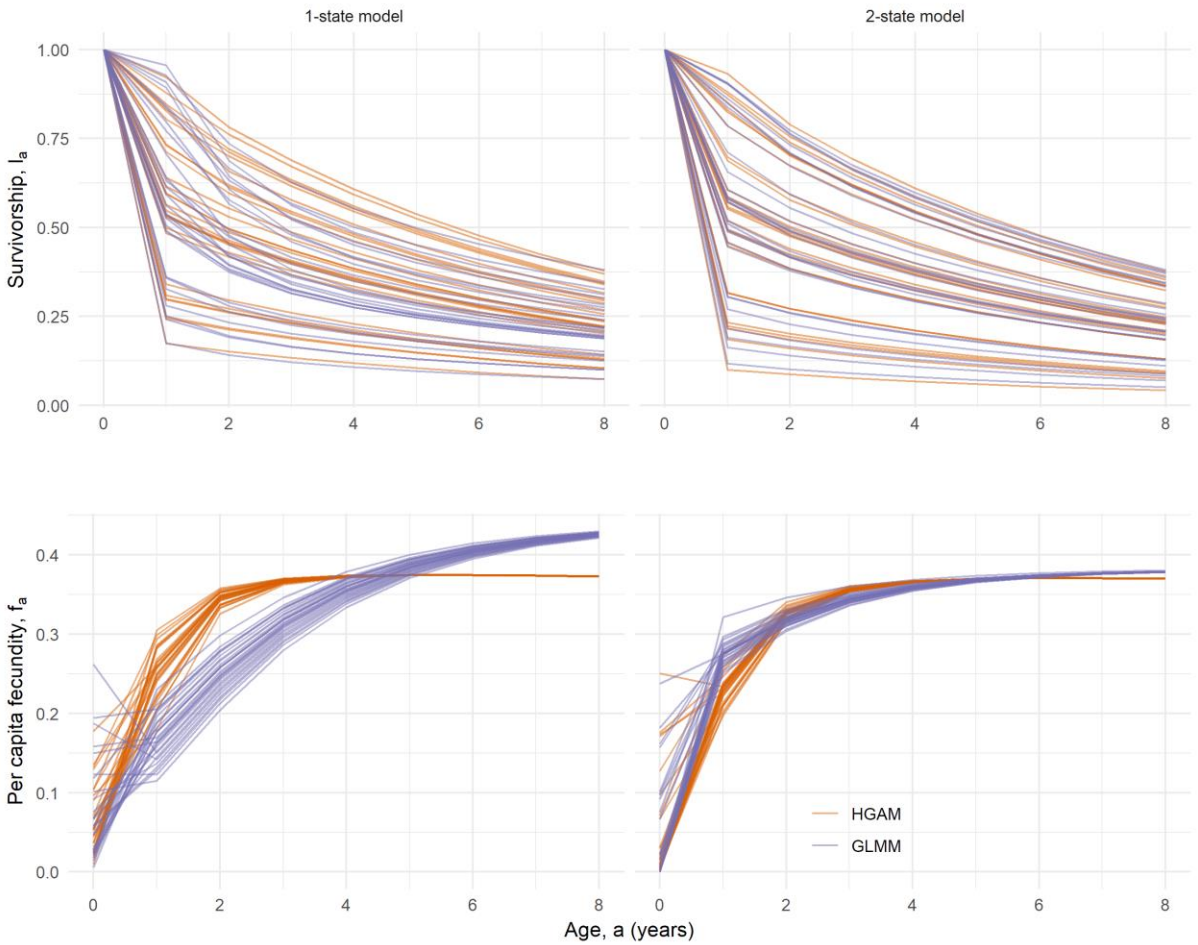


**Figure 4.3: Survivorship curves and fecundity curves.** Stochastically simulated probability of survival ($l_a$) and average per capita fecundity ($f_a$) of a surviving cohort of lambs for age ($a$) 0 to 8 with a starting size distribution derived from the mean size at first census of lambs in the Soay sheep population. Each line represents a starting cohort from each year. Survivorship and fecundity curves were generated from for types of IPM. Each IPM is constructed with one of two structures: a single state encompassing all sheep (left-hand column) or a two-state model with discrete states for lambs and adult sheep (right-hand column). For each IPM structure, one IPMs is constructed from vital rate functions fitted using generalised linear mixed models (GLMMs) (purple) or hierarchical generalised additive models (HGAMs) (orange).

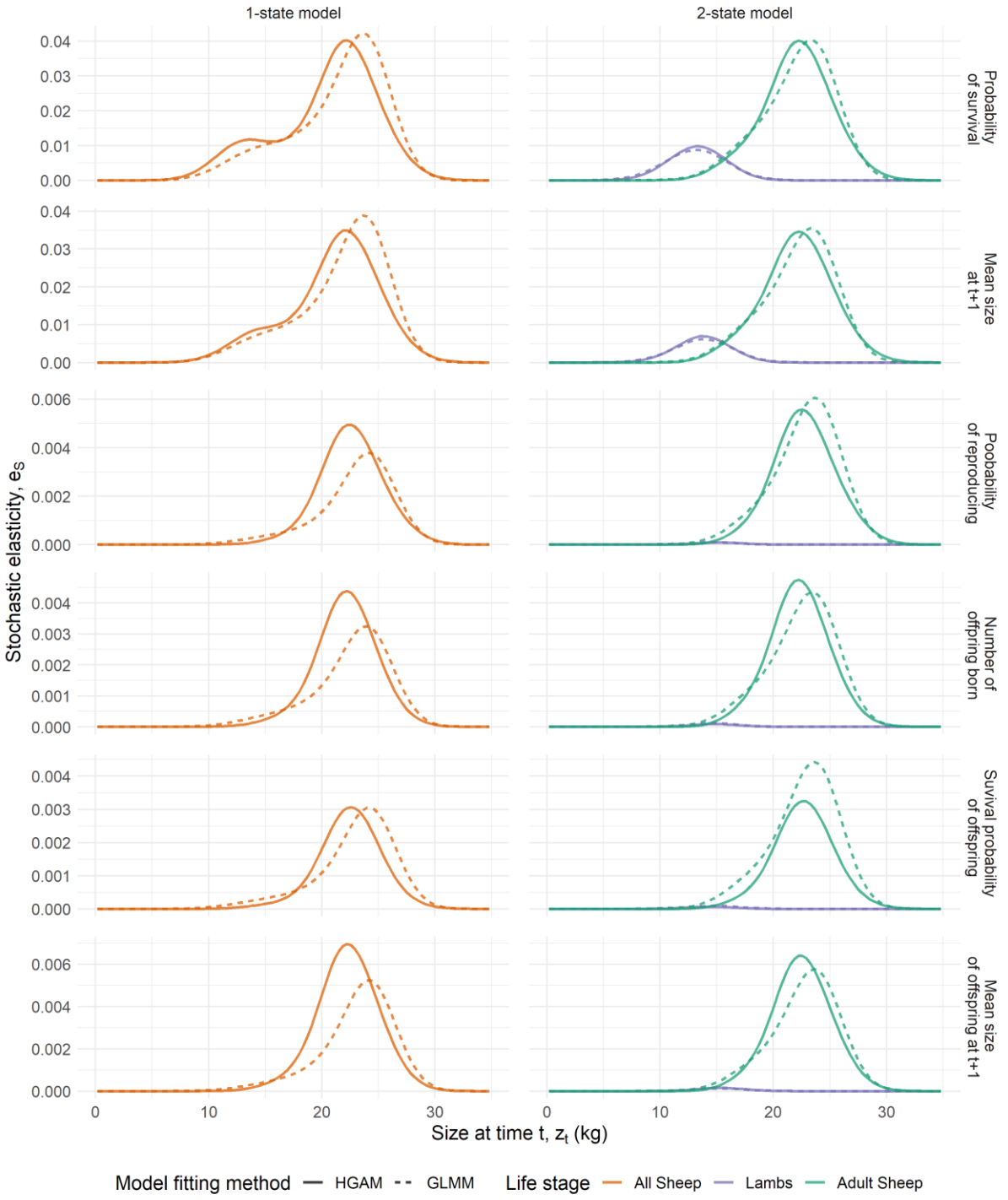


**Figure 4.4: The effect on the long-term growth rate of a perturbation to the vital rate function for six vital rates.** This perturbation analysis calculated the stochastic elasticity of six vital rates of survival, growth, probability of reproducing, number of offspring born, survival probability of offspring and mean size of offspring. The perturbations are applied to four different IPMs. Each IPM is constructed

with one of two structures: a single state encompassing all sheep (orange) or a two-state model with discrete states for lambs (purple) and adult sheep (green). For each IPM structure, one IPMs is constructed from vital rate functions fitted using generalised linear mixed models (GLMMs) (dashed line) or hierarchical generalised additive models (HGAMs) (solid line). These plots indicate the effect on stochastic long-term growth rate of an increase of vital rate at size z.

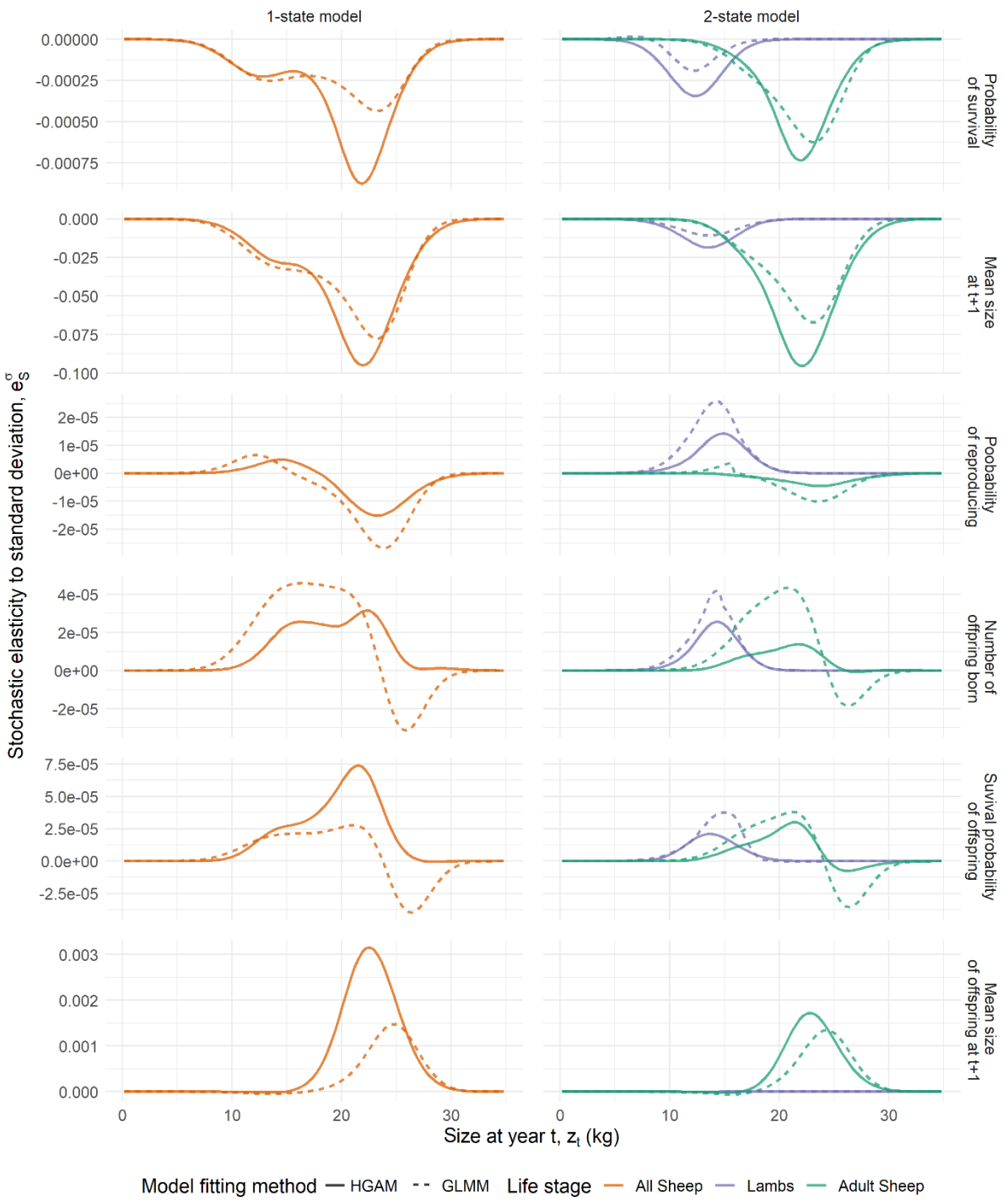


**Figure 4.5: The effect on the long-term growth rate of a perturbation to the standard deviation of the vital rate function for six vital rates.** This perturbation analysis calculated the stochastic elasticity to standard deviation of six vital rates of survival, growth, probability of reproducing, number of offspring born, survival probability of offspring and mean size of offspring. The perturbations are applied to four different IPMs. Each IPM is constructed with one of two structures: a single state

encompassing all sheep (orange) or a two-state model with discrete states for lambs (purple) and adult sheep (green). For each IPM structure, one IPMs is constructed from vital rate functions fitted using generalised linear mixed models (GLMMs) (dashed line) or hierarchical generalised additive models (HGAMs) (solid line). These plots indicate the effect on the stochastic long-term growth rate of an increase of vital rate at size z.

# Tables

**Table 4.1: Model comparison by Akaike information criterion (AIC) of vital rate models fitted to all sheep using generalised linear mixed models (GLMMs) and hierarchical generalised additive models (HGAMs).** HGAMs were fitted in different five configurations (G, GS, GI, S, I) of how features were shared across groups. The five types of HGAMs can be summarised as follows; G: A single common smoother, GS: a global smoother plus group-level smoothers that have the same wiggliness, GI: A global smoother plus group-level smoothers with differing wiggliness, S: group-specific smoothers without a global smoother, but with all smoothers having the same wiggliness, I: group-specific smoothers with different wiggliness.

| All sheep | GLMM | HGAM: G | HGAM: GS | HGAM: GI | HGAM: S | HGAM: I |
|---|---|---|---|---|---|---|
| Survival | 3471.298 | 3945.895 | 3335.480 | **3323.783** | 3386.283 | 3363.374 |
| Growth | 6424.557 | 6535.442 | 6326.513 | **6302.789** | 6336.081 | 6329.543 |
| Probability of reproducing | 3953.659 | 3613.480 | **3552.992** | 3557.098 | 3558.600 | 3582.649 |
| Number of offspring born | 6717.129 | 6731.233 | 6677.670 | **6690.854** | 6708.951 | 6711.112 |
| Survival of offspring | 2703.627 | 2699.030 | **2504.570** | 2506.565 | 2546.850 | 2557.539 |
| Mean size of offspring at t+1 | 7683.752 | 7741.156 | **7605.963** | 7610.518 | 7659.363 | 7643.601 |

**Table 4.2: Model comparison by Akaike information criterion (AIC) of vital rate models fitted to lambs using generalised linear mixed models (GLMMs) and hierarchical generalised additive models (HGAMs).** HGAMs were fitted in different five configurations (G, GS, GI, S, I) of how features were shared across groups. The five types of HGAMs can be summarised as follows; G: A single common smoother, GS: a global smoother plus group-level smoothers that have the same wiggliness, GI: A global smoother plus group-level smoothers with differing wiggliness, S: group-specific smoothers without a global smoother, but with all smoothers having the same wiggliness, I: group-specific smoothers with different wiggliness.

| Lambs | GLMM | HGAM: G | HGAM: GS | HGAM: GI | HGAM: S | HGAM: I |
|---|---|---|---|---|---|---|
| Survival | 1289.885 | 1608.7775 | **1268.1216** | 1269.3274 | 1300.9434 | 1279.6863 |
| Growth | 1487.879 | 1510.5105 | 1485.6327 | **1460.7522** | 1476.1097 | 1480.6526 |
| Probability of reproducing | 1385.446 | 1442.5562 | **1370.6728** | 1374.5792 | 1394.5350 | 1379.6249 |
| Number of offspring born | 866.334 | 908.1478 | **841.5500** | 850.5509 | 860.4697 | 888.6845 |
| Survival of offspring | 292.622 | 342.9099 | **263.5293** | 271.6001 | 271.8099 | 283.9249 |
| Mean size of offspring at t+1 | **314.592*** | **314.5927** | *Insufficient data for good model fit* | *Insufficient data for good model fit* | *Insufficient data for good model fit* | *Insufficient data for good model fit* |

**Table 4.3: Model comparison by Akaike information criterion (AIC) of vital rate models fitted to adult sheep using generalised linear mixed models (GLMMs) and hierarchical generalised additive models (HGAMs).** HGAMs were fitted in different five configurations (G, GS, GI, S, I) of how features were shared across groups. The five type of HGAMs can be summarised as follows; G: A single common smoother, GS: a global smoother plus group-level smoothers that have the same wiggliness, GI: A global smoother plus group-level smoothers with differing wiggliness, S: group-specific smoothers without a global smoother, but with all smoothers having the same wiggliness, I: group-specific smoothers with different wiggliness.

| Adults | GLMM | HGAM: G | HGAM: GS | HGAM: GI | HGAM: S | HGAM: I |
|---|---|---|---|---|---|---|
| Survival | 2087.366 | 2337.549 | **2064.568** | 2070.339 | 2076.477 | 2082.874 |
| Growth | 6424.557 | 6535.442 | 6326.513 | **6302.789** | 6336.081 | 6329.543 |
| Probability of reproducing | 2252.560 | 2143.873 | 2150.262 | **2140.118** | 2229.104 | 2193.075 |
| Number of offspring born | 5856.910 | 5820.482 | **5808.792** | 5813.531 | 5833.511 | 5851.761 |
| Survival of offspring | 2301.657 | 2355.093 | **2231.078** | 2235.506 | 2259.750 | 2260.154 |
| Mean size of offspring at t+1 | 7683.752 | 7420.550 | 7292.146 | **7280.628** | 7296.665 | 7299.753 |

**Table 4.4: Comparison of life history measures calculated from four different IPMs.** Each IPM is constructed with one of two structures: a 1-state IPM encompassing all sheep or a 2-state IPM with discrete states for lambs and adult sheep. For each IPM structure, one IPMs is constructed from vital rate functions fitted using generalised linear mixed models (GLMMs) or hierarchical generalised additive models (HGAMs). Notation of each life history measure follows table 3.3 of (Ellner et al., 2016a).

| Stochastic population measure | 1-state IPM | | 2-state IPM | |
|---|---|---|---|---|
| | GLMM | HGAM | GLMM | HGAM |
| Mean life expectancy, $\bar{\eta}(z_0)$ | 5.317313 | 5.012113 | 4.860881 | 4.795846 |
| Variance in lifespan, $\sigma_\eta^2(z_0)$ | 91.66789 | 58.31827 | 57.33409 | 55.99884 |
| Standard deviation in lifespan, $\sigma_\eta(z_0)$ | 9.574335 | 7.63664 | 7.571927 | 7.483237 |
| Mean probability of reproducing once, $B(z_0)$ | 0.7884714 | 0.750724 | 0.7461362 | 0.7386878 |
| Mean size at death, $\bar{\omega}(z_0)$ | 16.98803 | 17.51278 | 17.28827 | 17.28505 |
| Mean age at first breeding, $\bar{a}_R(z_0)$ | 0.312671 | 0.3390717 | 0.3214633 | 0.3609229 |
| Stochastic long term growth rate, $\lambda_S$ | 1.059735 | 1.062220 | 1.051862 | 1.051322 |

# Supplementary figures

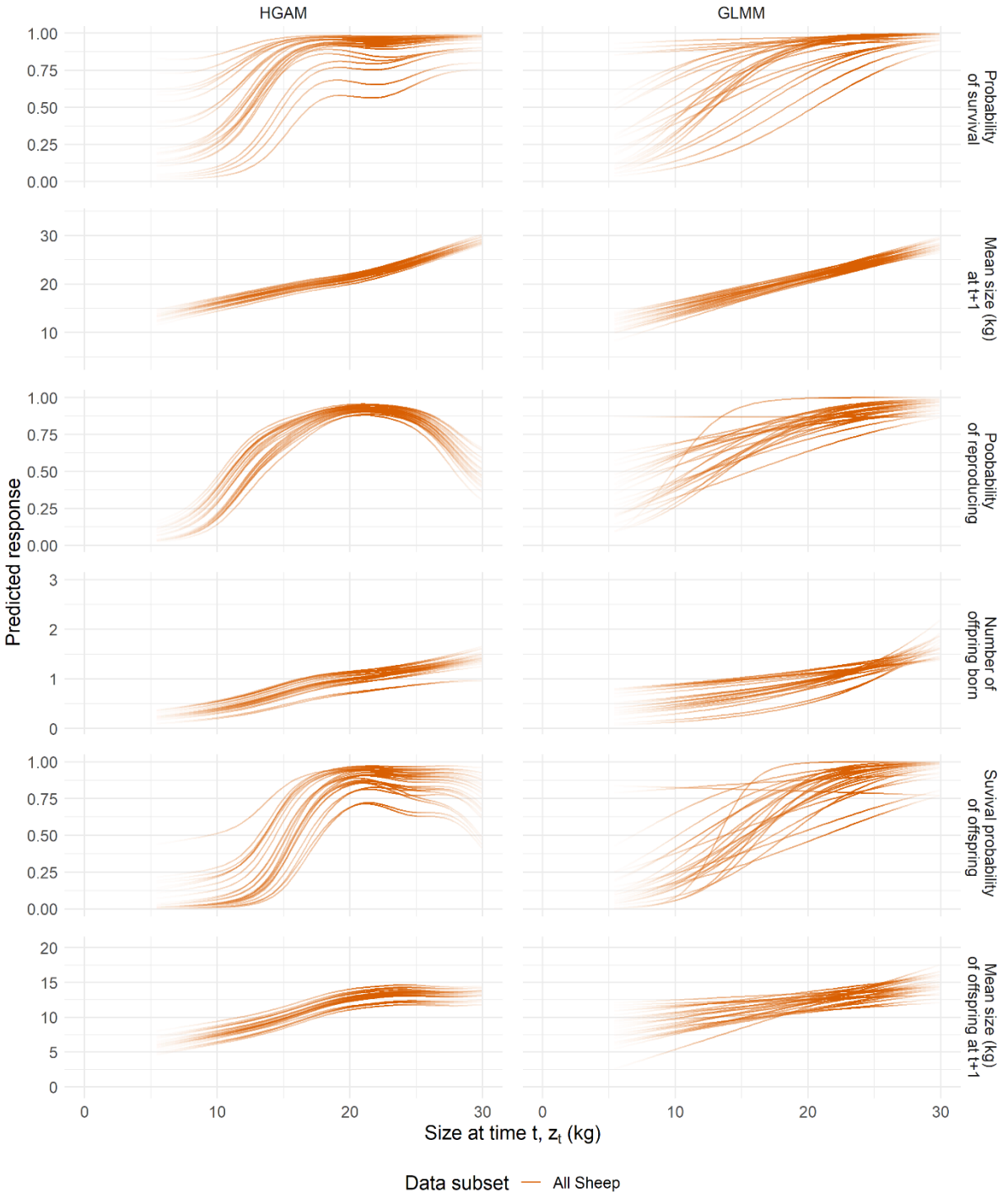


**Supplementary figure S4.1: Comparison of vital rate models fitted to all sheep by hierarchical generalised additive models (HGAMs) and generalized linear mixed-effects models (GLMMs).** Vital rate models for survival, growth, probability of reproduction, number of offspring, offspring

survival and mean size of offspring fitted to data from the Soay Sheep population using two modelling frameworks: HGAMs and GLMMs. Each line represents a model fit for each annual transition in the dataset. Transparency was adjusted by the population density at each size of a mean size distribution from a stochastic i.i.d. projection simulated for 10000 timesteps to highlight population density along with the vital rate functions.

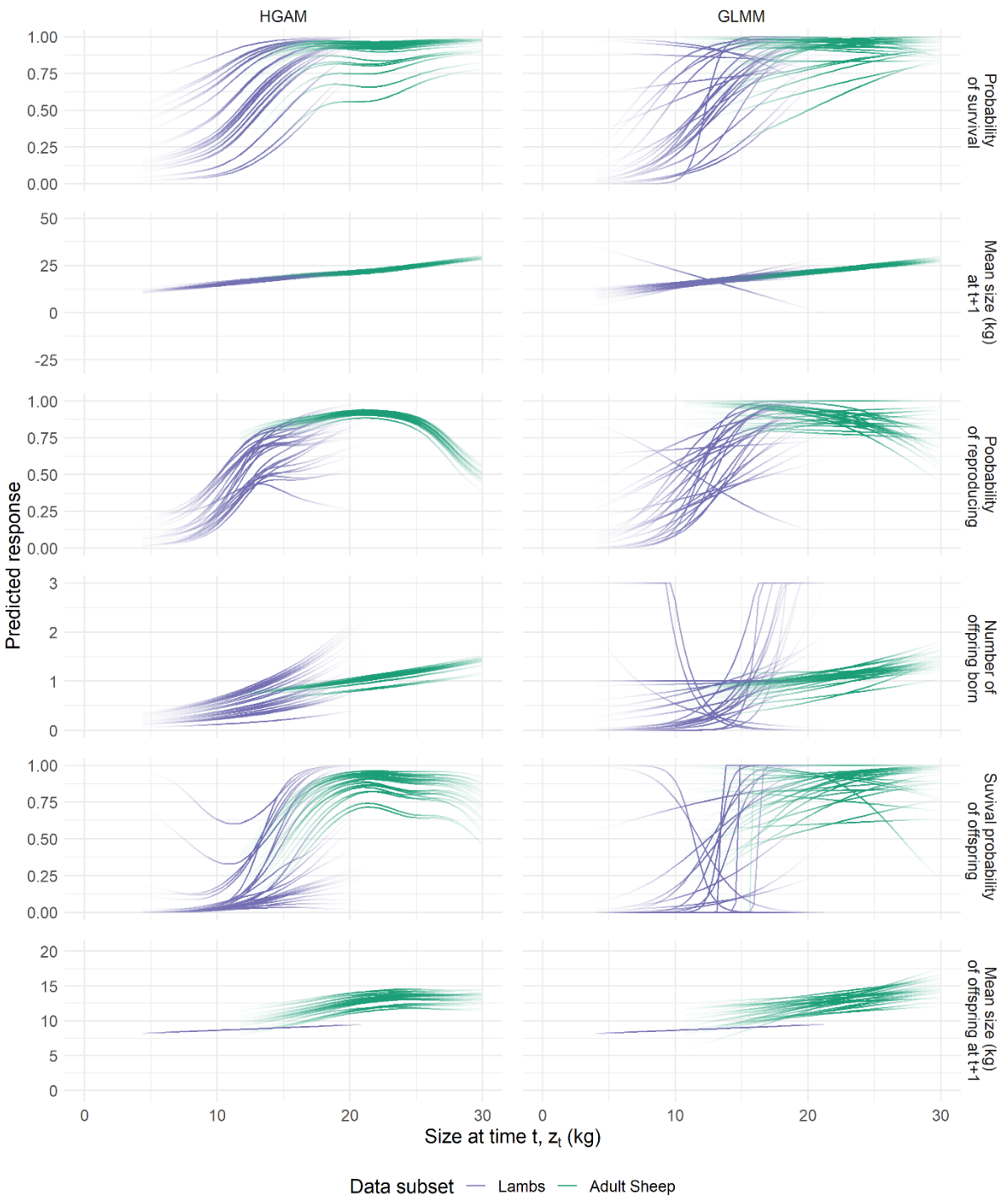


**Supplementary figure S4.2: Comparison of vital rate models fitted by adults and first-years by hierarchical generalised additive models (HGAMs) and generalized linear mixed-effects models (GLMMs).** Vital rate models for survival, growth, probability of reproduction, number of offspring, offspring survival and mean size of offspring fitted to data from the Soay Sheep population using two modelling frameworks: HGAMs and GLMMs. Each line represents a model fit for each annual

transition in the dataset. Transparency was adjusted by the population density at each size of a mean size distribution from a stochastic i.i.d. projection simulated for 10000 timesteps to highlight population density along with the vital rate functions.

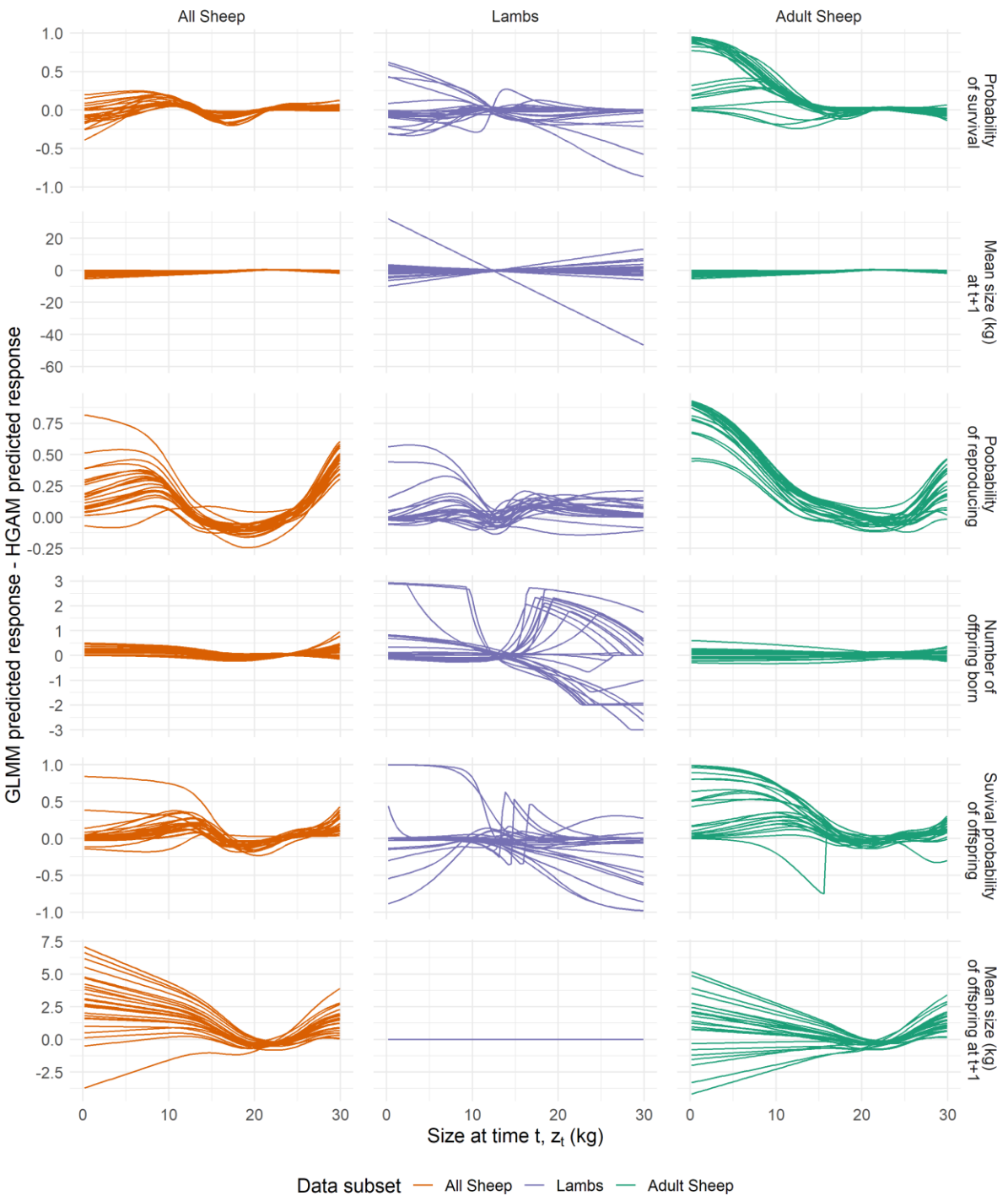


**Supplementary figure S4.3: The differences in vital rate models fitted by to all sheep, adults and lambs by hierarchical generalised additive models (HGAMs) and generalized linear mixed-effects models (GLMMs).** Difference between the predicted vital rate models for survival, growth, probability of reproduction, number of offspring, offspring survival and mean size of offspring fitted to data from the Soay Sheep population using two modelling frameworks: HGAMs and GLMMs. Each line

represents a model fit for each annual transition in the dataset. Large values (>0) mean that GLMM predicted higher values than HGAM and negative values mean that HGAM predicted higher values than GLMM.

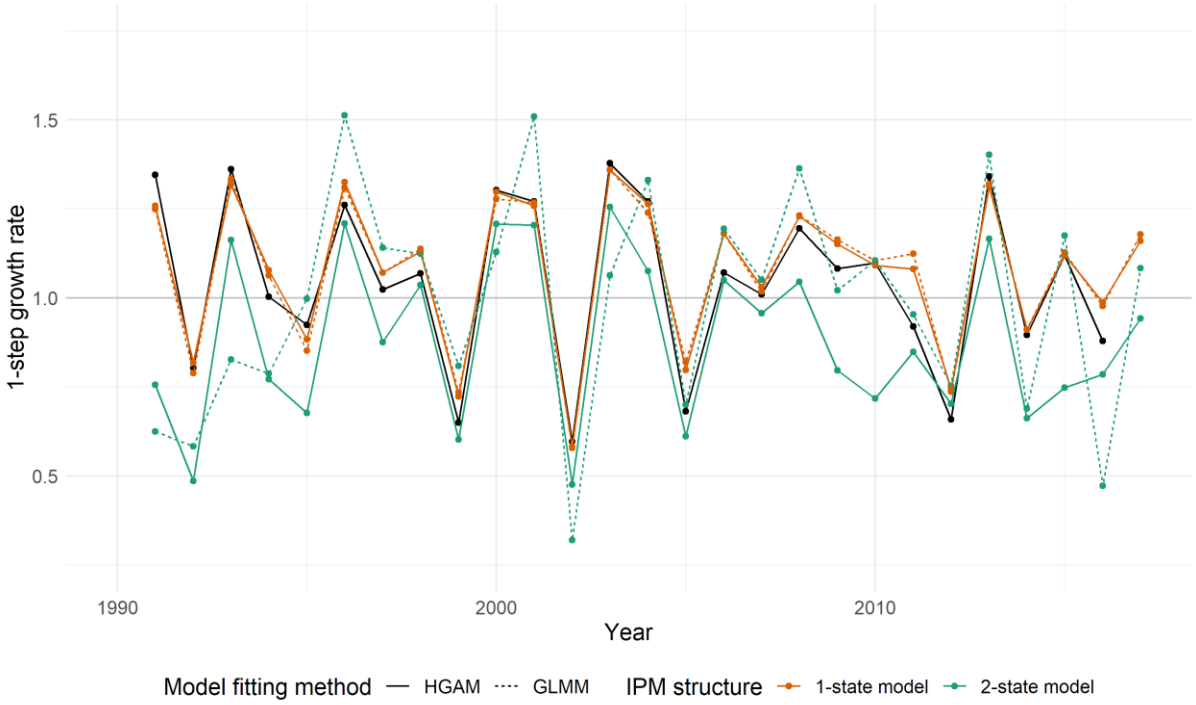


**Supplementary figure S4.4: 1-step growth rates from 1991 to 2017 for four integral projection models (IPMs) constructed from vital rates fitted to data from the Soay sheep population in St Kilda (green and orange lines).** These growth rates are compared to the growth rates derived from field population counts of the Soay sheep population (black line). Populations were projected for two model structures; a one-state model where all sheep were grouped and a two-state model where lambs and adult sheep were modelled separately where lambs transitioned to adult sheep after their first year. For each model structure, vital rates were fitted using two methods: hierarchical generalised additive models (HGAMs) and generalised linear mixed models (GLMM).

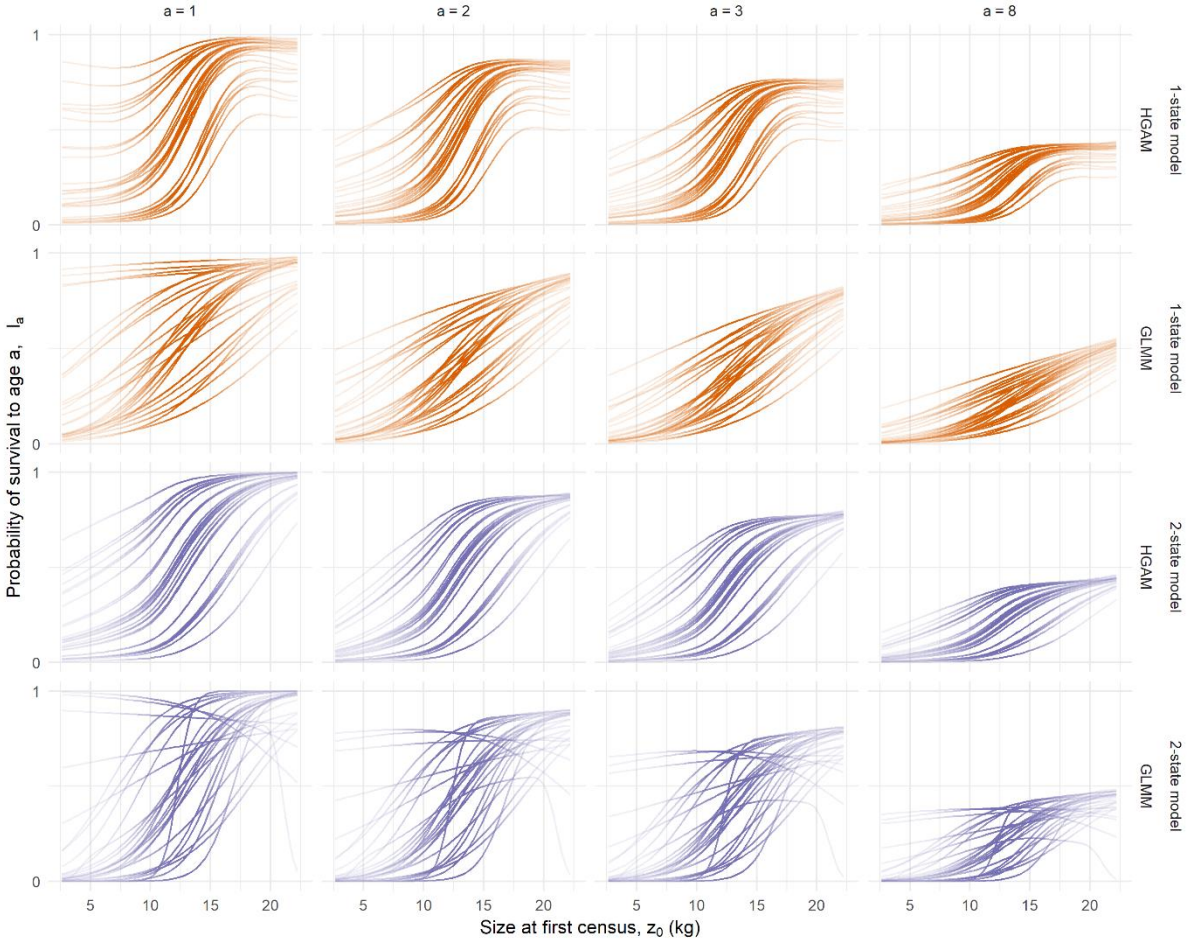


**Supplementary figure S4.5: Survivorship patterns across four different IPMs.** Probability of survival to ages 1,2,3, and 8 given size at first summer census (z0) for four different IPMs. Each IPM is constructed with one of two structures: a single state encompassing all sheep (orange) or a two-state model with discrete states for lambs and adult (purple). For each IPM structure, one IPMs is constructed from vital rate functions fitted using generalised linear mixed models (GLMMs) or hierarchical generalised additive models (HGAMs).

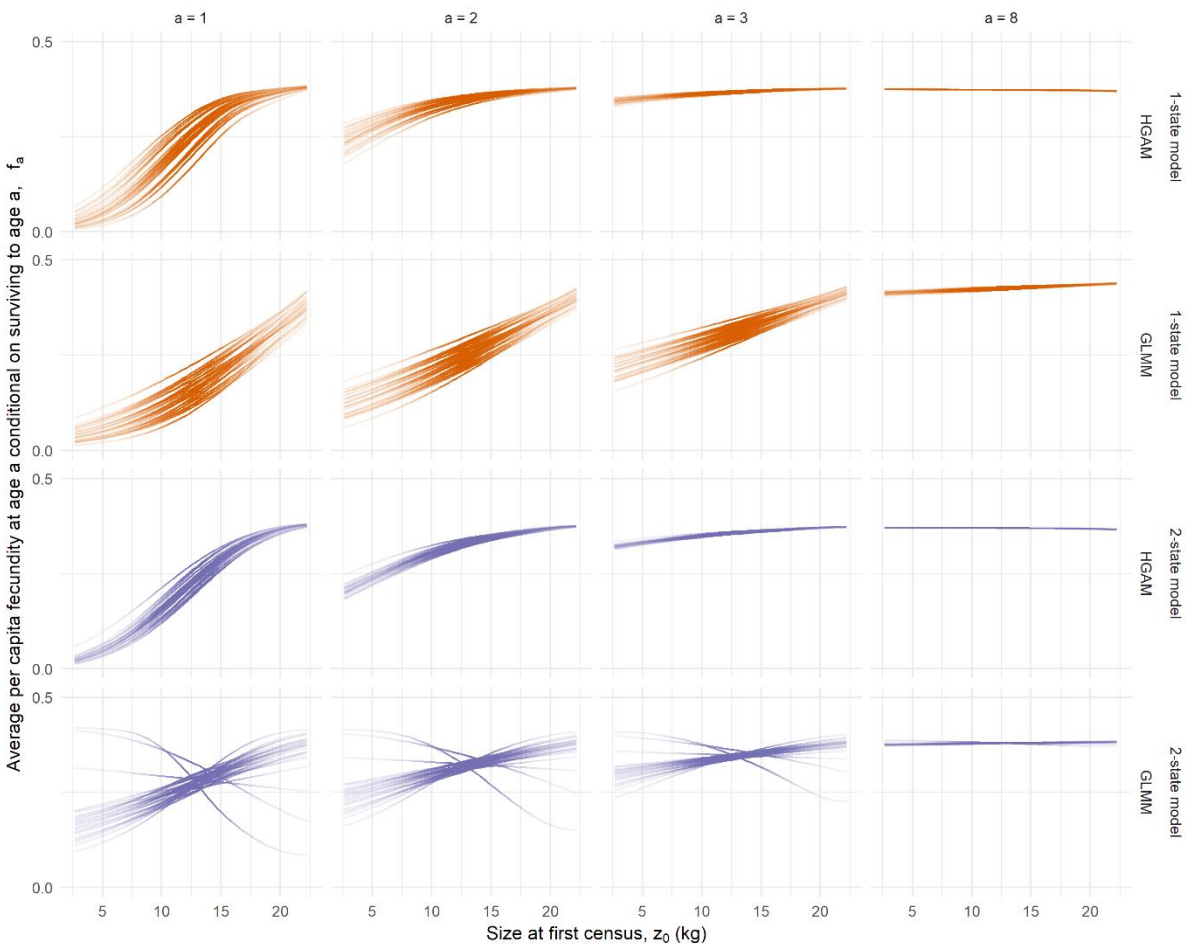


**Supplementary figure S4.6: Fecundity patterns across four different IPMs.** Average annual, per-capita fecundity at ages 1,2,3, and 8 given size at first summer census (z0) for four different IPMs. Each IPM is constructed with one of two structures: a single state encompassing all sheep (orange) or a two-state model with discrete states for lambs and adult sheep (purple). For each IPM structure, one IPMs is constructed from vital rate functions fitted using generalised linear mixed models (GLMMs) or hierarchical generalised additive models (HGAMs).

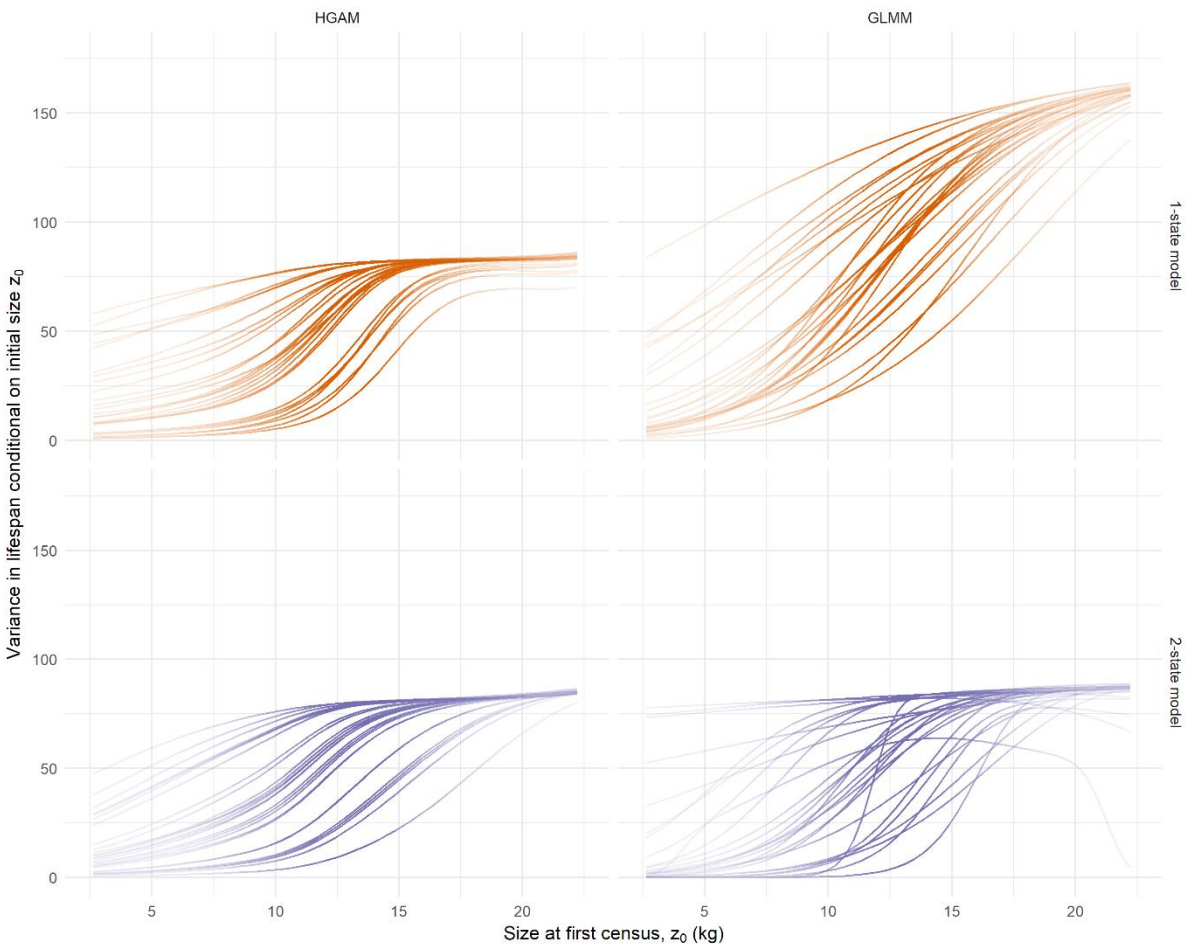


**Supplementary figure S4.7: Variance in lifespan given size at first summer census (z0) for four different IPMs.** Each IPM is constructed with one of two structures: a single state encompassing all sheep (orange) or a two-state model with discrete states for lambs and adult sheep (purple). For each IPM structure, one IPMs is constructed from vital rate functions fitted using generalised linear mixed models (GLMMs) or hierarchical generalised additive models (HGAMs).

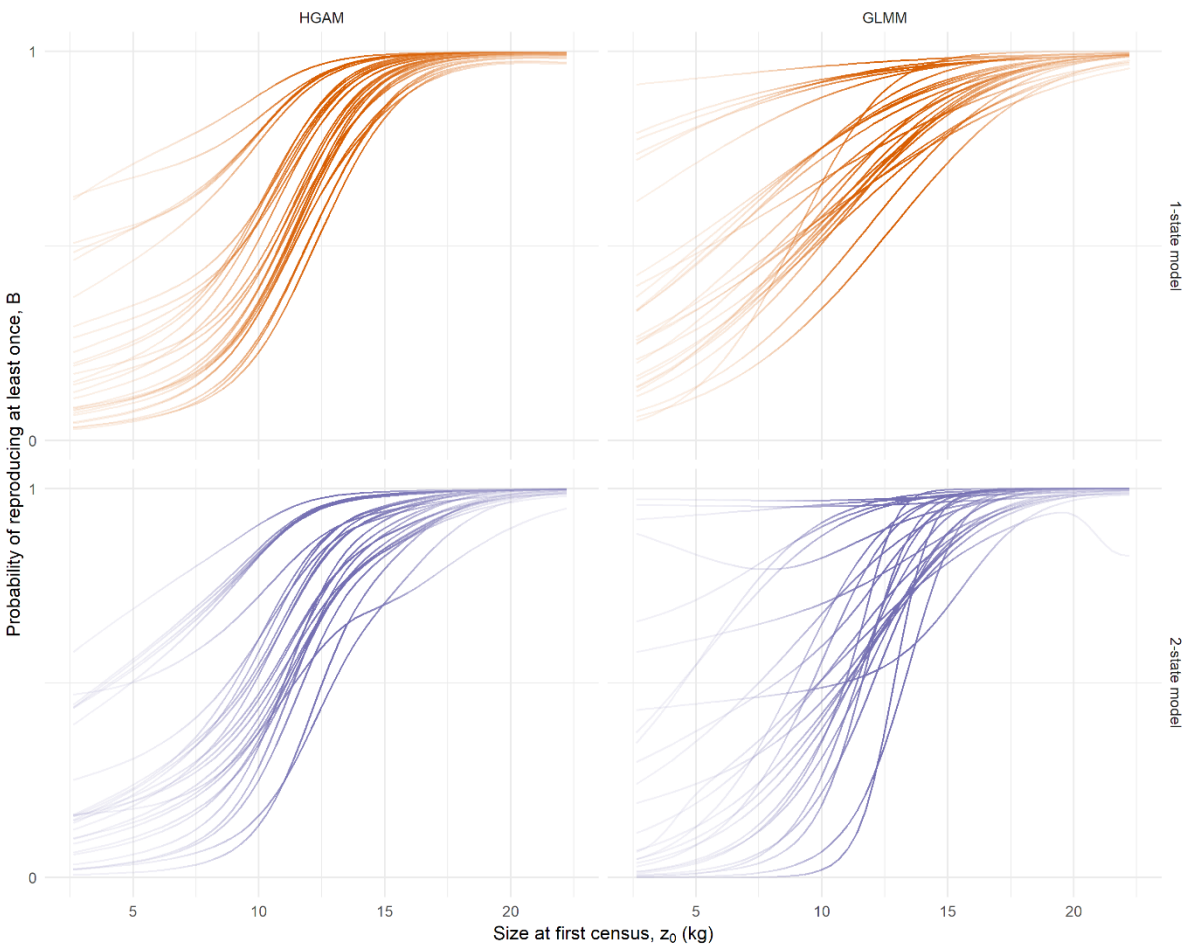


**Supplementary figure S4.8: Mean probability of reproducing at least once given size at first summer census (z0) for four different IPMs.** Each IPM is constructed with one of two structures: a single state encompassing all sheep (orange) or a two-state model with discrete states for lambs and adult sheep (purple). For each IPM structure, one IPMs is constructed from vital rate functions fitted using generalised linear mixed models (GLMMs) or hierarchical generalised additive models (HGAMs).

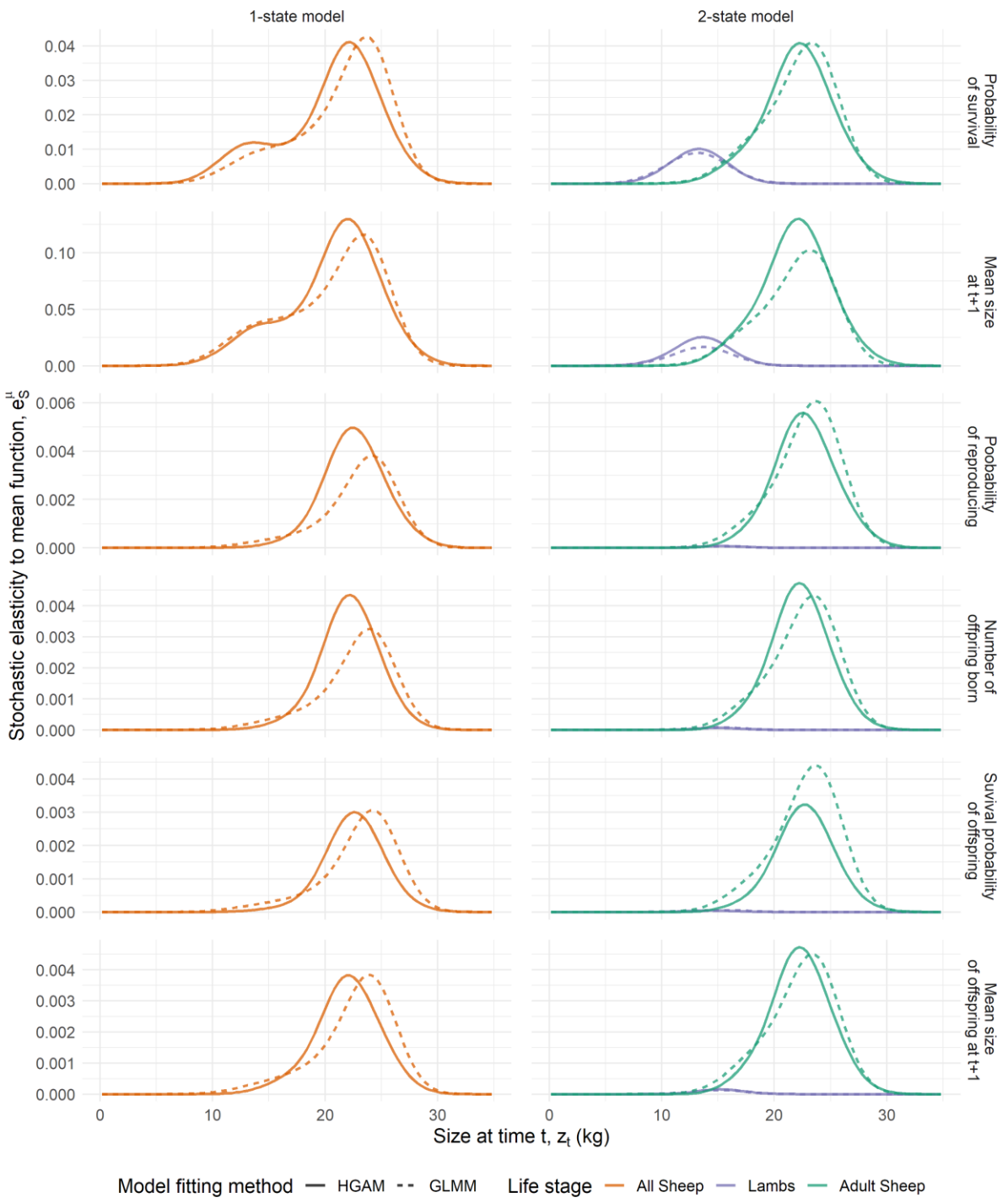


**Supplementary figure S4.9: The effect on the long-term growth rate of a perturbation to the mean vital rate function for six vital rates.** This perturbation analysis calculated the stochastic elasticity to mean function of six vital rates of survival, growth, probability of reproducing, number of offspring born, survival probability of offspring and mean size of offspring. The perturbations are applied to four different IPMs. Each IPM is constructed with one of two structures: a single state encompassing all

sheep (orange) or a two-state model with discrete states for lambs (purple) and adult sheep (green). For each IPM structure, one IPMs is constructed from vital rate functions fitted using generalised linear mixed models (GLMMs) (dashed line) or hierarchical generalised additive models (HGAMs) (solid line). These plots indicate the effect on the stochastic long-term growth rate of an increase of vital rate at size z.

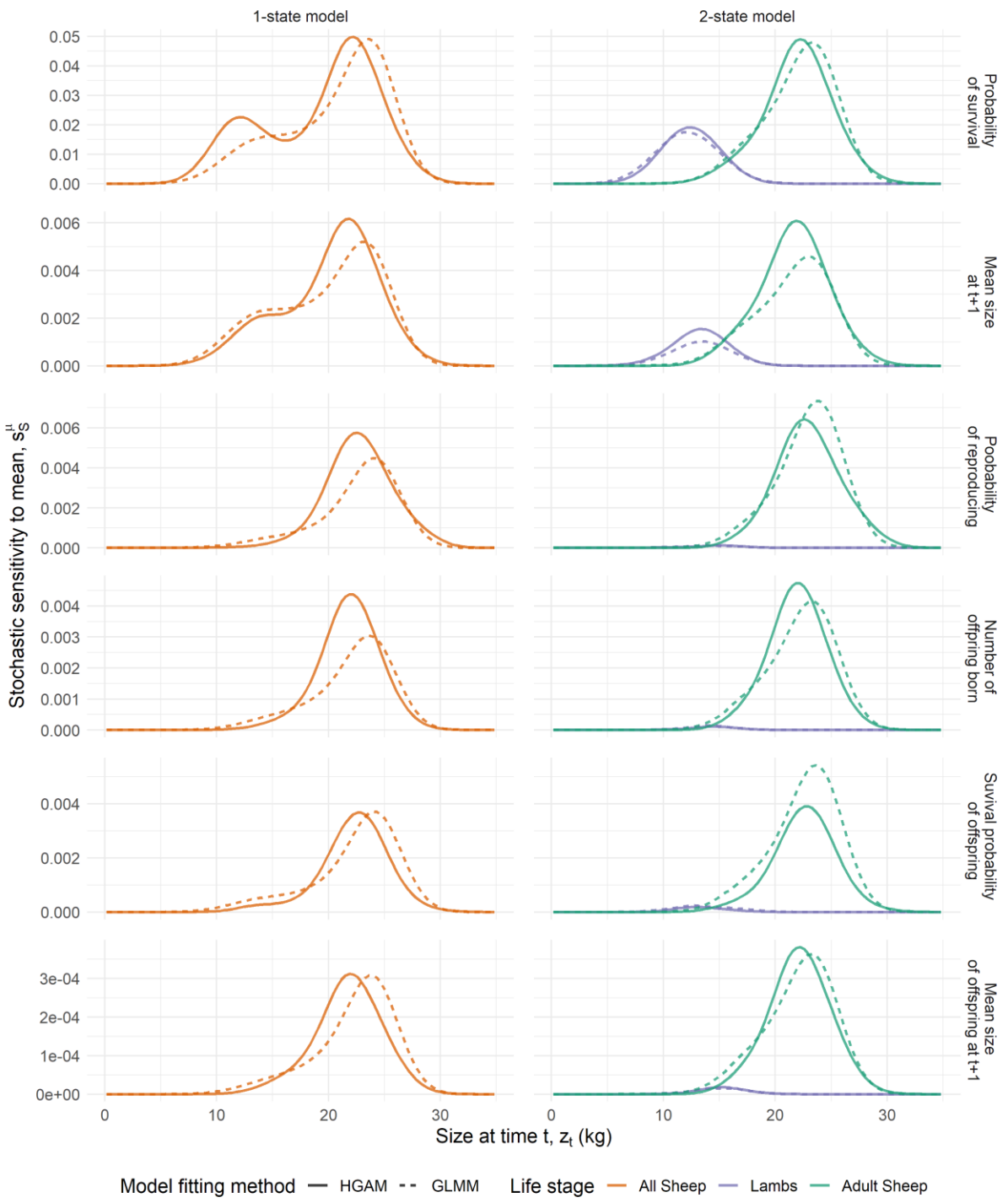


**Supplementary figure S4.10: The proportional effect on the long-term growth rate of a perturbation to the mean vital rate function for six vital rates.** This perturbation analysis calculated the stochastic sensitivity to mean function of six vital rates of survival, growth, probability of reproducing, number of offspring born, survival probability of offspring and mean size of offspring. The perturbations are applied to four different IPMs. Each IPM is constructed with one of two structures: a single

state encompassing all sheep (orange) or a two-state model with discrete states for lambs (purple) and adult sheep (green). For each IPM structure, one IPMs is constructed from vital rate functions fitted using generalised linear mixed models (GLMMs) (dashed line) or hierarchical generalised additive models (HGAMs) (solid line). These plots indicate the effect on the stochastic long-term growth rate of an increase of vital rate at size z.

# Supplementary tables

**Supplementary table S1:** R calls for the gam function in R package mgcv for fitting each vital rate. HGAMs were fitted in different five configurations (G, GS, GI, S, I) of how features were shared across groups. The five types of HGAMs can be summarised as follows; G: A single common smoother, GS: a global smoother plus group-level smoothers that have the same wiggliness, GI: A global smoother plus group-level smoothers with differing wiggliness, S: group-specific smoothers without a global smoother, but with all smoothers having the same wiggliness, I: group-specific smoothers with different wiggliness.

| Demographic function | Model type | R call in mgcv::gam |
|---|---|---|
| Survival | GLM | `gam(surv ~ t/ z -1 , family = binomial, method="REML")` |
| | HGAM: G | `gam(surv ~ z , family = binomial, method="REML")` |
| | HGAM: GS | `gam(surv ~ s(z,bs="tp") + s(z, t, bs="fs",m=2), family = binomial, method = "REML")` |
| | HGAM: GI | `gam(surv ~ s(z, bs="tp") + s(z, by =t, m=1,bs="tp") + s(t, bs="re"), family = binomial, data = method="REML")` |
| | HGAM: S | `gam(surv ~ s(z, t, bs="fs",m=2), family = binomial, method="REML")` |
| | HGAM: I | `gam(surv ~ s(z, by = t,bs="tp",m=2)+ s(t, bs="re"), family = binomial, method="REML")` |
| Growth | GLM | `gam(z1 ~ t/z-1 )` |
| | HGAM: G | `gam(z1 ~ s(z, bs="tp"), family = gaussian, method="REML")` |
| | HGAM: GS | `gam(z1 ~ s(z, bs="tp") + s(z, t, bs="fs",m=2), family = gaussian, method="REML")` |
| | HGAM: GI | `gam(z1 ~ s(z, bs="tp") + s(z, by =t, m=1,bs="tp") + s(t, bs="re"), family = gaussian, method="REML")` |
| | HGAM: S | `gam(z1 ~ s(z, t, bs="fs",m=2), family = gaussian, method="REML")` |
| | HGAM: I | `gam(z1 ~ s(z, by = t,bs="tp",m=2)+ s(t, bs="re"), family = gaussian ,method="REML")` |

| | | |
|---|---|---|
| Probability of reproduction | GLM | `gam(repr ~ t/ z -1 , family = binomial, method="REML")` |
| | HGAM: G | `gam(repr~ s(z, bs="tp"), family = binomial, method="REML")` |
| | HGAM: GS | `gam(repr~ s(z, bs="tp") + s(z, t, bs="fs",m=2), family = binomial, method="REML")` |
| | HGAM: GI | `gam(repr~ s(z, bs="tp") + s(z, by =t, m=1,bs="tp") + s(t, bs="re"), family = binomial, method="REML")` |
| | HGAM: S | `gam(repr~ s(z, t, bs="fs",m=2), family = binomial, method="REML")` |
| | HGAM: I | `gam(repr~ s(z, by = t,bs="tp",m=2)+ s(t, bs="re"), family = binomial, method="REML")` |
| Number of offspring | GLM | `gam(n_offspring ~ t/ z -1 , family = poisson, method="REML")` |
| | HGAM: G | `gam(n_offspring ~ s(z, bs="tp"), family = poisson, method="REML")` |
| | HGAM: GS | `gam(n_offspring ~ s(z, bs="tp") + s(z, t, bs="fs",m=2), family = poisson, method="REML")` |
| | HGAM: GI | `gam(n_offspring ~ s(z, bs="tp") + s(z, by =t, m=1,bs="tp") + s(t, bs="re"), family = poisson, method="REML")` |
| | HGAM: S | `gam(n_offspring ~ s(z, t, bs="fs",m=2), family = poisson, method="REML")` |
| | HGAM: I | `gam(n_offspring ~ s(z, by = t,bs="tp",m=2)+ s(t, bs="re"), family = poisson, method="REML")` |
| Offspring survival | GLM | `gam(win_l ~ t/ z -1 , family = binomial, method="REML")` |
| | HGAM: G | `gam(win_l~ s(z, bs="tp"), family = binomial, method="REML")` |
| | HGAM: GS | `gam(win_l~ s(z, bs="tp") + s(z, t, bs="fs",m=2), family = binomial, method="REML")` |
| | HGAM: GI | `gam(win_l~ s(z, bs="tp") + s(z, by =t, m=1,bs="tp") + s(t, bs="re"), family = binomial, method="REML")` |
| | HGAM: S | `gam(win_l~ s(z, t, bs="fs",m=2), family = binomial, method="REML")` |
| | HGAM: I | `gam(win_l~ s(z, by = t,bs="tp",m=2)+ s(t, bs="re"), family = binomial, method="REML")` |
| Size of offspring at t+1 | GLM | `gam(z_l~ t/z-1)` |

| | |
|---|---|
| HGAM: G | `gam(z_1~ s(z, bs="tp"), family = gaussian)` |
| HGAM: GS | `gam(z_1~ s(z, bs="tp") + s(z, t, bs="fs",m=2), family = gaussian)` |
| HGAM: GI | `gam(z_1~ s(z, bs="tp") + s(z, by =t, m=1,bs="tp") + s(t, bs="re"), family = gaussian)` |
| HGAM: S | `gam(z_1~ s(z, t, bs="fs",m=2), family = gaussian)` |
| HGAM: I | `gam(z_1~ s(z, by = t,bs="tp",m=2)+ s(t, bs="re"), family = gaussian)` |

# Chapter 5

# General Discussion

# Summary of thesis achievements

The aim of this thesis was to advance our understanding of the causes and consequences of demographic variation, with a particular focus on variation in population performance and life history. Demographic variation has many dimensions: demographic rates vary throughout an individual's lifetime, across individuals, across populations, across species, and across space and time. In this work I examined demographic variation using two approaches, species-level macroecological comparative demography and the in-depth study of a single system, to develop our understanding of the complex relationships between demography, life history and population dynamics. At these two levels of ecological complexity, across three data chapters, I have covered a range of parallel themes; how non-adaptive constraints play a key role in shaping demographic variation, synthesising demographic variation, the link between demography and life history, and how assumptions in demographic models can affect our interpretation of analyses. This thesis discussion first summarises the key findings from each data chapter. I then explore how the findings of this thesis can inform our broader understanding of demography and life history, the future of comparative demography, and provides a conceptual springboard for how we can apply the null model framework to approach new research questions.

In chapter two, *Density dependence limits the comparative analysis of demographic data*, I found that observed patterns of demographic (co)variation were consistent with patterns from simulated population models constrained by density dependence, a non-adaptive constraint. I simulated demographic models under the constraint that asymptotic growth rate, $\lambda$, in persistent populations converge to 1 or $\log(\lambda) \approx 0$. I compared the covariance patterns in life history metrics derived from our simulated demographic models to those derived from published MPMs sourced from the COMPADRE Plant Matrix Database. I saw substantial similarities in these patterns and therefore determined that the covariance patterns in demographic life history metrics might be attributed to density dependence. Furthermore, our work shows that we should assume that (co)variances patterns in demographic life history metrics are not attributed to budgetary trade-offs of investment in survival, growth, and reproduction. These findings prompt the re-evaluation of previous comparative analyses

that previously implied that these observed major axes of life-history variation are representative of budgetary trade-offs. This work provides a framework for further examinations of non-adaptive constraints.

In chapter three, *Linking life history to transient dynamics via population models*, I applied the simulated population model approach to achieve two aims. First, to assess how non-adaptive constraints affected (co)variance patterns in transient indices. Second, to explore the link between life history and transient dynamics. I used a different set of life-history metrics and a set of six transient indices but again found that non-adaptive constraints were ubiquitous in covariance patterns of MPM/IPM derived metrics. I found that (co)variance patterns within transient indices showed two main axes: magnitude of response and tendency towards amplification or attenuation. The most important axis of variation in life history traits and transient indices emerged as a prototypical fast-slow continuum from short-lived, highly reproductive populations to long-lived, less reproductive populations. This axis explained 50% of the magnitude of transient potential but subsequent latent variables were needed to improve predictions, and the tendency to amplify or attenuate was more poorly linked to life history. Non-adaptive constraints explained much of the (co)variance patterns in life history and transients which improved predictions of transient potential. Non-linear patterns in life history traits suggested that statistical approaches with assumptions of linearity such as PLS and PCA might not perform optimally. This work also proved that the simulated population models approach developed in chapter two could also be used as a standalone technique to answer the same research questions as empirical databases such as the COMPADRE Plant Matrix Database.

In chapter four, *Time-varying vital rates for population modelling: how flexible do we need to be?*, I stepped away from the comparative approach to explore the causes and consequences of demographic variation for a single population: the Soay sheep of St Kilda. I found that decisions in how we model time-varying vital rates, in terms of functional forms and how we pool parameters across years, affected trajectories of survival and reproduction having effects on life history metrics and vital rate sensitivities. I showed this by constructing time-varying IPMs with vital rates fitted with generalised linear mixed-effects models (GLMMs) and the more flexible hierarchical generalised additive models (HGAMs).

HGAMs scored better in model comparisons and the choice to use HGAMs or GLMMs had some effect on prospective projections and measures of life history. Differences in functional expressions of vital rates resulted in the average size distribution of HGAM-fitted IPMs to have smaller sheep than GLMM-fitted IPMs. This size change is reflected in perturbation analyses: HGAM-fitted IPMs showed that the stochastic long-term growth rate was more sensitive to changes in the vital rates of smaller sheep. Overall, this chapter found that HGAMs provide a robust approach for fitting non-linear time-varying vital rate models and might be especially useful in cases where there are hidden state variables.

# Life history through a demographic lens

Demography can provide powerful insights into life history. However, demographic data based on annual censuses can obfuscate important processes. Throughout this work I made a distinction between life history traits and life history metrics; life history traits were captured from direct field measurements whereas life history metrics were derived from population models. For example, work by Stearns (1983) explored covariances patterns in life history traits which captured timings of within-year developments such as gestation period and the number of offspring and are more direct measures of energetic investment. Conversely, Salguero-Gómez et al., (2016), which was presented as a continuation of Stearns' work, used demographic data to explore covariance patterns in life history metrics derived from demographic models. This demographic data describes transitions across annual censuses and these demographic rates represent the composite of many processes that occur between each census such as energetic investment into survival and reproduction, environmental factors, and density dependence. As a result, demographically derived life history metrics are good at capturing the timing and schedules of life history events but are not a direct measure of investment and therefore are less informative about allocation strategies. For example, MPM-derived mean sexual reproduction vital rate is incorporating several demographic processes (probability of reproduction, number of offspring, survival rate of offspring) and environmental factors. The key to using demographic data to explore patterns of life histories is our definition of 'life histories'. Sutherland et al., (1986) suggested over three decades ago that life histories "may be more profitably viewed as consequences of [organisms'] actions

(which may be evolved strategies), environmental effects and demographic constraints". (Co)variance patterns in demographically derived life history metrics do not describe axes of life-history strategies. Instead, we are observing axes of life history, of which life-history strategies are only one component.

Inconsistencies in the use of life history metrics for comparative analysis of demographic data have resulted in an unclear and ambiguous definition of the fast-slow continuum and reproductive strategies axes. Despite, technical ambiguity introduced by the use of different metrics, the generic messages of previous comparative analyses (Healy et al., 2019; Salguero-Gómez, 2017) are that life histories are structured along a 'pace of life' axis correlating with generation time, and a reproductive strategy axis going from iteroparity to semelparity. Having shown that these patterns are consistent with density-dependent constraints, it might be more productive to bypass the PCA approach and simply classify life histories using two or three metrics that explicitly capture these dimensions of life history. Alternatively, PCA and similar approaches are designed for dimension reduction and can accommodate many more metrics than the typical comparative demographic analysis. Why not include all robust metrics and allow the (co)variance patterns to emerge organically, rather than a preselection of metrics to fit the author's criteria of sufficiently describing different facets of life history? Otherwise, there is a risk that the emerging axes of variation are dictated as much by the author's choice of metrics, as the underlying life history of the study organisms. Going forward, authors should provide more transparency behind the motivation for each chosen life history metrics. In addition, authors could provide an alternate version of an analysis in which uses the same sets of life history metrics as other analyses; this would improve our ability to compare results between analyses.

Metrics used to classify life history should be independent of population performance. We need to be able to attribute observed correlations between life history and performance in empirical data to ecological mechanisms, rather than non-adaptive constraints. For example, $R_0$ is used as a measure of life history in Salguero-Gómez et al., (2016) but $R_0$ is mathematically constrained to be sign equivalent to $\log(\lambda)$. Therefore, when life history, as classified by major axes of variation in life history metrics including $R_0$, is found to correlate with $\lambda$, we cannot differentiate whether this correlation ecologically driven, or just an artefact of mathematic constraints. This classification of life history is also shown to

correlate with IUCN red list status (Salguero-Gómez, 2017); however, this is likely explained by a correlation with $\lambda$ because population growth rate is a factor in red list status. By conflating performance with life history, we undermine this comparative approach as a predictive framework. The simulated population model approach used in chapters two and three provide an appropriate tool for diagnosing these inherent correlations using simulated population models. By comparing whether a correlation is present in the empirical data and our null model, simulated population models, we can identify whether a link between life history and performance is inherent.

Chapters two and three were in-depth explorations of the effects of density-dependent constraints but we also know that mathematical constraints act on (co)variance patterns of life history metrics; however, we do not know the strength and shape of these constraints. A constraint is a mechanism that excludes some combinations of a set of variables. Mathematical constraints emerge in comparative demography when there are combinations of IPM/MPM-derived metrics that do not materialise despite every possible parameter combination for an IPM or MPM. For example, a mathematical constraint in transient indices is that maximum amplitude must be equal to or greater than first step amplification. In this simple case, it's easy to understand how the constraint acts. Other examples are less straightforward; for example, are there any mathematical constraints between generation time and degree of iteroparity? Other factors may also affect these constraints such as the matrix dimension of MPMs. It is important to understand the implications of mathematical constraints for the same reasons as density-dependent constraints; (co)variance patterns are likely shaped by these constraints and when examining a relationship found in empirical analyses, we need to know how much we can attribute to non-adaptive vs adaptive constraints. Reassuringly, the non-adaptive constraints observed in chapter two and three were not entirely mathematical because when we sampled population models to different mean $\lambda$ values, the covariance in life history metrics patterns was affected. A rigorous approach for a comprehensive examination of the impact of mathematical constraints would be the use of random matrix theory (RMT). A random matrix is a matrix in which some or all elements are random variables and originate in probability theory and mathematical physics but have been used to examine the stability of complex ecological systems (May, 1972; Stone, 2018) and transient dynamics (Grela, 2017). May (1972)

described interactions in ecological communities using matrices, which then were treated as random matrices to examine the inherent dynamics of the system. Similarly, we could treat MPMs as random matrices to examine the inherent mathematical properties of demographically structured populations.

Our findings in chapter two and three build on previous work (eg. Picard & Liang, 2014; Salguero-Gómez & Plotkin, 2010) and showed there was discretisation error in the majority of life history metrics and transient indices calculated from MPMs that were derived from our simulated IPMs. This discretisation induced error reduced the power of comparative analyses; in chapter three we found that the link between life history and transient dynamics was obscured when we analysed with discretely structured MPMs, as opposed to their continuously structured counterpart IPMs. We expect there to be an interaction between non-adaptive constraints and discretisation errors. For example, in the use of projection to latent space (PLS), the overall trends might persist, because of stabilising effect of non-adaptive constraints, whereas the position of a population model within the latent space may be affected considerably. As a result, emerging major axes of variation may hold true when derived from discretised models, because they are primarily attributed to non-adaptive constraints.

Adding an energetic underpinning to comparative demography would allow us to differentiate between energetic investments and environmental effects or non-adaptive factors. One tool that shows promise in this regard is dynamic energy budgets integral projection models (DEB-IPMs) (Smallegange et al., 2017). By incorporating a mechanistic understanding of vital rates, rather than a simply correlative approach as used in typical IPMs, DEB-IPMs provide an explicit link from individual-based investment in survival, growth, and reproduction to population-level processes. DEB-IPMs have been successfully used across a variety of taxa; in bulb mites (Smallegange & Ens, 2018), manta rays (Smallegange et al., 2017), and Japanese anchovy (Liao et al., 2020). The greater data requirements and method complexity are likely to be a barrier to mass adoption in the same scales as MPMs, thus making a macroecological comparative approach less feasible. However, simulating DEB-IPMs via a null model approach may offer some insights into what proportion of the (co)variance of life history metrics can be attributed to underlying energetic investments. If this were to show that energetic investments are detectable in the

comparative analysis demographic data, then this would provide confidence in the comparative methods (eg. Healy et al., 2019; Salguero-Gómez et al., 2016).

# Evaluation and opportunities of our simulated population model approach

In chapters two and three we used simulated population models to show that non-adaptive constraints played a crucial role in shaping species-level covariance patterns of life history traits and transient indices. Non-adaptive constraints may play a currently unrecognised role in other demographic analyses, such as our analysis of the Soay sheep population in chapter four. Here, we discuss the limitations of the current framework and changes required for applying the framework to comparative analysis of stochastic demographic models and single-species studies. In summary, our procedure for simulating population modes can be broken down into three stages, and this staging is used when describing how this approach could be adapted for future work. First, a plausible plant-like IPM is defined. In our implementation, this IPM had two discrete maturity stages with continuous size domains. Second, parameter sets for this IPM are sampled using a metropolis algorithm to fulfil the criteria of asymptotic long-term growth rate, $\lambda$, was approximately 1. Third, if the simulated population models need to be compared to MPMs from databases such as COMPADRE/COMADRE, the simulated IPMs are discretised to MPMs.

A key evaluation of this framework is determining how well the plant-like IPM we defined could express the demographic life history space. A quantitative evaluation asks how well the IPM could express the full diversity of combinations of life histories we could conceivably observe in natural populations. There are qualitative examples where a certain feature of life history couldn't be described. For example, our IPM did not contain dormant life stages, which are present in a range of organisms (Paniw et al., 2017). We saw evidence that our IPM was more constrained than MPMs from COMPADRE in terms of covariance of life history metrics: in simulated population models, a greater proportion of variance is explained by the fast-slow axis than our COMPADRE subset. This may in

part be due to MPM's freedom to express any combination of states and transitions between states, as opposed to our IPM's more constrained functional forms. Alternatively, it might have been that the IPM we defined was limited in describing life history diversity beyond the classical fast-slow continuum. Ultimately, the key messages of our work were not diluted by the relative inflexibility of our underlying IPM since the broad goal of this approach is to produce a sufficiently comprehensive approximation of the diversity of plausible life histories, which this work achieved. However, future applications of this framework may want to describe life histories beyond what we currently observe in databases such as COMPADRE. Therefore, simulated population models could provide a null model from which we can identify gaps in the life history space when compared to real populations. We could then look for explanations as to why certain possible combinations of life history metrics are not realised in real-world conditions.

Time-varying demographic models have been incorporated in comparative work, and we cannot currently apply our simulated population model to this setting. Paniw et al. (2018) utilised the time-varying demographic models in COMPADRE and COMADRE to show that slower life histories were less sensitive to temporal autocorrelation. However, the same question remains: how much of this pattern can we attribute to non-adaptive constraints such as density dependence? Another avenue of research uses the comparative analysis of time-variant population models to explore the demographic buffering hypothesis by determining how temporal variability in vital rates correlates with their contribution to fitness (Jongejans et al., 2010; McDonald et al., 2017). These studies have also used simulated population models to compare background patterns to empirical data from published population models. Simulated MPMS were generated with replicate matrices representing a set of annual transitions and demographic parameters sampled from separate distributions. Our approach presents several advantages over this approach. First, our life histories are underpinned by an IPM so we can use the functional basis of vital rates to generate more realistic life histories. Second, instead of independently sampling demographic parameters, we are simulating sets of parameters under a constraint that ensures realistic population dynamics. Third, IPMs can be discretised to MPMs,

providing a tool to determine whether the discretisation process biases the analyses, as we did in chapter three.

Comparative single species studies are another area that would benefit from a null model of simulated time-varying population models. For example, PlantPopNet is a globally distributed study of *Plantago lanceolata* looking to overcome a central challenge to single system and comparative studies: the lack of spatial replication (Buckley et al., 2014). By setting up field sites across the distribution of their target species, PlantPopNet looks to disentangle the factors underpinning the species' demography such as the environment, genetics, and local adaptation. However, when examining apparent trade-offs in the vital rates of survival, growth and reproduction, and the sensitivity of long-term growth rate to perturbations to these vital rates, how much is attributed to non-adaptive constraints? Again, it would be useful to contextualise the empirical demographic data against a background of simulated populations subject to minimal constraints on population growth rate. When simulating population models for a single species we would no longer be trying to explore the full diversity of life histories and can use prior knowledge of the study system to define a species-specific IPM. In addition, parameter sets could be sampled from target distributions of other population metrics such as generation time, in addition to the stochastic growth rate.

These opportunities to apply the simulated population model approach to time-varying comparative research and single species research will require more complex IPMs. There are conceptual and computation considerations with using a more complex population model. Conceptually, more complexity such as more flexibility in vital rate models risks the model expressing an implausible life history, e.g., an organism that is born large and shrinks as it matures. Computationally, every new parameter adds a new dimension to the parameter space and so will slow sampling and/or require greater computational resources. A more complex IPM also provides traps for different sets of parameters to express essentially the same demography. For example, with our relatively simple IPM, we experienced issues whereby immortal life histories that lived forever and never reproduced, thus satisfying the $\log(\lambda) \approx 1$ criterion, were oversampled. This is because once reproduction had been reduced to zero, parameters for now redundant vital rates such as the probability of flowering could freely vary to

produce unique parameter sets but essentially the same demographic model. Our solution was to implement some weak constraints to dissuade the sampler from doing this and thus adding model complexity may provide more opportunities to create immortal life histories and so might require additional constraints. However, I advise caution applying excessive constraints as it may detract from the conceptual aim to produce an unbiased sample of plausible life histories.

To incorporate stochasticity into the simulated population model approach we would need to define an IPM where vital rates can vary across a number of years. In chapter four we used kernel selection to simulate a stochastic population and assumed a stochastic population simulation randomly selects yearly transition kernels from independent identical distribution (i.i.d.). If assuming i.i.d., pseudo-duplicates of parameter sets might be sampled whereby the annual transitions are simply swapped between years. For example, for a stochastic IPM with vital rate parameters describe three years of annual transitions, if the parameters for year 1 and year 2 were switched, this would seem like two distinct parameter sets (the original and the switched set) to the sampler. Whereas in terms of stochastic population growth rate they are identical because of the i.i.d. assumption. Therefore, instead of kernel selection, we would use parameter selection whereby each parameter would have a mean and variance and unique kernels are generated for each time step by sampling from these parameter distributions (Ellner et al., 2016). We would need to determine appropriate assumptions for the covariances of these parameters. Whilst in chapter four we showed that HGAMs are appropriate for data-driven time-varying population models, they would be more obtuse to use for defining the stochastic IPM because HGAM parameters are less straightforward to interpret. Essentially, familiar challenges remain; the need to strike a balance between a model flexible enough to describe sufficient variability between years without adding too much model complexity which would hinder efficient sampling of parameters.

Preceding this work, several simulated population model approaches have been used in demography (e.g. Jongejans et al., 2010; McDonald et al., 2017; Takada et al., 2018). However, given the advantages and general applicability of this framework, some thought should be given to the reproducibility and standardisation of this approach. Reporting the use of the simulated population model approach would need to include a formal definition about the underlying IPM, the target distribution, any pseudo-priors

used to constrain the sampler, the sampling algorithm used and, if applicable, how the IPMs had been discretised to MPMs. The first step towards wider adoption of this approach is to provide access to the simulated population models generated as part of chapter two and three, in the form of their discretised MPMs, in the same format that MPMs from COMPADRE/COMADRE is distributed. This immediately provides a way that any comparative analyses can be run with simulated models, alongside their empirical data, to observe the effects of non-adaptive constraints. In addition, tools like the IPMr package developed by Sam Levine (https://github.com/levisc8/ipmr) could be useful tool for standard descriptions of the underlying IPMs from which parameter sets are sampled.

# Conclusions

The demographic approach is valuable; providing insight into how differences between individuals scale up to population-level dynamics. Here we've shown how we can use the demographic approach to interrogate comparative, and single system, patterns in life history and transient responses to perturbations. When modelling a single population, even the finest details in how we capture interannual variation in vital rates can impact our understanding of that population's life history and response to perturbations. At a comparative level, we showed using the demographic approach that density dependence is likely to explain a considerable proportion in (co)variance patterns in demographic life history metrics, and that these life history metrics can predict elements of transient. Alongside these important findings, we've stressed that the interpretation of demographic analyses requires consideration of non-adaptive constraints and how demographic models are constructed. We provide a solution to these challenges: using simulated population models are a useful tool to contextualise results against a null model. Ultimately, when doing macroecological analyses, before we attribute an explanation to an emerging pattern, we need to ensure that we have ruled out other explanations, which may be unrelated to the biology of the study organisms.

# References

Buckley, Y. M., Blomberg, S. P., Csergo, A., Ehrlén, J., Gonzalez, M. B., Garcia, … Wardle, G. M. (2014). PlantPopNet: A Spatially Distributed Model System for Population Ecology. *Ecology Society of Australia 2014 Annual Conference*.

Ellner, S. P., Childs, D. Z., & Rees, M. (2016). Environmental Stochasticity. In *Data-driven Modelling of Structured Populations: A Practical Guide to the Integral Projection Model* (pp. 187–227).

Grela, J. (2017). What drives transient behavior in complex systems? *Physical Review E*, *96*(2), 022316.

Healy, K., Ezard, T. H. G., Jones, O. R., Salguero-Gómez, R., & Buckley, Y. M. (2019). Animal life history is shaped by the pace of life and the distribution of age-specific mortality and reproduction. *Nature Ecology and Evolution*, *3*(8), 1217–1224.

Jongejans, E., De Kroon, H., Tuljapurkar, S., & Shea, K. (2010). Plant populations track rather than buffer climate fluctuations. *Ecology Letters*, *13*(6), 736–743.

Liao, B., Shan, X., Zhou, C., Han, Y., Chen, Y., & Liu, Q. (2020). A dynamic energy budget-integral projection model (DEB-IPM) to predict population-level dynamics based on individual data: A case study using the small and rapidly reproducing species Engraulis japonicus. *Marine and Freshwater Research*, *71*(4), 461–468.

May, R. M. (1972). Will a large complex system be stable? *Nature*, *238*(5364), 413–414.

McDonald, J. L., Franco, M., Townley, S., Ezard, T. H. G., Jelbert, K., & Hodgson, D. J. (2017). Divergent demographic strategies of plants in variable environments. *Nature Ecology and Evolution*, *1*(2), 0029.

Paniw, M., Ozgul, A., & Salguero-Gómez, R. (2018). Interactive life-history traits predict sensitivity of plants and animals to temporal autocorrelation. *Ecology Letters*, *21*(2), 275–286.

Paniw, M., Quintana-Ascencio, P. F., Ojeda, F., & Salguero-Gómez, R. (2017). Accounting for uncertainty in dormant life stages in stochastic demographic models. *Oikos*, *126*(6), 900–909.

Picard, N., & Liang, J. (2014). Matrix models for size-structured populations: Unrealistic fast growth or simply diffusion? *PLoS ONE*, *9*(6), e98254.

Salguero-Gómez, R. (2017). Applications of the fast-slow continuum and reproductive strategy framework of plant life histories. *New Phytologist*, *213*(4), 1618–1624.

Salguero-Gómez, R., Jones, O. R., Jongejans, E., Blomberg, S. P., Hodgson, D. J., Mbeau-Ache, C., … Buckley, Y. M. (2016). Fast-slow continuum and reproductive strategies structure plant life-history variation worldwide. *Proceedings of the National Academy of Sciences of the United States of America*, *113*(1), 230–235.

Salguero-Gómez, R., & Plotkin, J. B. (2010). Matrix dimensions bias demographic inferences: Implications for comparative plant demography. *The American Naturalist*, *176*(6), 710–722.

Smallegange, I. M., Caswell, H., Toorians, M. E. M. M., Roos, A. M., & de Roos, A. M. (2017). Mechanistic description of population dynamics using dynamic energy budget theory incorporated into integral projection models. *Methods in Ecology and Evolution*, *8*(2), 146–154.

Smallegange, I. M., & Ens, H. M. (2018). Trait-based predictions and responses from laboratory mite populations to harvesting in stochastic environments. *Journal of Animal Ecology*, *87*(4), 893–905.

Stearns, S. C. (1983). The influence of size and phylogeny on patterns of covariation among life-history traits in the mammals. *Oikos*, *41*(2), 173.

Stone, L. (2018). The feasibility and stability of large complex biological networks: A random matrix approach. *Scientific Reports*, *8*(1), 1–12.

Sutherland, W. J., Grafen, A., & Harvey, P. H. (1986). Life history correlations and demography. *Nature*.

Takada, T., Kawai, Y., & Salguero, R. (2018). A cautionary note on elasticity analyses in a ternary plot using randomly generated population matrices. *Population Ecology*, 1–11.